ESL-TR-87-03

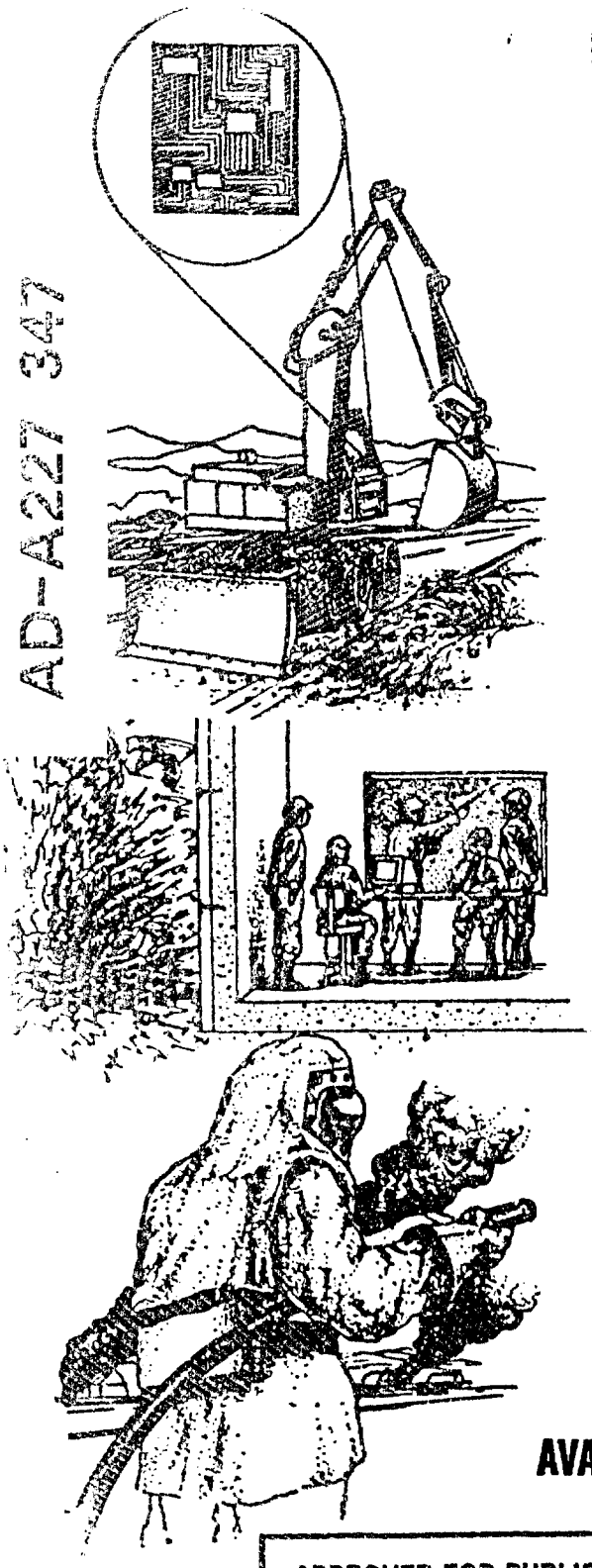

NEXT-GENERATION FIRE EXTINGUISHING AGENT PHASE II — LABORATORY TESTS AND SCOPING TRIALS

R.E. TAPSCOTT, J.H. MAY, J.P. MOORE,
M.E. LEE, J.L. WALKER

NEW MEXICO ENGINEERING
RESEARCH LABORATORY
UNIVERSITY OF NEW MEXICO
ALBUQUERQUE N.M. 87131

APRIL 1990

FINAL REPORT

AUGUST 1986 — JUNE 1988

ENGINEERING RESEARCH DIVISION
Air Force Engineering & Services Center
ENGINEERING & SERVICES LABORATORY
Tyndall Air Force Base, Florida 32403

NOTICE

PLEASE DO NOT REQUEST COPIES OF THIS REPORT FROM HQ AFESC/RD (ENGINEERING AND SERVICES LABORATORY). ADDITIONAL COPIES MAY BE PURCHASED FROM:

NATIONAL TECHNICAL INFORMATION SERVICE
5285 PORT ROYAL ROAD
SPRINGFIELD, VIRGINIA 22161

FEDERAL GOVERNMENT AGENCIES AND THEIR CONTRACTORS REGISTERED WITH DEFENSE TECHNICAL INFORMATION CENTER SHOULD DIRECT REQUESTS FOR COPIES OF THIS REPORT TO:

DEFENSE TECHNICAL INFORMATION CENTER
CAMERON STATION
ALEXANDRIA, VIRGINIA 22314

UNCLASSIFIED

SECURITY CLASSIFICATION OF THIS PAGE

REPORT DOCUMENTATION PAGE

1a. REPORT SECURITY CLASSIFICATION Unclassified	1b. RESTRICTIVE MARKINGS
2a. SECURITY CLASSIFICATION AUTHORITY	3. DISTRIBUTION/AVAILABILITY OF REPORT Approved for public release. Distribution unlimited.
2b. DECLASSIFICATION/DOWNGRADING SCHEDULE	
4. PERFORMING ORGANIZATION REPORT NUMBER(S) NMERI WA3-78 (3.21)	5. MONITORING ORGANIZATION REPORT NUMBER(S) ESL-TR-87-03
6a. NAME OF PERFORMING ORGANIZATION New Mexico Engineering Research Institute 6b. OFFICE SYMBOL (If applicable) NMERI	7a. NAME OF MONITORING ORGANIZATION Engineering and Services Laboratory
6c. ADDRESS (City, State and ZIP Code) University of New Mexico Albuquerque, New Mexico 87131	7b. ADDRESS (City, State and ZIP Code) Air Force Engineering and Services Center Tyndall Air Force Base, Florida 32403
8a. NAME OF FUNDING/SPONSORING ORGANIZATION 8b. OFFICE SYMBOL (If applicable)	9. PROCUREMENT INSTRUMENT IDENTIFICATION NUMBER Contract No. F29601-84-C-0080
8c. ADDRESS (City, State and ZIP Code)	10. SOURCE OF FUNDING NOS. PROGRAM ELEMENT NO. / PROJECT NO. / TASK NO. / WORK UNIT NO.
11. TITLE (Include Security Classification) NEXT-GENERATION FIRE EXTINGUISHING AGENT PHASE II--LABORATORY TESTS AND SCOPING TRIALS	
12. PERSONAL AUTHOR(S) Robert E. Tapscott, John H. May, Joanne P. Moore, Michael E. Lee, Joseph L. Walker	
13a. TYPE OF REPORT Final Report 13b. TIME COVERED FROM 8/86 TO 6/88	14. DATE OF REPORT (Yr., Mo., Day) April 1990 15. PAGE COUNT 137
16. SUPPLEMENTARY NOTATION This report is divided into five volumes, one for each phase. Availability of this volume is specified on reverse of front cover.	
17. COSATI CODES FIELD / GROUP / SUB. GR.	18. SUBJECT TERMS (Continue on reverse if necessary and identify by block number) halon, CFC, chlorofluorocarbon, ozone fire extinguishment, flame suppression laser Raman spectroscopy

19. ABSTRACT (Continue on reverse if necessary and identify by block number)

This project was established to originate concepts for next-generation fire extinguishing agents. In Phase II, laboratory tests and scoping trials were performed to initiate a program for replacement of halon fire extinguishants in Air Force fire protection and firefighter training. Facilities were also established to perform laser Raman spectroscopic investigations of flame suppression halon agents, and initial, baseline Raman studies were carried out.

20. DISTRIBUTION/AVAILABILITY OF ABSTRACT UNCLASSIFIED/UNLIMITED ☐ SAME AS RPT. ☐ DTIC USERS ☐	21. ABSTRACT SECURITY CLASSIFICATION Unclassified
22a. NAME OF RESPONSIBLE INDIVIDUAL JOHN R. FLODEN	22b. TELEPHONE NUMBER (Include Area Code) (904)283-6194 22c. OFFICE SYMBOL HQ AFESC/RDCF

DD FORM 1473, 83 APR EDITION OF 1 JAN 73 IS OBSOLETE.

UNCLASSIFIED

SECURITY CLASSIFICATION OF THIS PAGE

EXECUTIVE SUMMARY

A. OBJECTIVE

The objective of the overall effort is to originate concepts for a next-generation suppressant for multidimensional fires. The objective of this Phase II effort was to perform laboratory tests and scoping trials to begin a program for replacement of halons in Air Force fire protection and firefighter training. An additional objective was to initiate spectroscopic studies of flame/halon interactions.

B. BACKGROUND

Halon fire extinguishing agents have excellent dimensionality and they are clean; however, they give poor security and have poor deliverability, particularly outdoors with adverse winds. Moreover, halons have unacceptable environmental impacts. A particularly serious environmental problem is the suspected impact of common halon agents (Halons 1211 and 1301) on stratospheric ozone.

In Phase I, a study of flame suppression and fire extinguishment concepts was performed. A recommendation was made in the Phase I report that research efforts emphasize halons and halon-like materials. Due to the suspected global environmental impact of halons, a decision was made to continue work in Phase II with an emphasis on halon-like materials having a low potential to deplete stratospheric ozone.

C. SCOPE

The scope of the overall project is to originate concepts for new fire extinguishing agents. In Phase II, testing testing of halon-like agents that could serve as alternatives to the present halons was initiated. The Phase I analysis of combustion and suppression was reviewed and expanded, and laboratory studies on flame extinguishment and laser Raman spectroscopy

were initiated. A research plan for Phases III and IV on development of a low-ozone-impact training agent was prepared.

D. METHODOLOGY

Several techniques are available for testing fire extinguisment at the laboratory-scale; however, only cup burners have been widely used. Because of the available experience and data on cup burner testing, this technique was used to determine extinguishment concentrations of selected candidates. Laboratory cup burner tests of Halon 1211 alone and in blends with other halocarbons were conducted. Since it is a nonintrusive technique, laser Raman spectroscopy was selected for basic studies of halon flame extinguishment mechanisms. Raman studies were conducted on some halons of interest and on pyrolysis products from Halon 2402 to obtain baseline data.

E. TEST DESCRIPTION

A combustion laboratory with a standard cup burner apparatus was established. Flow meters were used to monitor flow rates for gaseous materials passing through the cup burner. A laser Raman spectrometer apparatus was assembled, and a slot burner was constructed for mixing fuel and halons.

F. RESULTS

The preliminary testing in this phase shows that inherent flame suppression ability increases in the order CFC-22 < CFC-12 < CFC-114 < Halon 1211. Synergistic effects were found in all mixtures tested on a laboratory cup burner apparatus: Halon 1211/CFC-12, Halon 1211/CFC-22, and Halon 1211/CFC-114. The synergism was particularly strong in the Halon 1211/CFC-22 mixture.

Both vacuum pyrolysis and flowing-nitrogen pyrolysis of Halon 2402 gave Halon 1301, Halon 1202, diatomic bromine, and tetrafluoroethene as the most

abundant products. These experiments provided experience in the construction, alignment, and operation of a flame Raman spectrometer, and provided a library of Raman spectra of many of the products that are expected to be encountered in later work.

G. CONCLUSIONS

The flame extingushment tests indicate that CFCs and HCFCs are potentially useful as clean fire-extinguishing agents. The observed synergistic effects show that the addition of a component having a high extinguishment concentration (such as CFC-22) may cause little decrease in the effectiveness of the mixture, and imply that blends of materials may be useful either to improve inherent suppression ability or to improve physical or toxicological characteristics. Laser Raman spectroscopy was shown to be a potentially useful tool for the study of the interactions between flames and halon-like agents.

H. RECOMMENDATIONS

It is recommended that HCFCs, CFCs, and their blends be targeted for investigation as alternative clean agents for halon replacement. Studies of flame-agent interactions with Raman or other spectroscopic tools are sufficiently complex that the basic spectroscopic studies should be established as a separate project.

(The reverse of this page is blank.)

PREFACE

This report was prepared by the New Mexico Engineering Research Institute (NMERI), University of New Mexico, Albuquerque, New Mexico 87131, under contract F29601-84-C-0080, for the Engineering and Services Laboratory, Air Force Engineering and Services Center, Tyndall Air Force Base, Florida 32403, and the Naval Air Systems Command, HQ NAVAIR, Washington, DC 20361. The report summarizes work done between August 1986 and June 1988. The HQ AFESC/RDCF Project Officers were Major E. Thomas Morehouse and Captain John R. Floden.

Professors Dana Brabson, Edward A. Walters, Donald R. McLaughlin, Thomas M. Niemczyk, and Fritz S. Allen, of the Department of Chemistry, University of New Mexico, provided comments, suggestions, and technical assistance on the spectroscopic studies. Dr. Mary Ann Smith of the College of Pharmacy, University of New Mexico, served as the toxicology consultant on this project.

This report has been reviewed by the Public Affairs Officer (PA) and is releasable to the National Technical Information Service (NTIS). At NTIS it will be available to the general public, including foreign nationals.

JOHN R. FLODEN, Capt, USAF
Project Officer

RICHARD N. VICKERS
Chief, Fire Technology Branch

JOSEPH L. WALKER
Chief, Engineering Research Division

RICHARD M. HANES, Col, USAF
Director, Engineering
and Services Laboratory

(The reverse of this page is blank.)

TABLE OF CONTENTS

TABLE OF CONTENTS
(CONCLUDED)

LIST OF FIGURES

LIST OF FIGURES
(CONCLUDED)

LIST OF TABLES

LIST OF ABBREVIATIONS

AFFF	Aqueous Film-Forming Foam
CFC	Chlorofluorocarbon
CW	continuous wave
FET	field effect transistor
GC	Gas Chromatography
GC-MS	Gas Chromatography-Mass Spectrometry
HAS	Hardened Aircraft Shelter
HCFC	hydrofluorochlorocarbon
ID	inside diameter
MCP	multichannel plate
MS	Mass Spectrometer
NFPA	National Fire Protection Association
OD	outside diameter
OMA	Optical Multichannel Analyser
PC	photocathode
SPA	Silicon Photodiode Array
Tem	transverse electric and magnetic
USAF	United States Air Force

LIST OF SYMBOLS

a	Viscosity divided by gas density
A	Pre-exponential term in Arrhenius equation
b	Burner slot width
c	Speed of light
C	Concentration in percent by volume
D	Diameter of burner hole
E	Arrhenius activation energy
$\vec{E}$	Oscillating electric field
$\vec{E}_0$	Amplitude vector of oscillating electric field
g	Specific gravity of a gas
G	Gibbs free energy
H	Enthalpy
k	Boltzmann constant
k_{AB}	Rate constant for reaction of reactants A and B
k'	Rate constant in units of molecules/cm^3-second
K_c	Correction factor for airflow measurements
ℓ	Burner slot length
L_m	Burner hole depth needed for laminar flow
N'_a	Concentration of species A in units of molecules/cm^3
p	Steric term in Arrhenius equation
P	Pressure
P_o	Standard pressure, 1 atmosphere (760 Torr)
q	Charge
Q	Air flow rate in mL/min
Q_k	Normal coordinate of kth vibration
R_e	Reynold's number

LIST OF SYMBOLS
(CONCLUDED)

$\vec{s}$	Vector along dipole direction
S	Entropy
S_g	Sensitivity gradient
t	Time
T	Temperature
v	Flame velocity
V	Gas velocity through burner
T_o	Standard temperature, 298.15 K
Z_{ab}	Average number of collisions of molecules A and B per cm^3-sec
α_{AB}	Radius of exclusion volume for molecules A and B
$\underset{\approx}{\alpha}$	Polarizability tensor
α_0	Polarizability at molecular equilibrium
α'_k	Change in polarizability with change in kth normal coordinate
ϵ_0	Permittivity of free space for an electric field
ΔG	Change in Gibbs free energy
ΔH	Change in enthalpy
ΔS	Change in entropy
ϵ	Activation energy
ϵ_o	Permitivity of free space for an electric field
μ	Reduced mass
$\vec{\mu}_0$	Amplitude vector of oscillating dipole
$\vec{\mu}$	Induced dipole moment
θ	Angle between oscillating dipole and r vector from dipole center
ω	Circular frequency

SECTION I
INTRODUCTION

A. OBJECTIVE

The objective of this effort is to originate concepts for a next-generation suppressant for multidimensional fires with analyses of the molecular basis for the agent action and of the quantitative burning inhibition obtained. The objective of the Phase II effort was to perform sufficient laboratory tests and scoping trials to start a program for replacement of halons in Air Force fire protection and firefighter training. The objective was also to initiate the spectroscopic study proposed in Phase I.

B. BACKGROUND

Although many new types of fire suppressants have been originated, improved agents are still needed. The fires of primary interest in ground-based fire protection for aerospace vehicles are Class B (liquid fuel) fires. Three types of agents are used by the Air Force and Navy for Class B fires (Reference 1). Foams, such as Aqueous Film-Forming Foam (AFFF), have low toxicities and provide excellent security against flashback and burnback of liquid fuels; however, foams are not three-dimensional and are dirty, leaving residues that can adversely affect aircraft engine and electronic components. Solid agents, such as potassium bicarbonate ($KHCO_3$), are excellent suppressants against liquid fuel fires (Reference 2), but they too are dirty, have poor deliverability, and give only moderate security. Halons (Reference 3) have excellent dimensionality and are clean; however, they give poor security and have poor deliverability, particularly outdoors with adverse winds. Moreover, halons have unacceptable environmental impacts. A particularly serious environmental problem is the suspected impact of common halon agents (Halons 1211 and 1301) on stratospheric ozone.

In Phase I, a study of flame suppression and fire extinguishment concepts was performed (Reference 4). A recommendation was made in the interim report that research efforts emphasize halons and halon-like materials (i.e., halocarbons). The Phase I study concluded that the most important criteria for a next-generation agent were the following:

1. Cleanliness
2. Acceptable toxicity and environmental impact
3. Good deliverability
4. Fuel securing capabilities
5. Good dimensionality

Toward the end of the Phase I study, the possibility that halon firefighting agents, like chlorofluorocarbons (CFCs), were depleting stratospheric ozone became increasingly apparent. Accordingly, a high priority was given to the development of clean fire extinguishants to replace halons, and a sixth criterion was added for a new agent: the agent must have a low Ozone-Depletion Potential (ODP). This emphasis on halon replacement necessitated a change in research direction. Development of a program to find chemical alternatives for Halons 1211 and 1301 was initiated. Since the greatest need within the Air Force is a replacement for Halon 1211, which is used for aircraft crash fires and protection of Hardened Aircraft Shelters (HAS), emphasis was placed on Halon 1211 alternatives. Halon 1301 replacements were not, however, totally ignored.

C. SCOPE

The scope of the overall Next-Generation Fire-Extinguishing Agent project is to originate concepts for new fire-extinguishing agents. The concepts may involve any combination of inhibitors that act by chemical and/or physical mechanisms or by new modes of utilization. Hypotheses are tested using laboratory-scale experiments. Fire parameters are monitored throughout the testing to provide information concerning mechanisms of action and to permit feedback for refinement of original concepts and

origination of new concepts. Research to determine the molecular mechanisms of extinguishment of selected agents is also performed. The next-generation agent(s) should be able to suppress one-, two-, or three-dimensional fires with minimal application under a range of ambient conditions. The final products of the overall project and of each phase are technical reports detailing all work accomplished, conclusions, and recommendations.

D. TECHNICAL APPROACH

The following tasks are required for Phase II of this project:

Tests shall be performed on halon derivatives determined as the most promising in Phase I using laboratory-scale burning tests. The types of tests that may be employed at this stage include (a) premixed gas flames (using flammability limits and/or burning velocities as criteria), (b) diffusion flames, and (c) pool fires. Additionally, special test systems may be constructed at a laboratory scale to test certain hypotheses. These tests may include laser diagnostic and spectral studies. Appropriate equipment to monitor burning conditions and extent of suppression shall be utilized in these and subsequent tests.

From the results of the studies outlined above, a detailed research plan for Phases III and IV on development of a low-ozone-impact training agent shall be prepared. This research plan will emphasize known materials for which significant toxicity and environmental impact data are available. The research plan will present hypotheses, the results of preliminary scoping trials, and the test procedures to be used.

In the following section, the Phase I analysis of combustion and suppression is reviewed and expanded. Following this, the results of laboratory studies on flame extinguishment and laser Raman spectroscopy are presented. In Phase I it was proposed that Raman studies, coupled with laboratory flame suppression studies, be used to elucidate flame extinguishment mechanisms (Reference 4).

SECTION II
REVIEW OF PHASE I WORK

A. HALON FIREFIGHTING AGENTS

Late in the 1800s, the halogenated hydrocarbon, carbon tetrachloride (CCl_4), was found to suppress fires (Reference 3). Despite the toxicity of this halocarbon, it was used in Europe at the turn of the century for fire suppression systems for combustion engines. The next halogenated hydrocarbon used as a fire suppressant, bromomethane (CH_3Br), was even more toxic. Despite its greater toxicity, this new agent was adopted by both England and Germany as their standard fire suppression agent in the late 1930s. The main use of CH_3Br was in aircraft and naval fire suppression systems, where it caused a number of casualties in the German Navy during World War II. Finally, a less toxic agent, trichlorobromomethane (CCl_3Br), was developed by the Germans in the late 1930s to replace CH_3Br. Because of low toxicity, this halogenated hydrocarbon fire suppressant was the first to be accepted by and used in the United States, where its primary user was the United States Air Force (USAF). The USAF used CCl_3Br in the on-board fire extinguishing systems for aircraft power plants, portable extinguishers aboard aircraft, and airport ramp patrol vehicle systems.

In 1948, the U. S. Army began a program to develop its own fire suppressing agent for use in tanks and other ground vehicles (Reference 5). This search started with 60 molecules, most of which were halogenated hydrocarbons that had shown some fire-suppressing ability in the past. Because of the cumbersome length of the halogenated hydrocarbon names, the halon nomenclature system was developed. The term "halon" is a contraction of "halogenated" and "hydrocarbon." In this system, a five-digit number is used to give the molecular formula. The first through fifth digits of the number represent, respectively, the numbers of carbon, fluorine, chlorine, bromine, and iodine atoms. For example, CCl_3Br becomes Halon 1031 when the trailing zero is dropped. The term "halon" is normally capitalized only when it is part or a designation number for a specific compound.

Of the agents investigated by the Army, Halons 1301 (CF_3Br), 1211 (CF_2ClBr), 1202 (CF_2Br_2), and 2402 ($C_2F_4Br_2$) were found to be the most effective fire suppressants. From these, the U.S. Army selected Halon 1301 for their small, 2-3/4 pound portable extinguisher. England chose Halon 1211 for both military and commercial uses, and the USAF chose Halon 1202 for its fire suppression systems. Halon 2402, the only agent cited above that exists as a liquid at room temperature, has found only limited use.

At first, these agents were used to protect only the power plants of military aircraft, naval ships, and land vehicles. Later, as the systems became more common, they were applied to other areas of these vehicles. The commercial use of Halon 1301 in the U.S. began in the 1960s when it replaced CO_2 in total-flood systems. During this period, Factory Mutual Research Corporation and the National Fire Protection Association (NFPA) began defining requirements for halon systems. From this work, a permanent standard for usage of these agents was established, a revised version of which is still in use today. At present, halons are used in portable extinguishers, total-flood systems, inerting systems, and explosion suppression systems. The versatility, cleanliness, and excellent fire suppressing capabilities of halon agents have pushed them to the front of the fire protection field, which they have revolutionized.

During the developmental period, many of the physical properties of the agent that are important in fire extinguishment were determined. Of particular importance are the observations below:

1. Halon effectiveness decreases in order of decreasing atomic weight of the halogen substituent: iodine > bromine > chlorine > fluorine. In fact, low molecular weight agents containing only fluorine are not much more effective than "inert" gases such as CO_2. Note, however, that effectiveness of totally fluorinated compounds increases markedly with increasing molecular weight.

2. One halogen atom in a compound causes a large increase in the effectiveness of the agent, whereas a second atom of the same halogen produces only a minor increase.

3. The concentration of an agent required to extinguish a flame is related to the following factors:

a. The type of fuel markedly affects the extinguishment concentration. For example, oxygenated or unsaturated hydrocarbon fuels require higher agent concentrations for extinguishment than do aliphatic hydrocarbon fuels.

b. Addition of halon agents to the air side of a flame requires a lower agent concentration for extinguishment than that required when agents are added to the fuel side.

c. Although temperature seems to increase the required concentration of these extinguishing agents, extinguishment of fires of some fuels, such as alkanes, exhibits little or no temperature dependence.

d. Diffusion flames require much lower halon-inerting concentrations than do premixed fuel-oxidizer flames.

e. Although halons extinguish flames rapidly, once they are removed from the combustion site, flames may reappear. This occurs with deep-seated fires for solid fuels and when the fuel or surroundings remain hot. To overcome these problems, higher concentrations and longer exposure times may be required.

4. Halon molecules are nonconductive and are, therefore, ideal for fires involving electronic components.

Determination of these characteristics has allowed fire suppression scientists to develop fire containment systems that are safe, effective, and designed to meet specific fire conditions.

During the 1970s and 1980s, scientists studied halons to (1) develop better application methods, (2) find new uses for the agents, and (3) determine the molecular processes occurring in halon-inhibited flames. The applied studies have contributed to the creation of safer, more effective halon delivery systems and have helped develop new applications. Studies of the chemistry of flame inhibition, however, have not been as successful in expanding halon use. It was originally believed that understanding the mechanisms of halon fire suppression would expand halon applications and would help develop new, improved agents. With the discovery of the depletion of stratospheric ozone during the 1980s, and the implication of halons as a major cause, it has now become imperative that new agents having decreased ozone impacts be developed. This effort is given increased urgency since a ban on the production of halons by the end of the century is likely.

B. COMBUSTION

1. Combustion Thermodynamics

Combustion is the process by which nearly all manmade energy is generated (References 6 and 7). The energy created by combustion runs automobiles, warms houses, generates electricity, and propels vehicles into space. Combustion is a dynamic process, which, when started, can proceed at an alarming rate. Uncontrolled combustion, termed "fire," is the cause of much destruction throughout the world; therefore, controlling fire is of major concern. To develop fire control methods, one must first understand combustion processes.

Combustion is the rapid conversion of high-energy reactants to lower energy products in a redox reaction with the emission of energy. This

conversion normally results from the oxidation of a fuel by oxygen. Fortunately, not all possible redox reactions result in combustion; only those that occur rapidly and spontaneously. For example, although the rusting of iron is the result of a redox reaction, it normally proceeds at a rate insufficient to produce combustion, fire, or flames.

From the preceding it is apparent that a redox reaction must be rapid, and it must generate energy in the form of heat in order to cause combustion. Two fields of physical chemistry involve the measurement of the rate and energy release of reactions: kinetics, which is a study of the rates at which reactions occur, and thermodynamics, which is a study of energy changes and reaction direction. The change in Gibbs free energy (ΔG) determines the spontaneity of a reaction. A negative value for ΔG indicates that a reaction can occur spontaneously in the forward direction; a positive value indicates that a reaction can occur spontaneously in the reverse direction.

Equation (1) gives the relationship between thermodynamic variables for a reaction.*

$$\Delta G = \Delta H - T\Delta S \qquad (1)$$

Here, ΔG is the change in the Gibbs free energy during a reaction, ΔH is the change in the enthalpy, ΔS is the change in the entropy (thermodynamic disorder), and T is the temperature at which the reaction occurs. This equation indicates that exothermic reactions (those that release energy and, therefore, have a negative ΔH) usually proceed spontaneously in the forward

---

*For the convenience of the reader, equation numbers are placed in parentheses and reaction numbers are placed in brackets throughout this report.

direction. Exceptions to this occur when the value of $T\Delta S$ is negative and larger than ΔH.

Spontaneity does not necessarily mean reactivity. For example, diamonds should spontaneously change to graphite, but under normal conditions, they do not. This is because an energy barrier, the activation energy, must be overcome before the reaction may proceed. Once sufficient energy is supplied to overcome the activation energy, reaction kinetics take over.

As stated earlier, kinetics is the science of reaction rates. This science also considers the mechanisms by which reactions proceed. It is often the rates of the elementary reactions making up a mechanism, and not the rate of the overall reaction, which are of primary interest in kinetic studies.

2. Combustion Mechanisms

As an example of the mechanism of a combustion reaction, consider Reaction [1] (References 6, 8, 9, and 10).

$$2H_2 + O_2 \rightarrow 2H_2 \qquad [1]$$

Although Reaction [1] seems uncomplicated, it does not actually proceed as shown. Hydrogen molecules do not collide with oxygen molecules producing water. The mechanism consists of a series of reaction steps, often termed "elementary reactions," that produce the final product. For combustion, these reaction steps are of four types: (1) chain-initiating, (2) chain-propagating, (3) chain-branching, and (4) chain-terminating. Each of these elementary reactions affects the overall combustion process differently, and together they provide the necessary driving force for combustion.

Before combustion can occur, free radicals must be produced by, or added to, the reactants. The chain-initiating elementary reactions are

those that produce free radicals from the reactants to start combustion. For Reaction [1], two initiation reactions predominate:

$$H_2 + M \rightarrow 2H\bullet + M \qquad [2]$$

and

$$O_2 + M \rightarrow 2O\bullet + M \qquad [3]$$

In these reactions, M represents any molecule that can supply, through a collision with H_2 or O_2, sufficient energy to overcome the decomposition activation energy for these diatomic molecules. Although reactions are usually initiated by energy transfer through collisions, they may also be initiated by processes such as photodissociation. The basic requirement is that free radicals are formed. Reaction-initiating microreactions are usually very endothermic and, therefore, require a continuous influx of energy to drive them. Once H• or O• free radicals are formed, they may react by any of the four types of elementary combustion reactions.

The second type of combustion reaction is chain propagation. During these reactions, free radicals react either with other free radicals or stable molecules with no change in the overall concentration of free radicals. The following reactions are examples of chain propagation steps for Reaction [1]:

$$H\bullet + O_2 + M \rightarrow HO_2\bullet + M \qquad [4]$$

$$HO_2\bullet + H\bullet \rightarrow 2OH\bullet \qquad [5]$$

$$H_2O + H\bullet \rightarrow H_2 + OH\bullet \qquad [6]$$

$$H_2O_2 + OH\bullet \rightarrow H_2O + HO_2\bullet \qquad [7]$$

$$H_2O_2 + H\bullet \rightarrow HO_2\bullet + H_2 \qquad [8]$$

These reactions may be either endothermic or exothermic; however, in either case, the energy difference between products and reactants is relatively small. The role of chain propagation reactions in combustion is the conversion of one free-radical species to another, possibly more reactive, free radical.

Chain branching, in contrast to chain propagation, produces a net increase in the number of free radicals. This can be seen in the branching microreactions for Reaction [2] given below:

$$H\bullet + O_2 \rightarrow O\bullet + OH\bullet \qquad [9]$$

$$H_2 + O\bullet \rightarrow H\bullet + OH\bullet \qquad [10]$$

$$H_2O + O\bullet \rightarrow 2OH\bullet \qquad [11]$$

$$H_2O + M \rightarrow H\bullet + OH\bullet + M \qquad [12]$$

$$H_2O_2 + O_2 \rightarrow 2HO_2\bullet \qquad [13]$$

$$H_2O_2 + M \rightarrow 2OH\bullet + M \qquad [14]$$

Like the initiation reactions, these chain-branching reactions produce free radicals and are endothermic. Unlike the initiation reaction, branching reactions have low activation energies.

Finally, termination reactions remove free radicals from the reaction. During this process, stable molecules, which may include the reactants and/or combustion products, are formed. The products of the termination reactions may, in turn, react by any of the above routes to produce free radicals and nonradicals, or they may pass out of the flame. For Reaction [2], two important termination reactions are shown below:

$$HO_2\bullet + H\bullet \rightarrow H_2 + O_2 \qquad [15]$$

$$HO_2^{\bullet} + OH^{\bullet} \rightarrow H_2O + O_2 \qquad [16]$$

These reactions are highly exothermic, and, therefore, can provide the driving energy for all the endothermic reaction steps shown earlier.

It is apparent that free-radical reactions are the dominant reactions occurring in flames. Since free radicals are lost by both termination reactions and by diffusion out of the flame, they must be generated continually and rapidly if the flame is to be sustained. In particular, the rate of free radical loss is balanced by the rate of generation in a stable flame.

3. Combustion Kinetics

Combustion kinetics treats three types of reactions: unimolecular, bimolecular, and trimolecular (Reference 10). In unimolecular reactions, a reactant molecule decomposes to form products. For this type of reaction to occur, energy must be supplied to overcome the activation energy. This is usually accomplished by collision of the reactant with another molecule, one capable of providing the necessary energy. Since these reactions, although unimolecular in reactants, require a second molecule for collision, they can be considered to be bimolecular. Reactions [2] and [3], are examples of pseudounimolecular reactions.

Trimolecular reactions are uncommon because of the extremely short duration of the collision process, which allows little time for three species to collide. Furthermore, many trimolecular reactions can be rewritten as two bimolecular reactions. Therefore, trimolecular reactions are unlikely and may proceed through two bimolecular reactions instead of one trimolecular reaction. Since real unimolecular reactions are not possible and since trimolecular reactions either have a low probability or result from two bimolecular reactions, only the reaction rates for bimolecular reactions will be considered in the following analysis.

During a bimolecular reaction, two reactant molecules collide, transfer energy, react, and form products. One can write an equation describing the rate at which products are formed. As an example, the rate equation for the general reaction A + B → C, can be written as follows:

$$d[C]/dt = k_{ab}[A][B] \tag{2}$$

In Equation (2), d[C]/dt is the rate of increase in the concentration of the product, k_{ab} is the rate constant for the reaction, and [A] and [B] are the concentrations of reactants A and B, respectively.

If the concentrations are expressed in units of molecules per cubic centimeter (Equation (3)), collision theory predicts that the average number of collisions occurring per cubic centimeter per second between molecules A and B is given by Equation (4).

$$d[N_c]/dt = k'_{ab}N'_aN'_b \tag{3}$$

$$Z_{ab} = 2[N'_aN'_b][\alpha^2_{ab}]\ (\frac{2\pi kT}{\mu})^{1/2} \approx 10^{-10}N'_aN'_b\ \frac{\text{molecules/cm}^3}{\text{sec}} \tag{4}$$

Here N'_a, N'_b, and N'_c are the concentrations of A, B, and C in units of molecules per cubic centimeter, k'_{ab} is the rate constant for the reaction in cubic centimeters per molecule per second, Z_{ab} is the average number of collisions that occur between molecules A and B per cubic centimeter per second, α_{ab} is the the radius of the volume excluded by molecules A and B (equal to the sum of the radii of molecules A and B), μ is the reduced mass, k is the Boltzmann constant, and T is the temperature. In the unlikely case that all collisions result in product formation, Equations (3) and (4) can be rewritten using collision theory as

$$d[N_c]/dt = Z_a = ZN'_aN'_b \tag{5}$$

Equation (5) shows that $k'_{ab} = Z$, a number approximately equal to 10^{-10} cm^3/molecule-second. This is a very large rate constant. Since reactions do not usually have rate constants this large, apparently all collisions are not effective. Several terms can be included in Equation (5) to correct for collision inefficiency. The first of these is a Boltzmann term, which accounts for the requirement that a collision must provide sufficient energy to the reactant molecules to overcome the activation energy. The resulting rate constant, k'_{ab}, from the inclusion of the Boltzmann factor is shown in Equation (6).

$$k'_{ab} = Ze^{-\epsilon/kt} = 2\alpha_{ab}^2(2\pi kT/\mu)^{1/2}e^{-\epsilon/kt} \tag{6}$$

In this equation, $e^{-\epsilon/kt}$ is the Boltzmann factor, ϵ is the activation energy, and all other terms were defined previously. This equation is very similar to the more familiar Arrhenius rate equation

$$k'_{ab} = Ae^{-E/kt} \tag{7}$$

where A is an experimentally determined constant, and E is equal to the Arrhenius activation energy, which is related to but not equal to ϵ in Equation (6).

Although the normal Arrhenius equation defines A as independent of temperature, Equation (6) indicates that this term should have some temperature dependence. In order to maintain the temperature independence of A, in accordance with the Arrhenius equation, and also to show a temperature effect in the pre-exponential term of the equation, A can be set equal to $2\alpha_{ab}^2(2\pi k/\mu)^{1/2}$ and a factor of $T^{1/2}$ can be included. This produces Equation (8) for the rate constant, k'_{ab}.

$$k'_{ab} = AT^{1/2}e^{-E/kt} \tag{8}$$

This extended Arrhenius equation now addresses the effect of both the temperature and the activation energy.

Combustion kineticists often further modify the Arrhenius equation to incorporate two other factors that play a part in determining the rate constant, and, therefore, the overall reaction rate. These terms, p and K, account for those reactions which, although having sufficient energy to overcome the activation energy, do not produce products. The term "p" (the steric factor) accounts for collisions that have an incorrect molecular orientation; K accounts for products that cannot dissipate the reaction energy sufficiently fast to avoid returning to the original reactants. Incorporation of these two terms into Equation (8) produces Equation (9).

$$k'_{ab} = AT^{n}e^{-E/kt} \tag{9}$$

Here A is not strictly equal to $2\alpha^{2}_{ab}(2\pi k/\mu)^{1/2}$ but now includes the magnitudes of p and K. Also, since p and K may have some temperature dependence, the pre-exponential term is dependent on T^{n} rather than the simple factor $T^{1/2}$. Although p and K can be determined theoretically, these determinations are normally inaccurate. Therefore, A and n in Equation (8) are best determined experimentally.

C. SUPPRESSION MECHANISM

At present, the best model for the suppression of flames by Halons is the hydrogen bromide catalytic mechanism shown in Reactions [17], [18], and [19].

$$Br\bullet + Br\bullet + M \rightarrow Br_2 \tag{17}$$

$$H\bullet + Br_2 \rightarrow HBr + Br\bullet \tag{18}$$

$$H\bullet + HBr \rightarrow H_2 + Br\bullet \tag{19}$$

During this catalytic mechanism, hydrogen radicals are consumed and reconverted to hydrogen molecules, thus effectively reducing the hydrogen radical concentration. This reduction in the hydrogen radical concentration slows the rate of radical formation through the reaction shown in Equation 10. Furthermore, slowing Reaction [9] also causes Reaction [10] to slow. Since Reactions [9] and [10] are considered to be the most important radical producers, reducing their rate even slightly can cause the rate of radical loss to become greater than that of radical production. This imbalance can result in the flame extinguishment.

SECTION III
LABORATORY-SCALE FIRE TESTS

A. OVERVIEW OF FIRE TESTS

An excellent discussion of laboratory tests for agent effectiveness is contained in an article by C. L. Ford (Reference 11). This reference contains a listing of selected fire extinguishing agent testing conducted up to 1975.

Ford divides fire tests into two types: dynamic and static. In dynamic tests, the fire products are carried away from the combustion source. Cup burner tests are an example of a dynamic test. Data from these tests are considered conservative: dynamic fires are more difficult to extinguish.

In static tests, the fire is allowed to burn in an enclosure. The products of the fire build up and limit the amount of fresh oxygen. This type of test is representative of a fire within a building and is usually easier to extinguish. Since the major Air Force requirement is for a streaming agent for outdoor delivery, static tests are not considered for the present work.

We define laboratory-scale tests as those whose apparatus is sufficiently small to be placed in a standard laboratory fume hood. The most common of such tests are cup burner tests, which appear in many different configurations and sizes. Cup burner tests are excellent for determining extinguishment characteristics of agents such as Halon 1301 that are applied in total-flood systems (Reference 12). For such applications, the agent concentration needed to effect extinguishment is of primary importance. The physical properties of the agent are of less importance as long as the agent is sufficiently gaseous to fill an enclosed space.

Cup burner tests, however, give only part of the data needed to evaluate a streaming agent, such as Halon 1211. For such agents, streaming

characteristics appear to be as important as extinguishment concentration, a conclusion that can be reached from observations presented in the Phase III work (Reference 13). Unfortunately, no laboratory-scale tests that require only limited amounts of agents and that evaluate extinguishment by discharge have been reported. Such apparatuses as the pot-fire test apparatus used at the Corps of Engineers Research and Development Laboratories require too much agent to be used in scoping trials (Reference 14). Existing pool fire tests, as used in the testing of portable fire extinguishers, are also inappropriate. It is, therefore, necessary to develop a laboratory-scale discharge test. This objective has been only partially met in the present effort, and, therefore, the work will be presented in the Phase III report (Reference 13).

B. CUP BURNER TESTS

The initial form of the cup burner apparatus used in the studies discussed here is described in Appendix A of Reference 4. The apparatus consisted of a 28-millimeter-diameter glass cup mounted on a 252-millimeter-long glass tube connected to a fuel supply (Figure 1). The cup and tube were housed in a glass chimney having a diameter of 85 millimeters. A rubber stopper with a hose connection leading to air and agent supplies was inserted in the bottom of the chimney. Glass beads assured an even air/agent flow. The gas temperature for each test run was determined by a thermocouple inserted in the bottom of the stopper. The entire apparatus was set up in an explosion-proof fume hood. The fuel was contained in a side-arm Erlenmeyer flask on a laboratory jack platform. A hose connected the flask side arm and the cup-burner tube. The fuel level in the cup was adjusted to the cup lip by raising or lowering the fuel flask. Flows of air and gaseous agents were determined with in-line Cole-Parmer Model 3217-45 rotameter flow meters.

JP-4 was used as the fuel for all tests reported here. Following initiation of the air-flow, the fuel was ignited by inserting a flame into the top of the chimney. The fuel was allowed burn for approximately 30

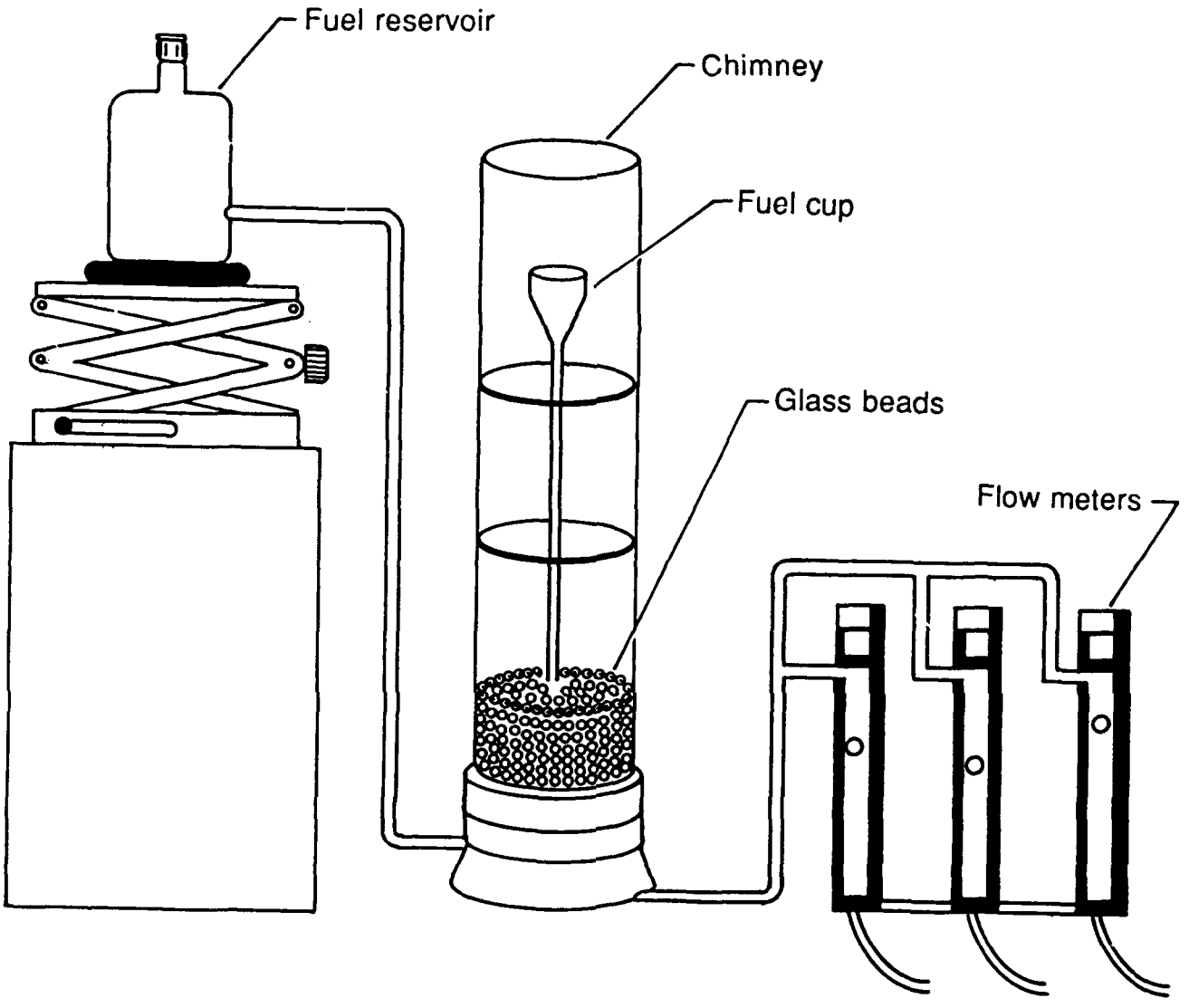

Figure 1. Cup Burner Apparatus.

seconds. Flows of the gaseous fire extinguishants were then initiated, and the flow settings required for flame extinguishment were determined and recorded. The agent concentrations required for flame suppression were calculated from the agent and air flows (Q in mL/min). The concentration in percent by volume was determined by

$$C = 100\ Q_{agent}/(Q_{agent} + Q_{air}) \tag{10}$$

The flow rates were obtained from data supplied by the rotameter manufacturer relating scale reading to flow rate for air (Table 1). The accuracy was stated to be ± 2 percent of the full scale. Two types of Cole-Parmer rotameter flow tube assemblies were used: FM044-40S for air and FM102-05G for agent gases. The rates were corrected for pressure, temperature, and (for gases other than air) density of the flowing gas. The correction factor, K_c, is a function of the gas temperature (T), pressure (P), specific gravity (g), and the standard temperature and pressure (T_o = 298.15 K, P_o = 1 atmosphere). The specific gravity of a gas is defined as the ratio of the density to that of air under the same conditions. For air, g = 1.

$$Q_{actual} = Q_{measured}/K_c \tag{11}$$

where

$$K_c = \sqrt{g(T/T_o)(P_o/P)} \tag{12}$$

The most important question to be answered in the cup burner tests is whether synergistic or antagonistic effects can be observed in mixed systems. If two agents operate independently, the concentration of a mixture required for flame suppression should be a linear function of the volume fraction of each agent. Nonlinear functions indicate synergistic effects if less agent than predicted is required and antagonistic effects if more agent is required (Figure 2). Weak evidence for synergism has been

observed in the Phase I work (Reference 4). Work done in the Purdue study on agents also indicates nonlinear dependencies of flame suppression concentration on mixture composition (Reference 5). Synergism could permit the development of blends that will perform better than either separate component. This could permit the use of a small amount of a component having some adverse properties (ODP, toxicity, cost) to give large improvements in agent performance.

TABLE 1. FLOW RATE CALIBRATION CHART FOR AIR.

Scale reading	Flow rate for air, mL/min	
	FM004-40S	FM102-05G
150	29500	4014
140	27200	3852
130	25390	3581
120	23060	3285
110	20790	3003
100	18840	2776
90	16810	2516
80	14770	2214
70	12740	1896
60	10680	1561
50	8560	1294
40	6830	901
30	4940	644
20	3000	379
10	980	127

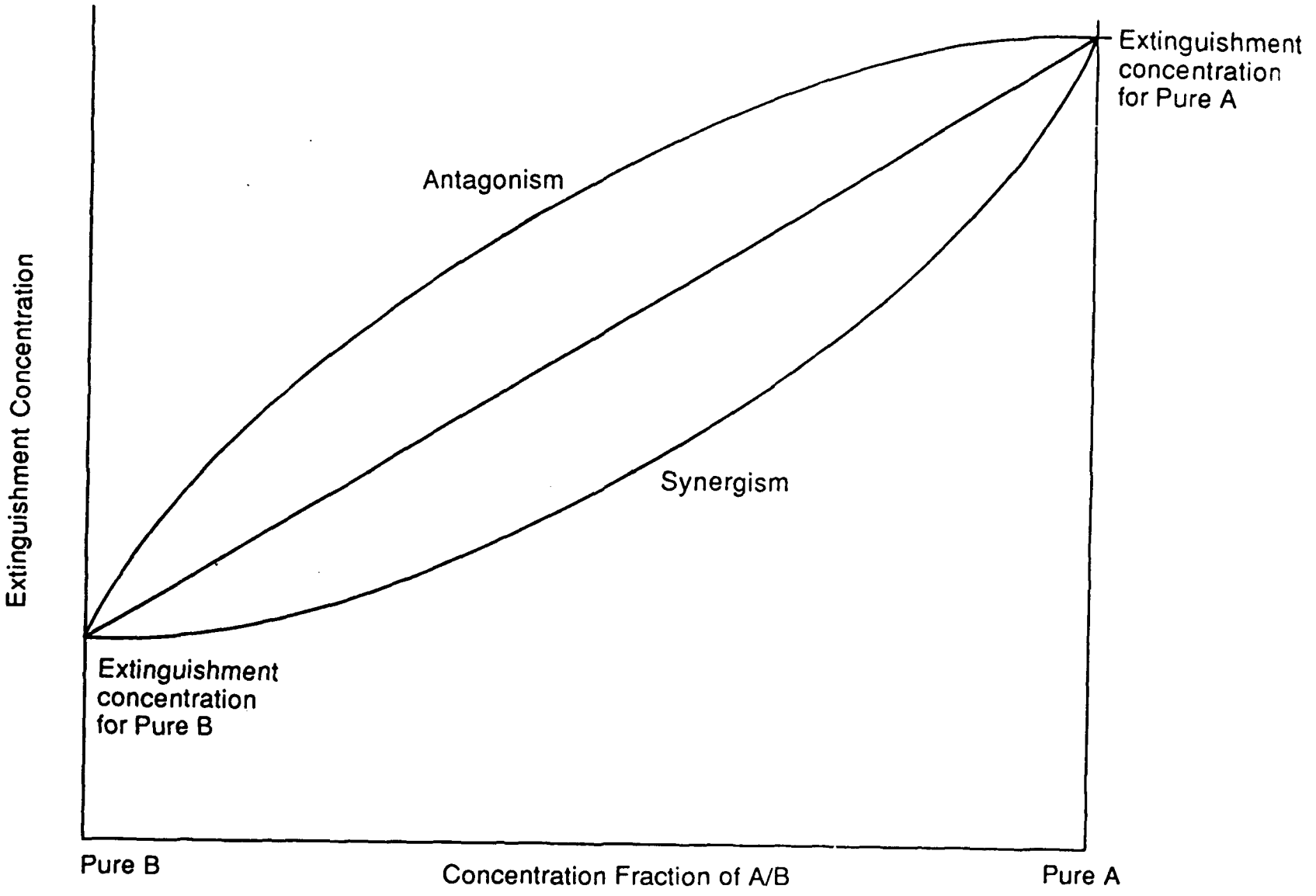

Figure 2. Synergism and Antagonism in Flame Suppression by Mixtures of Two Agents.

Halon 1211 alone was used in the first cup burner testing to establish a standard fire-extinguishing concentration for that compound. The results are presented in Table 2. The barometric pressure (P) on the day during which the testing was performed and the gas temperatures (T) are also given. The average Halon 1211 concentration needed for extinguishment was 3.04 percent.

These results were obtained in a high-altitude location, where the atmospheric pressure is about 83 percent of that at sea level. Extinguishment test results depend on the partial pressure of oxygen; the concentration required for extinguishment will generally decrease as the oxygen concentration in the air decreases. As shown below, however, a reverse trend is possible.

The HCl- or HBr-catalyzed recombination of hydrogen free radicals into H_2 by an extinguishing agent follows the following mechanism, where "X" represents a chlorine or bromine atom (Reference 15). The reference cited presents data on chlorine inhibition only; however, the same mechanism is believed to hold also for bromine, as shown earlier in Reactions [17] - [19].

$$HX + H\bullet \rightarrow H_2 + X\bullet \qquad [20]$$

$$2X\bullet + M \rightarrow X_2 + M \qquad [21]$$

$$H\bullet + X_2 \rightarrow HX + X\bullet \qquad [22]$$

The net result is the conversion of highly reactive monoatomic hydrogen into less reactive diatomic hydrogen:

$$H\bullet + H\bullet \rightarrow H_2 \qquad [23]$$

A second mechanism involves the direct removal of hydrogen free radicals by the termolecular reaction shown in Reaction [24].

TABLE 2. CUP BURNER TEST RESULTS FOR HALON 1211.[a]

Test no.	Scale reading		Q, mL/min		Temperature of air, K	Extinguishment concentration, %
	Air	Halon	Air	Halon		
1	110	54	18901	539	295.1	2.77
2	110	68	18894	703	295.3	3.59
3	110	60	18891	600	295.4	3.08
4	110	58	18891	580	295.4	2.98
5	110	55	18891	549	295.4	2.82
6	110	60	18891	600	295.4	3.08
7	110	60	18904	600	295.0	3.08
8	110	60	18904	600	295.0	3.08
9	110	60	18904	600	295.0	3.08
10	110	60	18907	600	294.9	3.08
11	110	60	18907	600	294.9	3.08
12	110	60	18904	600	295.0	3.08
13	110	60	18904	600	295.0	3.08
14	110	60	18904	600	295.0	3.08
15	110	65	18904	665	295.0	3.40
16	110	65	18904	665	295.0	3.40
17	110	65	18904	665	295.0	3.40
18	110	65	18904	665	295.0	3.40
19	110	65	18904	665	295.0	3.40
20	110	53	18904	528	295.0	2.72
21	110	50	18904	498	295.0	2.57
22	110	48	18904	462	295.0	2.41
23	110	45	18904	422	295.0	2.18
24	110	50	18904	498	295.0	2.57
25	110	50	18904	498	295.0	2.57
26	110	70	18886	729	295.0	3.72
27	110	54	18886	539	295.0	2.77
28	110	65	18886	665	295.0	3.40
29	110	65	18870	665	295.0	3.40
30	110	58	19045	575	295.1	2.93
31	110	58	19045	575	295.1	2.93

[a]P = 630 Torr = 0.829 atmosphere; T = 289.8 K.

$$H\bullet + X\bullet + M \rightarrow HX + M \qquad [24]$$

Both Reaction [23] and Reaction [24] are pressure-dependent. Thus, at high pressures, inhibition will increase. However, at lower pressures, the effect of oxygen partial pressure cancels this expected pressure dependence.

To determine the effect of volumetric air flow rate on the Halon 1211 extinguishment concentration, the concentration of Halon 1211 required for flame suppression was measured for varying flow rates (Table 3). The results were as expected: as the air flow was increased, more Halon 1211 was required for flame extinguishment. As the air flow was decreased, less Halon 1211 was required. Figure 3 contains a graph showing the dependence of the Halon 1211 fire extinguishing concentration on the air flow rate. The relationship is nearly linear; however, a better fit is obtained with the quadratic

$$C = 2.219 + 1.102 \times 10^{-5} Q + 2.298 \times 10^{-9} Q^2 \qquad (13)$$

where C is the flame extinguishment concentration in percent by volume and Q is the air flow rate in mL/min. This equation, whose curve is shown in Figure 3, gives a standard deviation based on N-1 data points of 5.46 percent. The r^2 value (the coefficient of determination) is 0.8926. The closer r^2 is to 1, the better is the fit between calculated and experimental data (Reference 16).

The average extinguishment concentration from all data collected for flow rates from 9695 to 23271 mL/min was 3.04 percent by volume in air. It must be recognized that these data were collected in a location where the atmospheric pressure was only 630 Torr at the time of the experiment.

Since extinguishment concentration depends on air flow, this variable was, to the extent possible, kept constant in the studies performed on mixed-agent systems.

TABLE 3. HALON 1211 EXTINGUISHMENT CONCENTRATION FOR VARYING AIR FLOW.[a]

Test no.	Scale reading		Q, mL/min		Temperature of air, K	Extinguishment concentration, %
	Air	Halon	Air	Halon		
32	130	84	23271	901	293.2	3.70
33	130	85	23239	913	294.0	3.78
34	130	85	23251	913	294.0	3.78
35	130	77	23251	818	293.7	3.40
36	130	85	23251	913	293.7	3.78
37	120	78	21128	830	293.4	3.78
38	120	76	21132	806	293.3	3.67
39	120	71	21132	744	293.3	3.40
40	120	76	21146	806	292.9	3.67
41	120	71	21146	744	292.9	3.40
42	120	71	21150	744	292.8	3.44
43	120	70	21150	732	292.8	3.35
44	60	35	9795	298	292.8	2.95
45	60	33	9795	278	292.8	2.76
46	60	30	9698	249	298.7	2.50
47	60	30	9697	249	298.8	2.50
48	60	31	9695	258	298.9	2.60
49	80	44	13528	409	293.6	2.93
50	80	45	13544	424	297.9	3.03
51	80	40	13482	348	295.6	2.52
52	80	40	13482	348	295.6	2.52
53	80	41	13478	363	295.8	2.62
54	80	42	13473	378	296.0	2.73
55	80	42	13478	378	295.8	2.73
56	60	30	9742	249	296.0	2.49
57	110	65	18965	667	296.0	3.40
58	110	60	18961	603	296.1	3.08
59	110	61	18965	616	296.0	3.14
60	110	65	18961	662	296.1	3.40
61	110	62	18952	629	296.4	3.11
62	40	20	6201	145	294.5	2.29
63	40	21	6201	155	294.5	2.44
64	40	20	6201	145	294.5	2.29
65	40	20	6193	145	294.8	2.29

[a]P = 630 Torr = 0.829 atmosphere; T = 289.8 K.

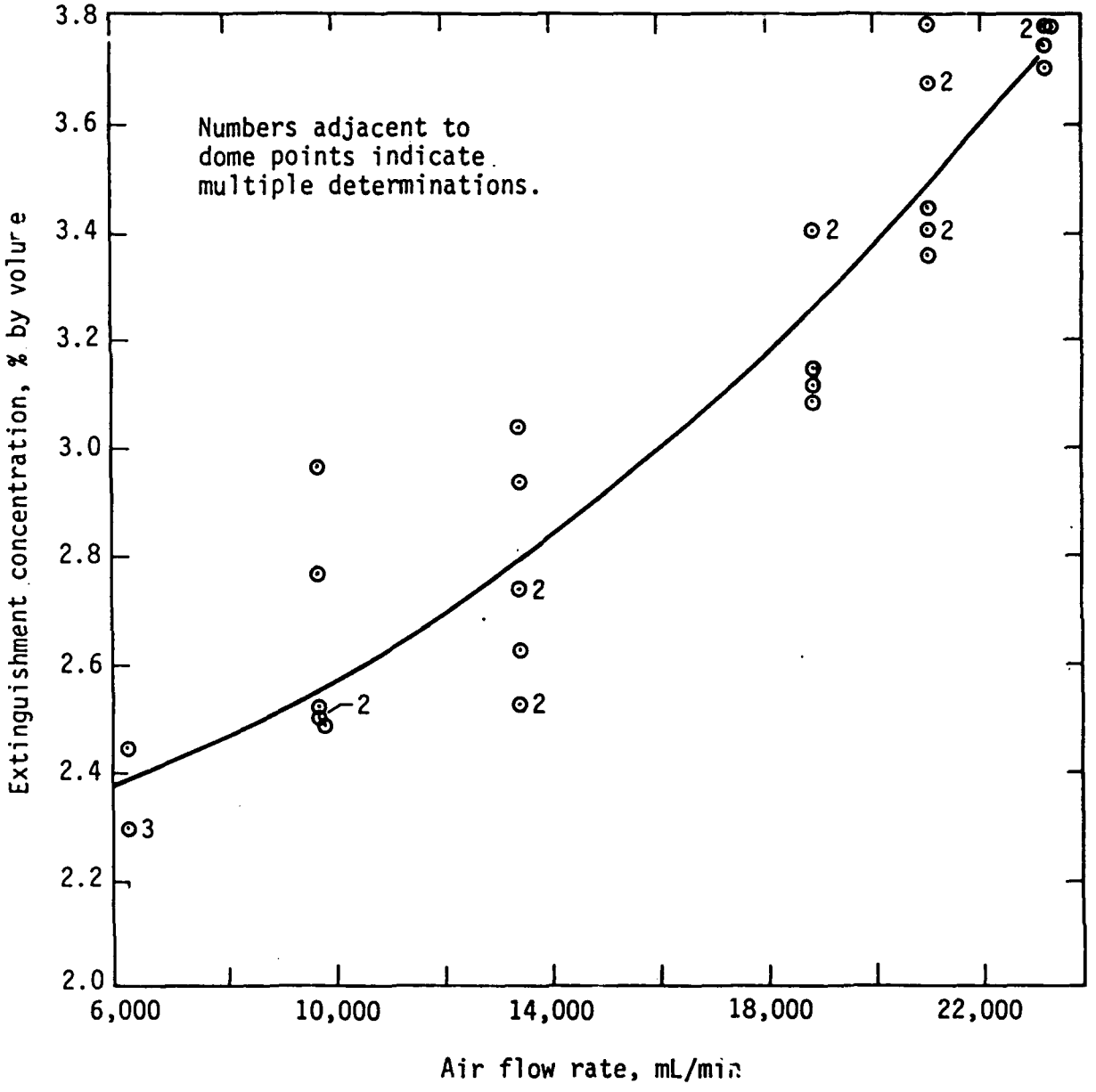

Figure 3. Extinguishment Concentration for Halon 1211 as a Function of Air Flow Rate.

In the first tests for synergism, mixtures of dichlorodifluoromethane (CCl_2F_2, CFC-12) and Halon 1211 were studied. Extinguishment concentrations were determined for mixtures containing approximately 50 percent of each component and for pure CFC-12. The results, presented in Table 4, indicate significant synergistic effects. Table 4 shows an average CFC-12 concentration of 6.68 percent for suppression compared to 3.04 percent required for Halon 1211. A 50:50 mixture of the two agents requires an average of 3.45 percent for flame extinguishment, compared to the value of 4.86 percent predicted for a linear relationship. This indicates that the performance of a relatively poor suppressant, such as CFC-12, can be significantly improved by addition of another agent.

Since the air velocity was allowed to vary in the first tests with mixtures of Halon 1211 and CFC-12, additional determinations were performed. The additional tests encompassed a wider range of mixtures to permit a determination of the functional dependence of flame extinguishment concentration on mixture composition. The mixtures contained approximately 20, 40, 60, 80, and 100 percent CFC-12. The results are presented in Table 5 and are shown graphically in Figure 4, which includes data from the earlier 50:50 mixture study. The data in Figure 4, can be fit by the quadratic presented in Equation (14).

$$C = 2.952 - 0.4288\ F + 4.269\ F^2 \qquad (14)$$

where F is the volume fraction of CFC-12 in the mixture. The coefficient of determination, r^2, is 0.8053.

Chlorodifluoromethane ($CHClF_2$, CFC-22) was tested both alone and in combination with Halon 1211 (Table 6). Note that the designation "CFC" rather than "HCFC" (hydrochlorofluorocarbon) is used here for simplicity. CFC-22 requires a relatively high concentration for extinguishment, greater than 10 percent. Combinations of CFC-22 and Halon 1211 appear to exhibit an even stronger synergism (Figure 5) than that observed for CFC-12 with Halon

TABLE 4. FLAME EXTINGUISHMENT CONCENTRATIONS FOR PURE CFC-12 AND FOR 50:50 MIXTURES OF CFC-12 AND HALON 1211.[a]

Test no.	Scale reading		Q, mL/min			Ratio of halon/CFC	Extinguishment concentration, %	
	Halon	CFC	Halon	CFC	Air		Halon	CFC
1	30	27	248	239	17197	1.01	1.40	1.35
2	35	32	297	295	17197	1.01	1.67	1.66
3	35	32	297	295	17197	1.01	1.67	1.66
4	35	32	297	295	17197	1.01	1.67	1.66
5	35	32	297	295	17197	1.01	1.67	1.66
6	0	105	0	1224	17197	0	0	6.65
7	0	120	0	1392	17197	0	0	7.49
8	0	110	0	1272	17197	0	0	6.89
9	0	110	0	1272	17197	0	0	6.89
10	0	105	0	1224	17197	0	0	6.65
11	0	113	0	1308	17197	0	0	6.64
12	0	110	0	1272	17197	0	0	6.89
13	0	109	0	1263	17197	0	0	6.27
14	0	110	0	1272	17197	0	0	6.89
15	0	112	0	1296	17197	0	0	6.43
16	0	108	0	1264	19171	0	0	6.18
17	0	109	0	1274	19171	0	0	6.23
18	45	41	419	402	19100	1.04	2.10	2.02
19	44	40	404	385	19119	1.05	2.03	1.93
20	44	40	404	385	19123	1.05	2.03	1.93
21	40	36	344	341	19061	1.01	1.74	1.73
22	40	36	344	341	19064	1.01	1.74	1.73
23	39	36	334	341	19061	0.98	1.69	1.73
24	44	40	404	385	19061	1.05	2.03	1.94
25	39	36	334	341	19045	0.98	1.69	1.73
26	40	37	344	352	19048	0.98	1.74	1.78
27	38	35	324	330	19045	0.98	1.65	1.68
28	38	35	324	330	19045	0.98	1.65	1.68
29	38	35	324	330	19041	0.98	1.65	1.68
30	37	34	314	319	19041	0.98	1.60	1.62
31	38	35	324	330	19038	0.98	1.65	1.68
32	37	35	314	319	19035	0.98	1.60	1.62

[a]Ambient pressure (P) = 630.6 Torr = 0.83 atmosphere; T (Halon 1211) = 289.8 K; T (CFC-12) = 288.6 K; T (air) = 295.0 K (Test Numbers 1-13), 295.1 K (Test Numbers 14-30).

TABLE 5. FLAME EXTINGUISHMENT CONCENTRATIONS FOR PURE CFC-12 AND FOR VARYING MIXTURES OF CFC-12 AND HALON 1211.[a]

Test	Scale reading			Q, mL/min			Ratio of	Extinguishment concentration, %	
no.	Halon	CFC	Air	Halon	CFC	Air	halon/CFC[b]	Halon	CFC
1	50	30	110	496	273	18852	1.8	2.53	1.39
2	50	17	110	496	129	18820	3.86	2.54	0.66
3	50	17	110	496	129	18845	3.86	2.55	0.66
4	50	16	110	496	116	18848	4.29	2.55	0.59
5	51	17	110	506	129	18845	3.93	2.60	0.66
6	50	17	110	506	129	18826	3.94	2.60	0.66
7	43	29	110	390	262	18826	1.49	2.00	1.34
8	48	33	110	466	306	18820	1.52	2.38	1.56
9	45	31	110	420	284	18813	1.48	2.15	1.45
10	45	31	110	420	284	18813	1.48	2.15	1.45
11	44	31	110	405	284	18813	1.43	2.08	1.46
12	54	70	110	537	803	18807	0.67	2.66	3.99
13	46	60	110	436	661	18810	0.66	2.19	3.32
14	44	55	110	405	605	18070	0.67	2.12	3.18
15	33	45	110	276	465	18070	0.59	1.47	2.47
16	36	45	110	306	465	18804	0.66	1.56	2.38
17	36	46	110	306	482	18798	0.63	1.56	2.46
18	38	46	110	326	482	18794	0.68	1.66	2.46
19	40	119	110	345	1380	18788	0.25	1.68	6.7
20	30	84	110	247	989	18791	0.25	1.23	4.9
21	25	69	110	196	789	18791	0.25	0.99	3.99
22	25	69	110	196	789	18794	0.25	0.99	3.99
23	26	69	110	203	789	18794	0.26	1.03	3.99
24	26	70	110	203	803	18785	0.25	1.03	4.06

[a]Ambient pressure (P) = 628 Torr = 0.826 atmosphere; T (Halon 1211) = 289.8 K; T (CFC-12) = 288.6 K; T (air) = 295.4 to 297.3 K (individual values were recorded and used in the flow calculations).

[b]Ratios of 4.0, 1.5, 0.67, and 0.25 correspond to respective values of 20, 40, 60, and 80 percent CFC-12 in the mixture.

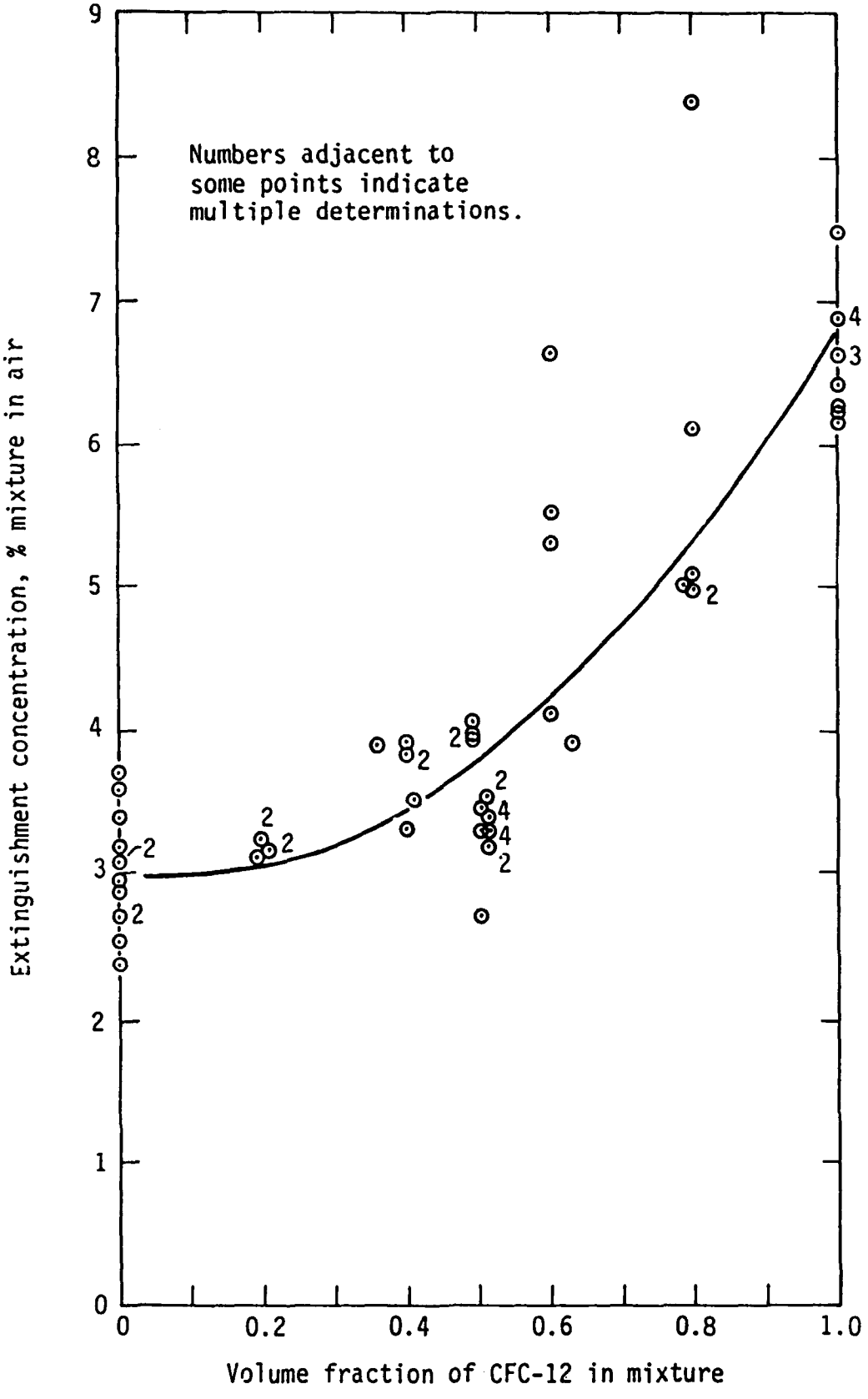

Figure 4. Extinguishment Concentration for Mixtures of Halon 1211 and CFC-12.

TABLE 6. FLAME EXTINGUISHMENT CONCENTRATIONS FOR PURE CFC-22 AND FOR VARYING MIXTURES OF CFC-22 AND HALON 1211.[a]

Test no.	Scale reading			Q, mL/min			Ratio of halon/CFC	Extinguishment concentration, %	
	Halon	CFC	Air	Halon	CFC	Air		Halon	CFC
1	0	150	105	0	2147	17436	0	0	10.96
2	0	150	105	0	2147	17438	0	0	10.99
3	0	150	105	0	2147	17371	0	0	11.00
4	45	36	110	425	427	19070	0.996	2.14	2.14
5	45	36	110	425	427	19070	0.996	2.14	2.14
6	44	35	110	410	413	19037	0.993	2.07	2.08
7	46	36	110	441	427	19037	1.03	2.21	2.14
8	48	39	110	471	468	19031	1.01	2.36	2.34
9	46	37	110	441	441	19018	1.00	2.21	2.21
10	59	16	110	597	150	19143	3.99	3.0	0.75
11	57	16	110	576	150	19115	3.85	2.90	0.75
12	57	15	110	576	136	19115	4.23	2.91	0.69
13	57	16	110	576	150	19121	3.85	2.90	0.75
14	57	15	110	576	136	19115	4.23	2.91	0.69
15	50	30	110	503	346	19121	1.45	2.52	1.73
16	48	28	110	473	318	19121	1.49	2.38	1.60
17	51	29	110	514	332	19121	1.55	2.57	1.66
18	51	30	110	514	346	19115	1.48	2.57	1.73
19	51	30	110	514	346	19128	1.48	2.57	1.73
20	41	40	110	366	484	19134	0.75	1.83	2.42
21	45	47	110	427	632	19128	0.68	2.12	3.13
22	43	45	110	396	590	19126	0.67	1.97	2.93
23	45	47	110	427	632	19121	0.68	2.12	3.13
24	45	47	110	427	632	19115	0.68	2.12	3.13
25	94	40	110	351	1409	19112	0.25	1.68	6.75
26	30	69	110	251	1001	19115	0.25	1.23	4.92
27	35	79	110	301	1173	19121	0.26	1.46	5.70
28	34	78	110	291	1156	19105	0.25	1.41	5.62
29	35	81	110	301	1206	19092	0.25	1.46	5.86
30	36	83	110	311	1239	19083	0.25	1.51	6.00

[a]Ambient pressure (P) = 639 Torr = 0.841 atmosphere (Test Numbers 1-9), 645 Torr = 0.849 (Test Numbers 10-30); T (Halon 1211) = 289.9 K (Test Numbers 1-9), 289.8 K (Test Numbers 10-30); T (CFC-22) = 288.6 K; T (air) = 292-296 K (individual values were used in the flow calculations).

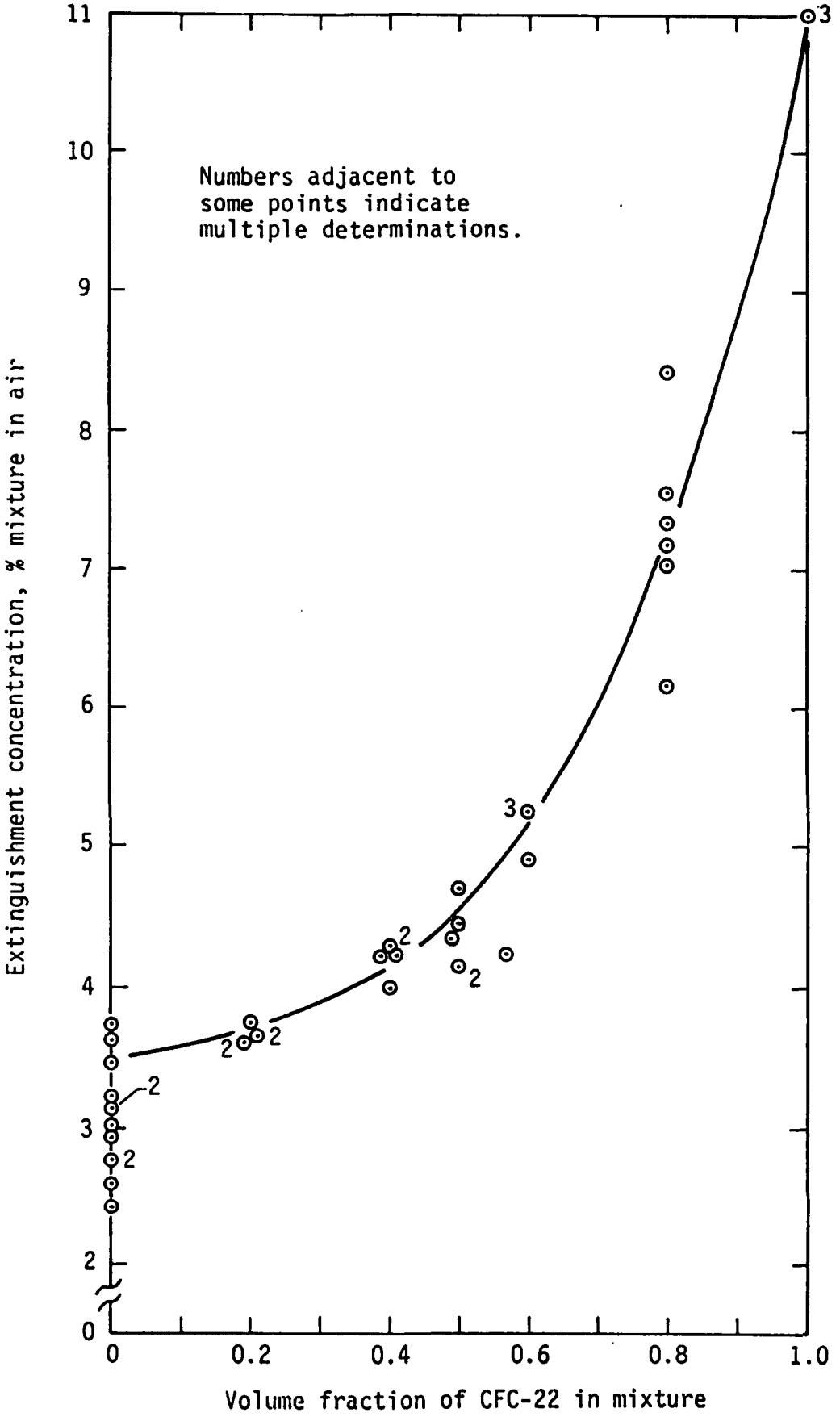

Figure 5. Extinguishment Concentration for Mixtures of Halon 1211 and CFC-22.

1211 (Figure 4). A 50:50 mixture exhibits an extinguishment concentration only a little higher than that of pure Halon 1211. The quadratic curve that best fits these data is given by the Equation (15), where F is the volume fraction of CFC-22. The r^2 value is 0.9523.

$$C = 3.111 - 1.801\ F + 9.207\ F^2 \qquad (15)$$

In a final series of cup burner tests, CFC 114 was combined with Halon 1211 to give approximate concentrations of 20, 40, 60, 80, and 100 percent CFC 114. See Table 7 for the results of this testing. CFC 114 is marginally more effective than CFC 12 and much more effective than CFC 22. Figure 6 gives the combined percent extinguishing concentrations versus the Halon 1211 percentage. The curve shown in this figure is obtained from the quadratic fit given in Equation (16). The r^2 value for this fit is 0.8951.

$$C = 3.012 + 1.076\ F + 1.952\ F^2 \qquad (16)$$

TABLE 7. FLAME EXTINGUISHMENT CONCENTRATIONS FOR PURE CFC-114 AND FOR VARYING MIXTURES OF CFC-114 AND HALON 1211.[a]

Test no.	Scale reading		Q, mL/min			Ratio of halon/CFC[b]	Extinguishment concentration, %	
	Halon	CFC	Halon	CFC	Air		Halon	CFC
1	0	118	0	1209	18838	0	0	6.03
2	0	120	0	1230	18844	0	0	6.13
3	0	118	0	1209	18844	0	0	6.42
4	0	116	0	1188	18844	0	0	5.93
5	45	46	424	426	18844	0.995	2.15	2.16
6	40	41	348	352	18841	0.988	1.78	1.80
7	42	43	378	382	18847	0.991	1.93	1.95
8	41	42	363	367	18847	0.990	1.85	1.87
9	42	43	378	382	18847	0.991	1.93	1.95
10	48	37	469	309	18835	1.52	2.39	1.57
11	47	36	454	299	18838	1.52	2.32	1.53
12	47	36	454	299	18832	1.52	2.32	1.53
13	56	19	561	133	18866	4.24	2.87	0.68
14	55	20	551	142	18857	3.88	2.82	0.73
15	57	20	572	142	18840	4.02	2.92	0.73
16	57	19	572	133	18835	4.32	2.93	0.68
17	33	53	278	515	18832	0.50	1.42	2.62
18	38	50	328	504	18841	0.65	1.67	2.56
19	40	51	348	514	17092	0.68	1.94	2.86
20	40	51	348	514	18863	0.68	1.76	2.61
21	26	78	208	837	18847	0.25	1.04	4.21
22	25	74	197	787	18841	0.25	1.00	3.97
23	25	74	197	787	18832	0.25	1.00	3.97

[a]Ambient pressure (P) = 637 Torr = 0.838 atmosphere, T (CFC-22) = 298.9 K, T (air) = 300 K, Air Setting FM 044-40S = 110.

[b]Ratios of 4.0, 1.5, 0.67, and 0.25 correspond to respective values of 20, 40, 60, and 80 percent CFC-12 in the mixture.

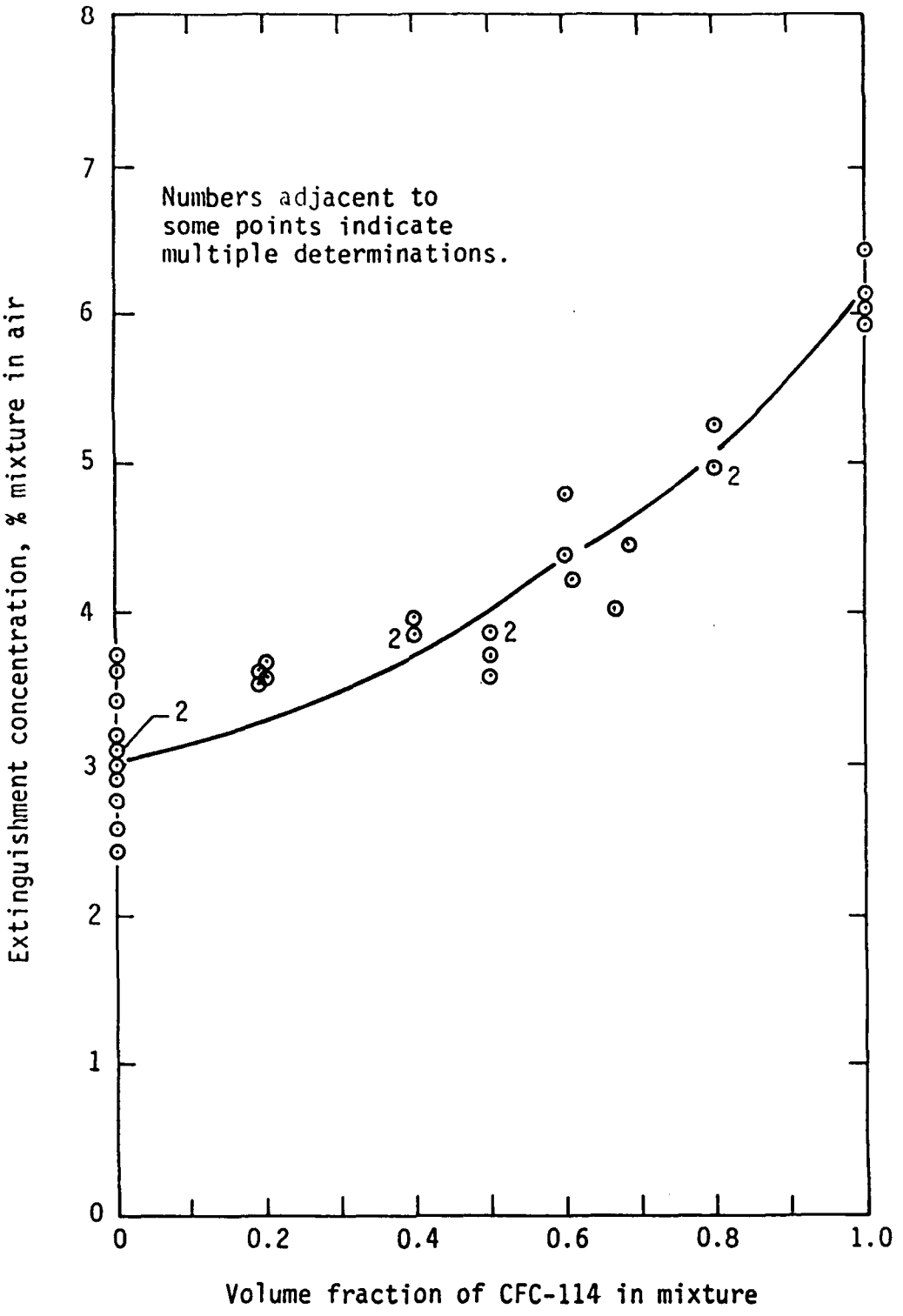

Figure 6. Extinguishment Concentration for Mixtures of Halon 1211 and CFC-114.

SECTION IV
RAMAN SPECTROSCOPY STUDIES

A. INTRODUCTION

At the turn of the century, halogenated hydrocarbons (halons) were found to be effective in extinguishing flames. Unlike water, which acts as a heat sink, halons appeared to extinguish flames by another method. In addition, because of the relative inertness and low boiling points (many were gases at room temperature), halons caused little or no damage to the area surrounding the fire and required no cleanup. This property contrasted with that of water and solid extinguishants, which often caused more damage than the actual fire and required cleanup. These advantages of the halons, along with their excellent ability to extinguish many different types of fires, made them one of the most useful extinguishing agents available. Consequently, investigations of the mechanism by which halon agents extinguished flames were undertaken.

Early studies of fire suppression by halons dealt solely with such bulk processes as flame temperature and velocity. These studies, although helpful in providing information on agent performance, provided little information on the actual mechanisms involved in flame suppression (Reference 17). More recent studies, using molecular beam mass spectrometers, provided data on the initial reactions that occurred in flames containing halons (References 18 and 19); however, since solid probes and low pressures were required for mass spectrometry, the mechanisms deduced were questionable. One way to remove these questions was to analyze atmospheric flames using nonintrusive methods.

A method that first showed promise in the 1970s for analyzing atmospheric flames is Raman spectroscopy (References 20 through 28). This method is of particular interest because it works with atmospheric flames and, since it uses lasers that emit light at wavelengths outside the absorption bands of flame molecules, causes little or no perturbation of the

flame. For these reasons, Raman spectroscopy was selected for the present work as a technique for investigation of the chemical mechanism for combustion inhibition by halons.

B. RAMAN SPECTROSCOPY

1. Background

Of the many useful techniques available to study the chemistry of flames, optical methods have the advantage of being nonintrusive. In addition, optical techniques often have excellent spatial resolution and can simultaneously determine flame temperatures and species concentrations. These properties make optical techniques well suited to flame investigation.

Spontaneous Raman spectroscopy has been chosen as the optical method for investigation of flame species for this work. Raman was chosen over such other optical techniques as fluorescence, coherent anti-Stokes Raman scattering, and absorption spectroscopy for the reasons listed below.

a. Instrumentation for Raman spectroscopy (laser, triple monochromator, diode array detector) was available.

b. Raman spectroscopy can measure the vibrational, rotational, and in some special cases, the electronic spectrum of molecules or atoms and is, therefore, information intensive.

c. Raman spectroscopy allows a choice of the electromagnetic spectral region for detection of the vibrational, rotational, or electronic spectra.

d. Raman spectroscopy is noninvasive, can have high spatial resolution, and can provide information on species concentration and temperature.

e. Raman spectroscopy has been used successfully in the past to investigate flame species.

These reasons all played important roles in the choice of Raman spectroscopy as the principal method in this project for the investigation of halon-inhibited flames. Most important, a great amount of information was available through the vibrational and rotational Raman spectrum of molecules.

2. Classical Raman Theory

Raman spectroscopy has been practiced for over 60 years. It was first observed by K. S. Krishnan and C. V. Raman in 1928. The Raman effect is caused by the interaction of the electromagnetic field of light with the electric field of a molecule. During this interaction, a photon of the incident light may be annihilated with the simultaneous creation of a new photon. This new photon may have the same frequency as the incident light, or it may have a frequency equal to the incident frequency plus or minus the vibrational or rotational frequency of the molecule interacting with the light. The first of these effects, no frequency change, is termed "Rayleigh scattering." The second effect, frequency change, is the Raman effect, with which this work is concerned. From this brief description, it is apparent that the position of a Raman band in the electromagnetic spectrum is not characterized by its absolute position but rather by the magnitude of its frequency displacement from the frequency of the incident light. To further explain the Raman effect, the remainder of this section contains a highly condensed development of the classical model for Raman scattering (Reference 29).

The Raman phenomenon results from the inelastic scattering of radiation incident on a molecule. For a molecule to be Raman active, vibration along at least one of its normal coordinates must cause a change in the molecular polarizability. The polarizability of a molecule may be described by Equation (17).

$$\vec{\mu} = \underset{\approx}{\alpha}\,\vec{E} \tag{17}$$

In this equation, $\vec{\mu}$ is a vector representing the dipole moment induced in the molecule by the electric field vector $\vec{E}$ incident on the molecule, and $\underset{\approx}{\alpha}$ is the polarizability tensor of the molecule along its principal coordinates. The time dependence of the incident electric field can be expressed as shown in Equation (18).

$$\vec{E} = \vec{E}_0 \cos(\omega_0 t) \tag{18}$$

Here, $\vec{E}_0$ is the amplitude vector of the incident field, ω_0 is the circular frequency of the incident electric field, and t is time.

Since $\underset{\approx}{\alpha}$ is defined as the polarizability of a molecule along its principal coordinates, the mathematical description of $\underset{\approx}{\alpha}$ for a molecule using classical mechanics requires the development of 3N-6 normal coordinates (Q_k) of vibration for a nonlinear molecule of N atoms (3N - 5 for linear molecules). These normal coordinates, derivable from the 3N Cartesian coordinates that describe the displacement of the molecular atoms, represent an irreducible set of orthogonal vibrational coordinates. Therefore, any possible vibration of the molecule can be represented by the linear combination of these irreducible normal coordinates. Vibration along any normal coordinate of a molecule may cause a change in the polarizability tensor of the molecule with time. Thus, variations in the polarizability tensor with respect to the normal coordinates can be mathematically expressed using a Taylor series expansion. Using such an expansion and appropriate trigonometric relationships, one can derive an equation for the induced dipole moment of a molecule interacting with electromagnetic radiation:

$$\vec{\mu} = \alpha_0 \cdot \vec{E}_0 \cos(\omega_0 t) + [\alpha'_k \cdot \vec{E}_0 Q_{k,0} \cos\{(\omega_0 + \omega_k)t + \delta_k\} \cdot \cos\{(\omega_0 - \omega_k)t - \delta_k\}] \tag{19}$$

In Equation (19), α_k' is the change in polarizability with a change in the kth normal coordinate, Q_k, and α_0 is the value of α when the molecule is in its equilibrium state.

Equation (19) indicates that $\vec{\mu}$ has the following three distinct frequency dependencies:

a. ω_0, which is at the frequency of the incident light. It is this frequency dependence of the induced dipole that causes Rayleigh Scattering.

b. $\omega_0 + \omega_k$, which is at a frequency higher than the incident frequency by an amount equal to the frequency of the molecular vibration along the k^{th} normal coordinate. This frequency dependence of the induced dipole with the incident radiation is called "anti-Stokes Raman scattering."

c. $\omega_0 - \omega_k$, which is at a frequency lower than the incident frequency by an amount equal to the frequency of the molecular vibration along the k^{th} normal coordinate. This frequency dependence of the induced dipole with the incident radiation is called "Stokes Raman scattering" and is the effect of concern in the present study.

It is also apparent that while Rayleigh scattering has the same phase as the incident light, both Stokes and anti-Stokes Raman scattering are phase shifted by an amount equal to δ_k, a point that is of little concern to this work.

It can be concluded from this simple mathematical model that light interaction with a molecule may induce an oscillating dipole. Furthermore, this induced dipole may oscillate at frequencies equal to the incident frequency, ω_0, and at frequencies displaced from ω_0 by an amount equal to plus or minus the vibrational frequency of the molecule, ω_k, along one of

its normal coordinates. Therefore, the frequencies observed in Raman scattering may be considered beat frequencies between the frequencies of the incident light and the molecular vibration of the molecule.

3. Raman Intensity

Of particular importance for this work is the relationship between the concentration of a species and the intensity of the Raman bands caused by that species. In order to develop the theoretical model for the intensity of a Raman band, the relationship between the magnitude of an oscillating dipole and the intensity of the emitted radiation must be developed.

An oscillating dipole may be described by the equation

$$\vec{\mu} = q\vec{s} \tag{20}$$

where $\vec{s}$ is a vector oriented from -q to +q having a magnitude equal to the charge separation, q is the charge, and $\vec{\mu}$ is the dipole moment vector.

The time dependence of the harmonic oscillation of such a dipole can be expressed by the equation

$$\vec{\mu} = \vec{\mu}_0 \cos(\omega t) \tag{21}$$

where $\vec{\mu}_0$ is the amplitude vector of the oscillating dipole, ω is the circular frequency of the oscillating dipole, and t is time. Starting with these relationships, one can derive the following equation for intensity of a Raman signal at any point in space.

$$I = [(\omega_0 \pm \omega_k)^4 \underset{\approx}{\alpha}^2 \vec{E}^2 \sin^2\theta]/[32\pi^2 \epsilon_0 c^3] \tag{22}$$

Here, r is the distance from the center of the dipole, c is the speed of light, ω is the circular frequency of the oscillating dipole, ϵ_0 is the

permitivity of free space for an electric field, and θ is the angle between the direction of r and the direction of the oscillating dipole.

Many important properties of Raman spectroscopy are illustrated in Equation (22). Of importance to this work are the following:

a. Since Equation (22) represents the intensity of the Raman scattering due to a single dipole, the intensity of the Raman signal from an assembly of N dipoles (molecules) must simply be N x I. Therefore, the intensity of the Raman signal is proportional to the concentration of the molecules present in incident light beam.

b. Increasing the intensity of the electric field of the excitation source will linearly increase the Raman signal.

c. The intensity of the Raman signal is proportional to the square of the ease $\underset{\approx}{\alpha}$ with which electrons can be displaced to produce an electric dipole under the action of an electric field.

C. INSTRUMENTATION

The development of the instrumentation required to investigate chemical processes can be as difficult as the experiments themselves. In this case, Raman spectroscopy is a well-known method with many interesting and useful capabilities; however, the application to flames has been limited. Because of the dynamic nature, natural radiance, and gaseous state of the matter in a flame, each component of the Raman instrument must be optimized to produce the highest measurable intensity possible for the already weak Raman signal. Here is described the instrumentation and modifications used to obtain the spatially resolved Raman spectrum of a flame.

Raman spectrometers contain a high-intensity light source, a double or triple monochromator, a detector, and data acquisition and storage electronics. A sample cell, laser optics, and sample to monochromator coupling

optics are also needed. Proper selection and adjustment of these components are required to provide Raman spectra for any given experiment. For the flame Raman spectrometer, a high power argon ion laser was chosen as the light source, a triple monochromator with high stray light rejection was selected for dispersion, and an Optical Multichannel Analyzer (OMA) was used to detect the Raman signal. A block diagram of the laser Raman spectrometer is shown in Figure 7. The details are discussed in the following portions of this report.

1. Laser

A Coherent, I-52-4 wavelength-selectable, argon ion laser was used as the light source in this spectrometer. This laser was nominally capable of producing 4 watts of continuous power while in the multiline mode and approximately 1.8 watts when running in single line mode for the 488-nanometer and 514.5-nanometer argon lasing wavelengths. Actual values for the power outputs can be expected to exceed these values by as much as 50 percent, a value obtained from actual power readings in the vicinity of 2.5 watts for either the 488-nanometer or 514.5-nanometer lines.

A further increase in the power output was achieved by replacing the long, approximately 10-foot focal length, output coupler with a shorter, approximately 5-foot focal length, coupler. Single-line power output began to approach the 3.4-watt values for the 488-nanometer and 514.5-nanometer argon laser lines using the shorter focal length mirror. The power increase resulting from changing the output coupler can be attributed to the change from the 00 transverse electric and magnetic lasing mode (Tem00) of the long focal length coupler to the Tem01 lasing mode of the shorter focal length coupler. The change from the Tem00, power-centered Gaussian beam, to the doughnut shaped, Tem01 beam had little effect on the focusing of the beam in the flame, since the beam diameter in the flame was only 50 micrometers. Consequently, no spatial resolution was lost by using the higher power Tem01 laser line.

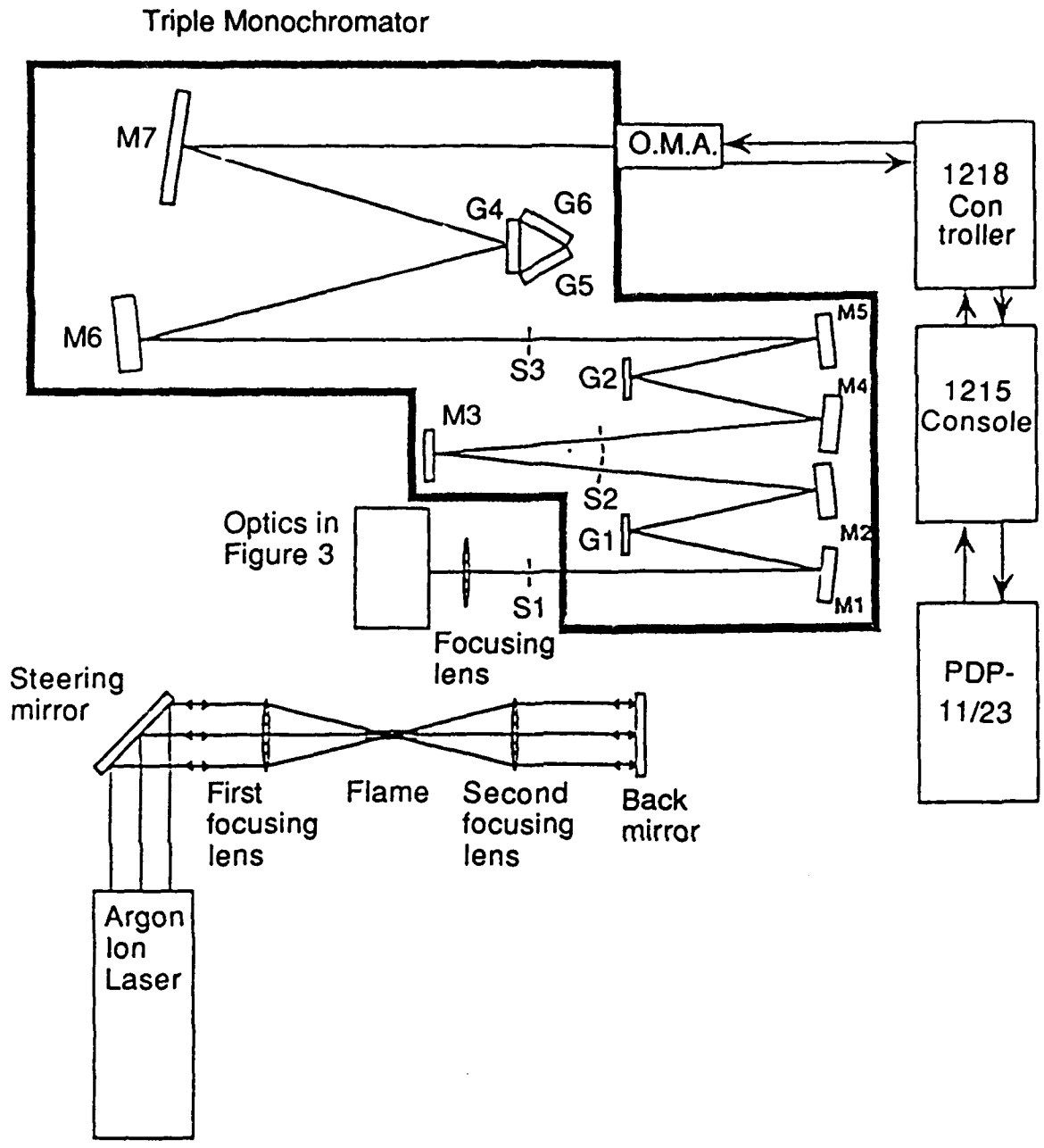

Figure 7. Raman Spectrometer.

2. Spectrometer

A Spex model 1877 Triplemate spectrometer was used as the light dispersion device for the Raman instrument. Triple monochromators of this type are ideally suited for Raman spectroscopy and for multichannel detectors since they provide high stray light rejection and a flat, undistorted focal plane for the detectors. A triple monochromator contains two main sections. For the Spex Triplemate, the first section is a 0.22-meter double monochromator with gratings locked in subtractive dispersion mode. This section acts as a wavelength-variable, bandpass-selectable filter. Radiation from the first section is fed into the entrance slit of the second, 0.5-meter, single-monochromator spectrograph section, which, in turn, disperses the radiation over the detector.

The Spex model 1877 has a variable grating turret that allows the selection of one of three possible gratings without dismantling the device; however, this feature was used very little for this work. The 1200 grooves/millimeter grating was used for all data collection. This grating provides a dispersion of 0.035 nanometers per 25 micrometers (14 nanometers per centimeter) at the detector. The dispersion gives a resolution of better than 0.2 nanometers for the system. Wavenumber resolution varies from 4 cm^{-1} to 7 cm^{-1} for the 514.5-nanometer excitation wavelength and from 5 cm^{-1} to 8 cm^{-1} for the 488.0-nanometer excitation wavelength.

Variation in the wavenumber resolution for the two different excitation wavelengths is caused by the nonlinear relationship between wavelength and wavenumber and by the fact that gratings disperse light approximately linearly on the wavelength scale. The nonlinear relationship causes higher wavelength excitation lines to have higher wavenumber resolutions than lower wavelength excitation lines. From this, one might assume that it would be best to use the highest wavelength available so that the best resolution could be achieved; however, since the intensity of the Raman signal is inversely proportional to the wavelength of the excitation source to the fourth power (Equation (22)), using higher wavelength

excitation lines reduces the Raman signal intensity. Consequently, a trade-off must be made between increased signal intensity and increased resolution in any Raman experiment. Because the only two laser lines of appreciable intensity for an argon ion laser, 488-nanometers and 514.5-nanometers, are close together, no real compromise need be considered. In fact, both laser lines were used to provide complementary, and (in the case of C_2 fluorescence caused by the 514.5-nanometer laser wavelength) different information.

3. Detector

The detector consists of a Princeton Applied Research OMA, Model 1420, equipped with a Model 1218 controller and Model 1215 console. The OMA, an intensified silicon linear diode array, contains a proximity-focused microchannel plate (MCP) intensifier coupled by fiber optics to a Silicon Photodiode Array (SPA). The intensifier incorporates a semitransparent photocathode (PC) that emits electrons when struck by photons. The emitted electrons are accelerated by the PC to MCP potential and cross the small space between the PC and MCP. Most of the electrons enter the MCP, which consists of a bundle of fine glass tubes having partially conductive walls. The potential difference of about 700 volts between the ends of the microchannels accelerates the electrons along the channels and causes them to collide with the microchannel walls as they move. Each collision results in additional electrons being liberated, allowing the microchannels to act as optically resolved electron multipliers. The electron packet exiting from the MCP is accelerated toward the phosphor screen by the 5-kilovolt potential difference between the MCP and the phosphor screen. These electrons strike the phosphor, causing it to emit photons.

The light output of the phosphor is coupled by fiber optics to a linear Silicon Photodiode Array. The photodiode array consists of 1024 photodiodes, which are reverse-biased so that they are, in effect, charged capacitors. When light strikes one of these diodes, electrons are freed leaving electron hole pairs that discharge the capacitance of the diodes.

Access to each diode is controlled by an array shift register that serially opens and closes the FET (field effect transistor) switches connected to each photodiode. In this way, each diode is independently connected to the summing junction, which is connected to a charge-sensitive preamplifier. This amplifier has a capacitor connecting its output and input so that it behaves as a charge detector. As each diode is connected to the amplifier, it is charged. The amount of charge required to recharge the diode equals the amount of discharge caused by the light that struck the diode since the time the diode was last connected to the charge-sensitive preamplifier. As a result of the charge transfer, a voltage change at the output of the preamplifier is effected. This voltage change is amplified and then digitized by the 1218 controller. The controller then sends the digitized signal to the 1215 console for display and storage.

A typical spectral response curve for this detector can be seen in Figure 8. The detector is cooled to below 0 ^{o}C by an internal Peltier cooler to reduce the dark current of the tube. At this temperature, the dark current limits integration time on the detector to no more than 23 seconds. A further decrease in the maximum integration time to 8 seconds is caused by the flame background.

4. Optics

The optics of the Raman system consists of three parts: the monochromator, laser optics, and sample-to-monochromator optics. The monochromator was described earlier. The laser optics consisted of two high-reflectivity, first-surface mirrors and two 50-millimeter lenses. The first mirror was used to steer the laser beam toward the flame. This mirror was necessary because of space problems, which required that the large argon ion laser be placed out of a direct line with the flame. The beam coming off the steering mirror was focused into the flame by one of the 50-millimeter lens such that the focal point of the lens was at the center of the burner flame slot and the beam traveled parallel to the slot.

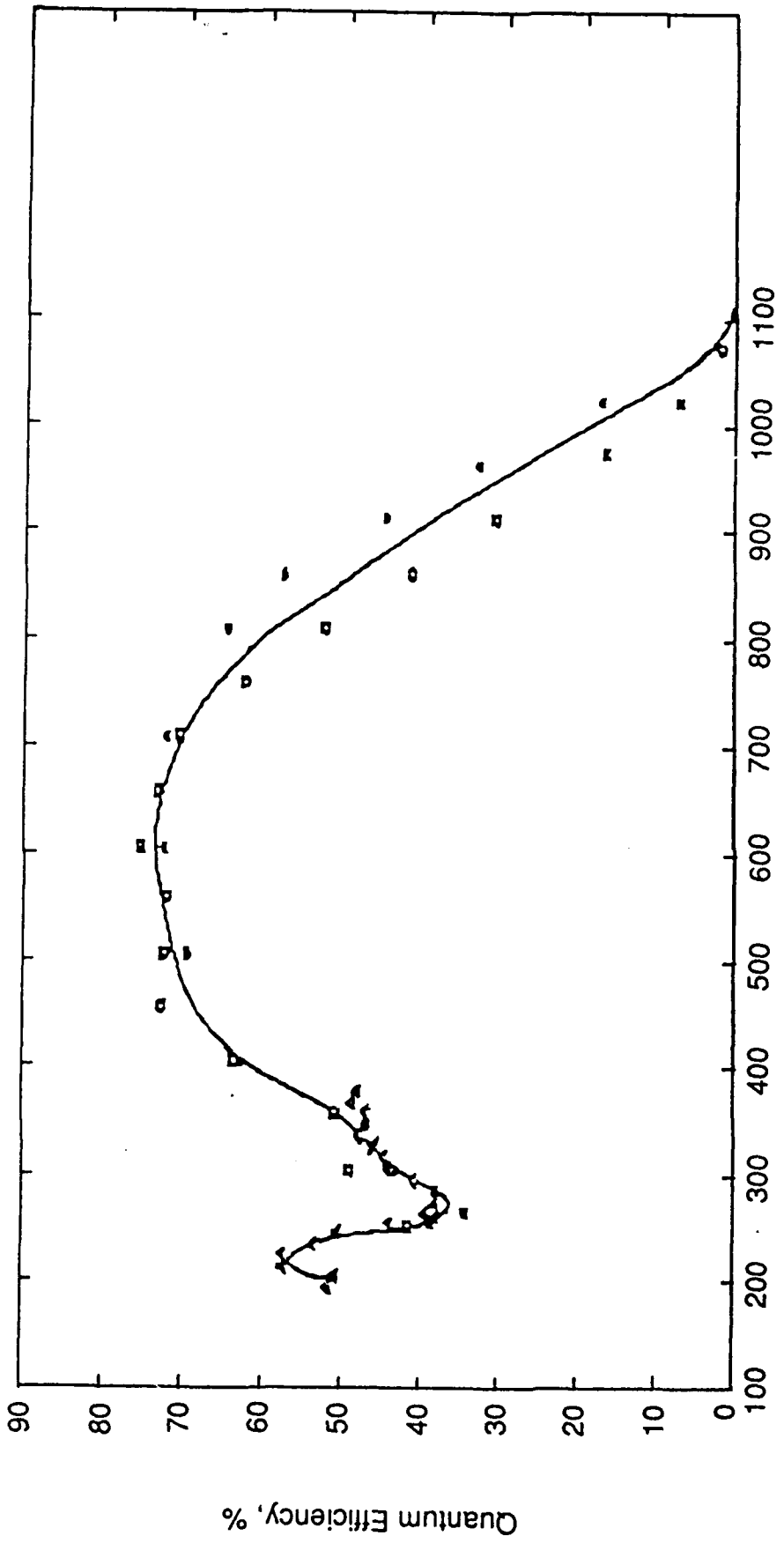

Figure 8. Response Curve for the OMA Detector.

The focused beam then encountered the second lens place on the opposite side of the burner. Ideally, this second lens should be placed such that its focal point is the same as that of the first lens. In this configuration, the focused laser beam is be collimated by the second lens. This collimated beam is then reflected by the second mirror so that the laser beam retraces its path to the laser cavity. This design not only allows double passing of the laser beam through the sample without loss of spatial resolution but also, if aligned properly, generates an exterior laser cavity.

Generation of an exterior cavity increases the laser intensity striking the sample, and, therefore, increases the Raman signal. To obtain the maximum exterior laser cavity effect, one must position the second mirror slightly farther away from the burner than its focal point. When the mirror is moved back, the returning laser beam is focused in much the same way as an output coupling mirror on the laser does in the cavity.

Evidence of this exterior cavity can be seen in Figure 9, which shows the intensity of the oxygen vibrational spectrum both with and without the multipass mirror lens system. In this figure, the lower intensity spectrum was obtained with the back mirror blocked; the higher intensity spectrum was obtained with the back mirror installed. As can be seen, the intensity of the oxygen spectrum is greater than twice the intensity that would be expected for double passing the beam through the system. This increase can be attributed to the generation of the exterior cavity. The actual increase is about four times the single-pass intensity.

The coupling of the Raman signal generated by the laser beam passing through the flame to the monochromator slit requires two high-reflection, first-surface mirrors: a 7.5-centimeter quartz lens and a removable 350-nanometer high-pass filter. The two mirrors were used to translate the horizontal path of the laser beam as it passed through the flame to the vertical direction of the monochromator slit (Figure 10). This configuration allowed for maximum filling of the monochromator slit.

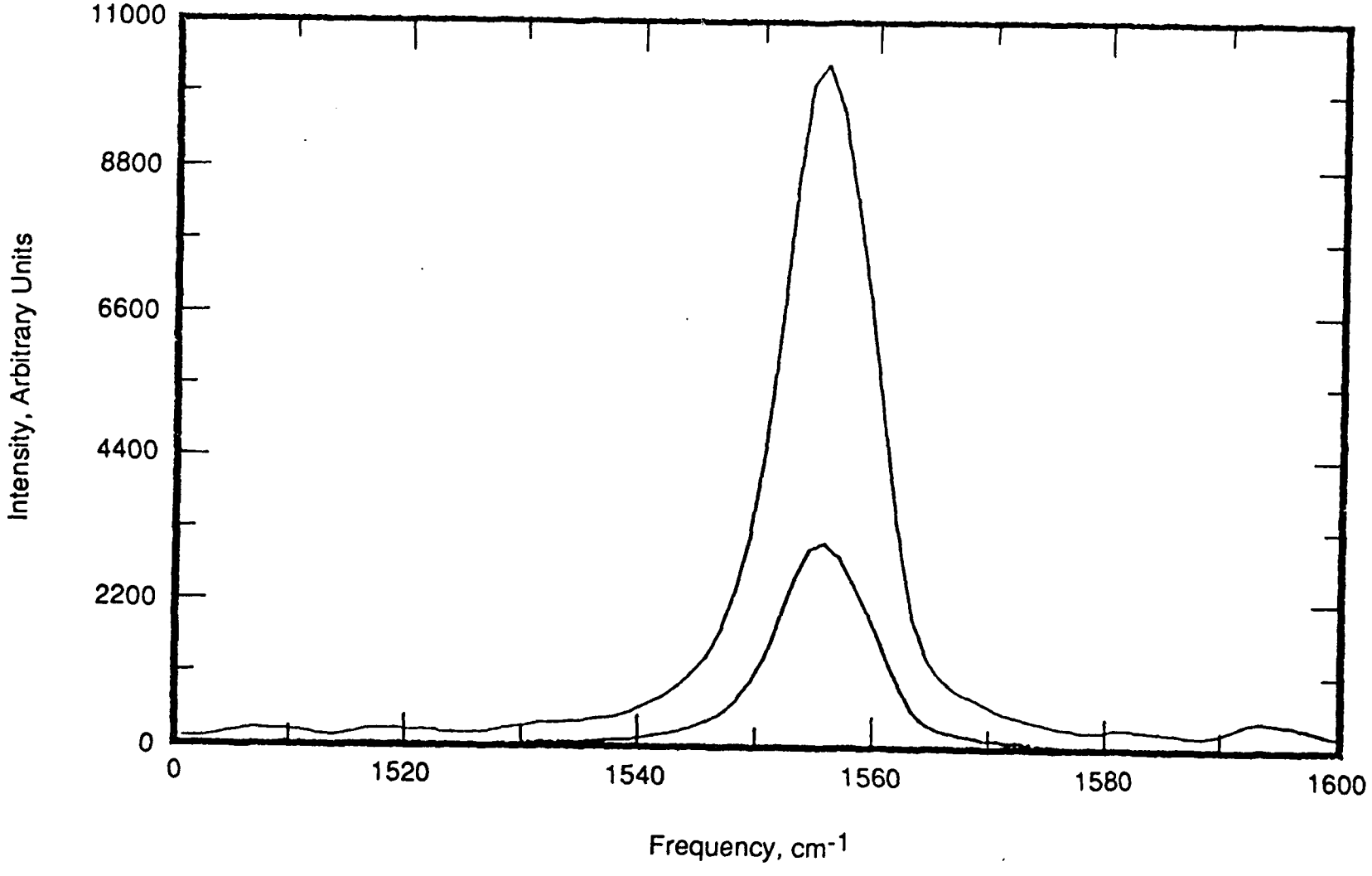

Figure 9. Increase in Signal with Exterior Laser Cavity (Raman Spectrum of Oxygen in Air).

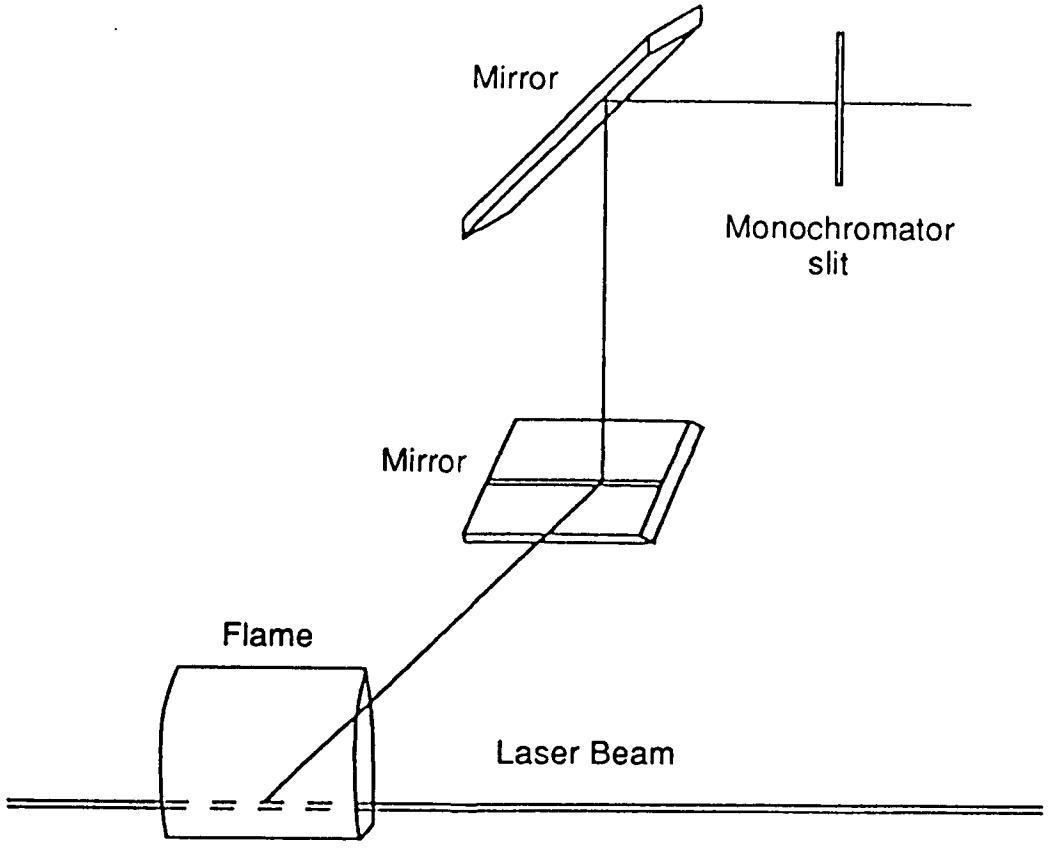

Figure 10. Optics Used to Translate the Horizontal Image to the Vertical Axis.

The 5.1-centimeter diameter, 7.5-centimeter focal length lens was set approximately 16.4 centimeters from the monochromator slit and 13.8 centimeters from the point where the laser beam passes through the flame. This configuration produces a sample to monochromator magnification of 1:1.2 and an f-number of approximately 3.2 for the lens system. With a monochromator f-number of 6.8, overfilling of the monochromators optics by the f(3.2) lens system was expected; however, due to the high stray light rejection of the triple monochromator, this overfilling was not of concern. Furthermore, by overfilling the optics, one is assured that complete filling of the monochromator optics and, therefore, maximum spectral intensities are obtained.

A 350-nanometer high-pass filter was placed in the optical path to block the hydroxyl (OH) emission spectrum, which could be seen in the 600 to 700-nanometer spectral range. The shift in the OH spectrum from its normal 300 to 350-nanometer spectral region to the higher 600 to 700-nanometer spectral region can be attributed to the passage of the second-order spectrum of the gratings. Since the gratings in this monochromator are designed to run in first order, the higher order spectra can normally be ignored unless the intensity of the signal is very high. In this case, the OH emission was so great that even the third-order spectrum could be seen in the region of 900 to 1050 nanometers. An advantage to using the higher orders of a grating is that one obtains an increase in the resolution over the lower orders. This effect was actually used when calculating the temperature profiles of the hydrogen-oxygen flame using the rotational-vibrational spectrum of the OH electronic transition. The 350-nanometer, high-pass filter was used to keep the OH emission from entering the monochromator where it would interfere with the Raman spectra and reduce the signal-to-noise level.

5. Burner

A laminar flow premixed hydrogen-oxygen slot burner was designed and constructed for this work. The design allows operation over a wide

variety of hydrogen-oxygen mixtures without flashback. One of the key design criteria was ease of machining, a feature that has resulted in considerable flexibility in the dimensions of the slots and the positioning of the sheath slots relative to the flame slot. The flame produced shows high stability and distinct regions, which makes it ideal for fundamental combustion diagnostic studies. Appendix A contains a manuscript of a submitted paper describing the burner. A discussion of the burner design is presented below.

a. Background

Most combustion processes are the result of diffusion flames. The many examples of diffusion flames include processes as varied as a campfire or a welding torch. An important advantage of diffusion burners is that flashback cannot occur. Thus, diffusion burner designs are simple, and no problems are associated with the use of high burning velocity fuel-oxidant mixtures. The major drawback to diffusion flames is that they are both audibly and optically noisy. This problem has been somewhat alleviated by burner designs in which the reactants are combined in a laminar mixing zone (Reference 30). This design is certainly an improvement in terms of flame noise and offers no possibility of flashback.

Premixed laminar flow flames have been widely used in spectroscopic studies over the last decade. When compared to diffusion flames they demonstrate lower flame flicker, reduced rise velocities, increased dimensional stability, and improved homogeneity. They have become particularly popular for flame atomic absorption studies, for which a variety of manufacturers supply premix laminar flow burners. The great popularity is, in part, due to the properties of the nitrous oxide-acetylene flame, which gives an excellent flame cell. Nitrous oxide-fuel mixtures have relatively low burning velocities and, thus, can be used in premix burners with a reasonable degree of safety.

When oxygen is used as the oxidizer, much higher burning velocities are encountered than when nitrous oxide is used. This is particularly the case when hydrogen is used as the fuel. Thus, relatively few reports of flame studies have involved a premixed laminar flow hydrogen-oxygen flame, in spite of the advantages of a hydrogen-oxygen flame. These advantages include a relatively high temperature, a simple flame composition, and a relatively low background, all of which can be important in many situations. The low background and simple flame composition are particularly important when performing combustion diagnostics.

Denton and coworkers have studied the burning parameters of hydrogen-oxygen flames (Reference 31) and have pointed out the usefulness of a premixed hydrogen-oxygen flame in flame emission studies (Reference 32). The burner used in those studies employs a head containing a pattern of very small diameter holes, through which the premixed hydrogen-oxygen mixture flows. The holes have a small diameter to achieve laminar flow. Though the work cited provides the data needed to design hydrogen-oxygen burners, the design is difficult to machine due to the need for deep, very narrow holes.

Another design is the slot burner. Mossholder, Fassel, and Kniseley (Reference 33) have evaluated a high-flow, premixed hydrogen-oxygen flame supported on a slot burner originally designed by Fiorino, Kniseley, and Fassel (Reference 34). The results obtained with their design are not encouraging, due, in part, to the slot sides not being parallel. Thus, laminar flow was most likely not achieved.

Review of past efforts permitted the development of a premixed laminar flow hydrogen-oxygen burner that is safe to operate and easily constructed. The burner incorporates argon sheathing, an important feature for a burner used for combustion diagnostics.

b. Burner Design

The theoretical equations required to predict the burner dimensions needed to produce a laminar flame are

$$Re = VD/a \tag{23}$$

and

$$Lm = 0.05(Re)(D) \tag{24}$$

where Re is the Reynolds number, V is the average gas velocity, a is the viscosity of the gas divided by its density, D is the diameter of the hole though which the gas flows, and Lm is the depth required to establish the boundary layers needed for laminar flow for this hole (References 7, 35). In the case of a slot, the equation for D is

$$D = (2)(\ell)(b)/(\ell+b) \tag{25}$$

where ℓ is the length of the slot and b is its width. When ℓ is much greater than b, D can be approximated to be equal to 2b (Reference 35). A Reynolds number less than 2300 indicates laminar flow. Since the depth of the slot is proportional to the square of its width, decreasing the slot width reduces the depth required to establish laminar flow. A width of 400 micrometers was chosen. This width requires a slot depth of approximately 3 centimeters. The calculated Reynolds number of 900 for an hydrogen-oxygen gas mixture flowing at an average velocity of 4000 centimeters/second is then within the laminar region. These same considerations were also given to the dimensions of the sheathing slots.

Specialized machining is necessary to produce a burner satisfying the above constraints. Previous laminar hydrogen-oxygen burners have generally used a capillary design in which the holes were approximately 500 micrometers in diameter (Reference 31). The actual hole depth is not

given in Reference 31; however, calculations indicate that the depth of these holes was approximately 3 centimeters. Drilling a hole, 0.05 centimeters in diameter and 3 centimeters in depth, into stainless steel is very difficult. An alternative design employing a slot, rather than round holes, also presents extreme machining constraints. The design used here solves the problem of producing deep, narrow slots to allow for simple construction and flexible dimensions and to produce a stable and well-structured flame.

A diagram of the burner is shown in Figure 11. Appendix B contains outline drawings of the original engineering drawings. The burner has three sections: the top section consisting of four pieces (A, B, C, and D), the baseplate (E), and the bottom section, which serves as the gas mixing chamber (F). Parts A and D are 7.0 x 5.0 x 3.0 centimeter blocks with 0.04-centimeter indents machined into them. Part B is a 7.0 x 0.3 x 3.0 centimeter spacer with a 0.4-centimeter indent. The dimensions of part E are 7.0 x 5.0 x 1.0 centimeters. The slot in the center of the piece is 3.0 x 0.1 centimeters. Part F is a 5.0-centimeter piece of tubing having an outside diameter of 3.0 centimeters and an inside diameter of 2.0 centimeters. All parts of the burner are made of stainless steel.

The key to the design is the four top pieces. The problem of machining deep narrow slots is overcome by grinding an indent into three of the four pieces. The mating surfaces of the pieces are polished flat. When these pieces are pulled together, the indents form the slots necessary to achieve laminar flow. The indents in A and D form the argon-sheath slots. The argon is introduced into the sheath slots by means of two 0.125-inch holes drilled through each of parts A and D. The holes are positioned to match the bottom of the argon-sheath slots. A cavity and connections for water cooling have also been incorporated into these pieces. The water cooling cavities are formed by drilling a 0.250-inch hole through the part, parallel to the slots. The piece labeled B serves as a spacer, and C has the indent that forms the slot for the flame. Two alignment pins, purposely offset to each other, are used to provide an accurate and unique assembly of

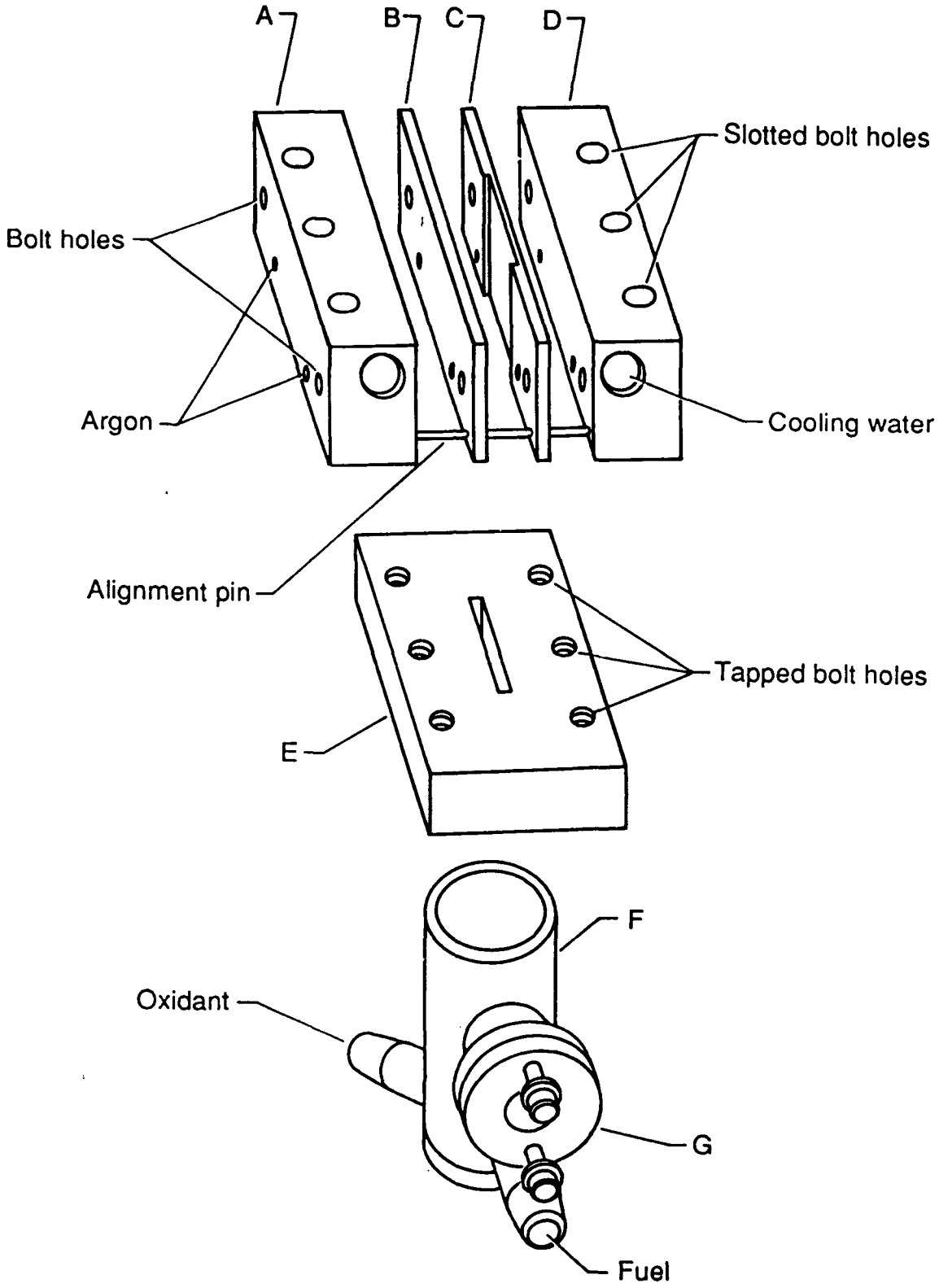

Figure 11. Burner Assembly.

the pieces (only one pin is shown in Figure 11). The entire group is connected by two bolts that pass horizontally through the pieces. Once the top section is assembled, it is bolted onto the baseplate (E).

The dimensions and spacing of the slots are flexible. The distance from the argon sheath to the flame is set by the width of pieces B and C. By making vertical slots for the bolts in pieces A and D, different dimensions can be used without remachining the entire burner. Extremely narrow slots are possible with this design.

The baseplate (E) was constructed in a manner similar to that used for the burner head. The plate was first cut in half, and an indent was ground into one of the two halves. The two halves were then welded back together to form a 0.10-millimeter slot in the center of the plate. This slot allows the gas mixture in the bottom section (F) to pass through only the middle flame slot of the burner head.

The bottom section (F) serves as the burner mount, as well as gas-mixing chamber. The top of this piece was welded to the bottom of the baseplate (E). Three connections, of which only two are visible in Figure 11, are located at the bottom for introducing gases into the mixing chamber.

The pressure relief valve (G) was constructed by welding a short section of tubing having an outside diameter of 2.0 centimeters and an inside diameter of 1.5 centimeters to a hole bored into the side of the mixing chamber. The cover piece is secured in a closed position by springs.

The burner slot used here is 0.040 centimeters wide, 2.0 centimeters long, and 3.0 centimeters deep. The argon sheath slots are 0.040 centimeters wide, 3.0 centimeters long, and 3.0 centimeters deep. These dimensions were chosen to ensure laminar flow under all flow conditions that might be encountered. Consideration was also given to the fact that the burner walls quench the flame reaction. This quenching makes very narrow slots, such as the burner slot, useful for conditions where the

flow rate through the slot might be lower than the absolute burning velocity of the fuel oxidant mixture (Reference 31). Quenching allows design of a burner that will work safely over a wider set of operating conditions than those that would be predicted from the burning velocity of the flame.

c. Burner Results and Discussion

A major drawback to the use of a premixed hydrogen-oxygen flame is the possibility of flashback. To minimize flashback, the gas flow through the burner slot must be higher than the burning velocity of the fuel-oxidant mixture, taking into account any wall quenching effects. The gas velocity through the slot must also be in a range that produces a stable, well-structured flame. The slot dimensions used in this design were chosen such that the flow rate of oxygen required for normal operation was 3 liters/minute. With this oxygen flow, the hydrogen flow required for normal operation was 3.5 to 9.5 liters/minute depending on the desired oxidizing or reducing nature of the flame. Conditions producing a flashback were determined by setting one of the flows (oxygen or hydrogen) and slowly decreasing the other until flashback occurred or a zero flow was obtained.

The data produced in these studies are plotted in Figure 12. The conditions that produce flashback are a function of both the total flow rate through the burner slot and the hydrogen to oxygen ratio. The conditions necessary to produce flashback also depend on the burner temperature (Reference 31). Since the burner is water cooled, it rapidly reaches an equilibrium and flashback conditions remain constant.

The data also show that the total flow rate required to produce flashback for any hydrogen-oxygen mixture is more than a factor of two below the normal operating conditions. Thus, the burner is normally operated without any significant possibility of flashback. Indeed, no unintentional flashbacks have occurred during burner operation. Further reduction or complete elimination of flashback could be accomplished by using even narrower slots than the ones used here.

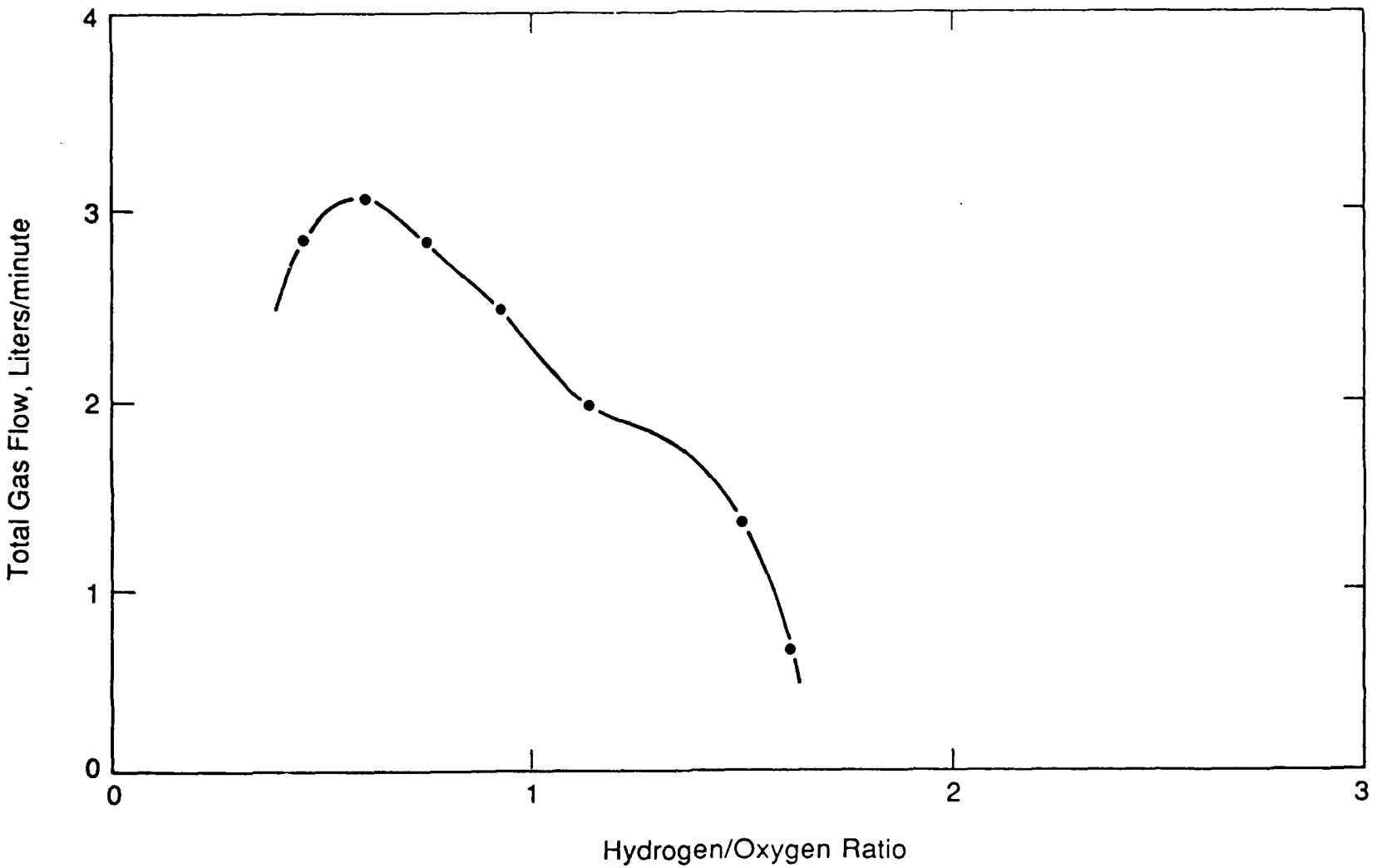

Figure 12. Total Gas Flow at Flashback as a Function of the Hydrogen to Oxygen Ratio.

Another goal of the burner design was to produce a stable flame with well-defined reaction zones. Such a flame has temperature zones that characterize the processes occurring at each region in the flame. The results of a temperature measurement as a function of height above the burner head are shown in Figure 13. The temperature was determined by measuring the relative intensities of OH vibrational-rotational bands and calculating the temperature according to the method of Zinman and Bogdan (Reference 36). When one views the flame operating under the conditions used here, the primary reaction zone begins approximately 1.5 millimeters above the burner head. The bright blue primary reaction zone is approximately 2 millimeters high. Above that is a very light blue mantle that extends up to 20 to 30 centimeters above the burner head. One would expect that the temperature of the flame gases would increase rapidly with height in the preheat zone, reach a maximum in the primary reaction zone, and taper off with height above the primary reaction zone. This is exactly the behavior seen in Figure 13. The precision and stability of the system are indicated by the data, where two separate temperature determinations were carried out at each height above the burner.

D. HALON 2402 PYROLYSIS

The initial investigation into the halon-inhibition mechanism involved pyrolysis of Halon 2402 in several environments. This was done in hopes of separating the complex problem of combustion into smaller, more easily understood parts. The actual chemical mechanisms, however, will not be evident in this type of experiment since only stable pyrolysis products are identified. The main purpose of this experiment was to lay the foundation for later flame analysis of halon inhibition. Since standard Raman spectra of Halon 2402 and its pyrolysis products are not available in the literature, this experiment permits the generation of a library of Raman spectra for later use. Furthermore, the experiment allowed development of the skills and knowledge in diagnostics of gaseous matter needed for later development of the flame Raman spectrometer. Halon 2402 was pyrolyzed in three environments: vacuum, flowing nitrogen, and flowing oxygen. The

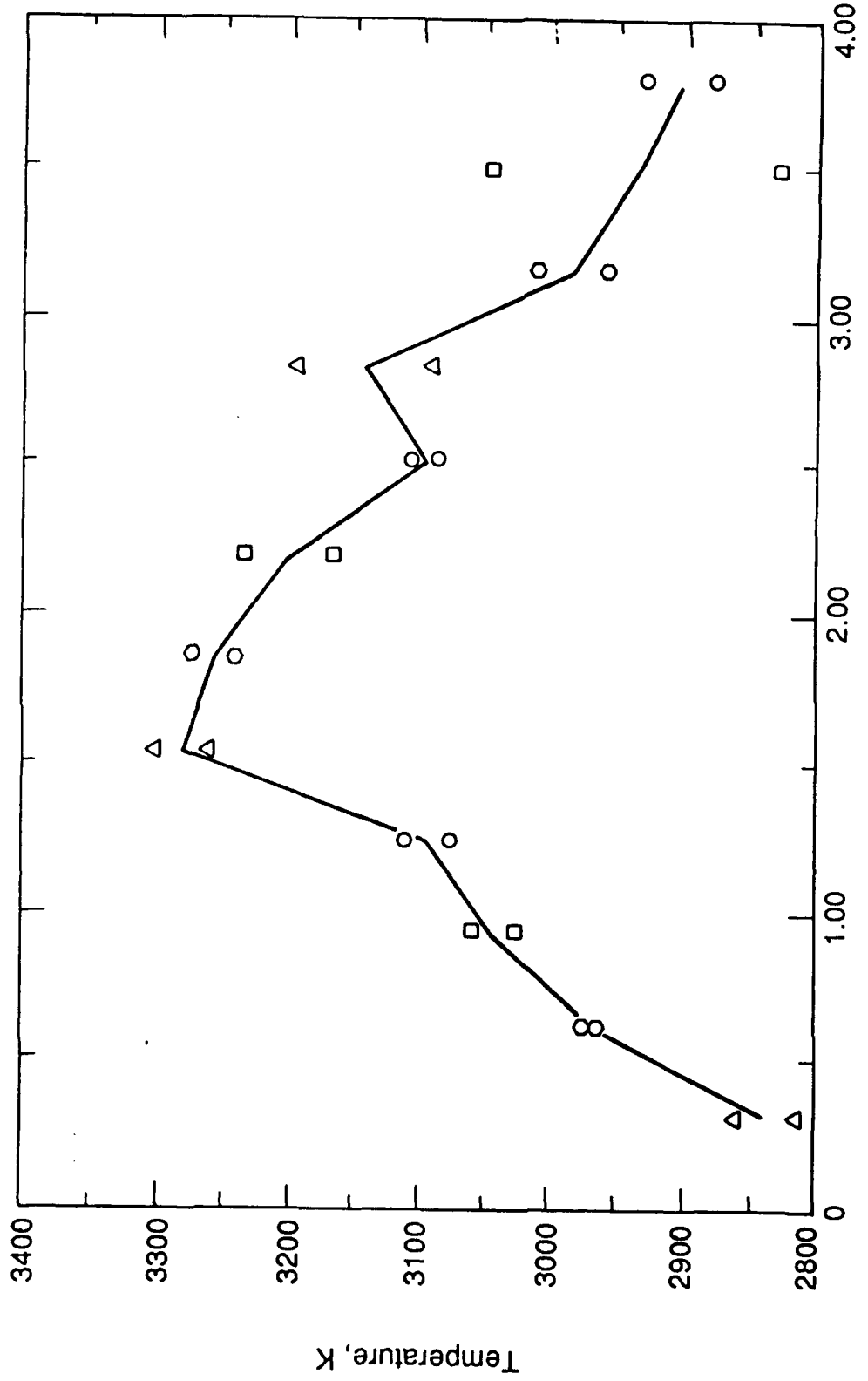

Figure 13. Flame Temperature as Determined from OH Rotational-Vibrational Spectra as a Function of Height above Burner.

results for these three experiments provided a wealth of experience and standard spectra for later use in the flame experiments. A description of the apparatus and procedures used in this experiment follows, as well as the final results of the halon pyrolysis in the three environments. A preliminary paper on this series of experiments has been presented at a meeting of the American Chemical Society (Appendix C).

1. Apparatus

A special quartz pyrolysis tube was constructed for pyrolysis of Halon 2402 in controlled environments (Figure 14). This tube was constructed of three parts: two sealable U-Tubes and one straight quartz tube, each having an outside diameter of 1 inch and a length of 1.5 feet. The U-Tubes had stopcocks placed on either side of the U-shaped region to permit isolation or opening of the tubes. One end of each U-Tube terminated with a female ball joint connector; the other end terminated with a standard 1/4-inch tubing connector. This configuration allowed each U-Tube to be connected to the quartz tube through the male ball joints. When assembled, these three parts created an isolatable system that could be placed inside a tube furnace with the straight quartz tube extending out of both sides of the furnace. The inside environment of the pyrolysis tube system could be controlled by connecting the outer ends of each U-Tube to the conditions desired.

2. Vacuum Pyrolysis Procedure

In the vacuum pyrolysis experiments, a vacuum line was attached to both ends of the tube system, and the quartz tube was placed in the tube furnace. The system was evacuated while heating the quartz tube to 800 ^{o}C. After approximately 30 minutes, stopcock B was closed. The vacuum line on U-Tube 1 was then removed and brought to atmospheric pressure. Halon 2402 was injected into U-Tube 1 through stopcock A, and the vacuum line was reattached. After several seconds of evacuation to remove air, liquid nitrogen was applied to the exterior of U-Tube 1 to freeze the Halon 2402.

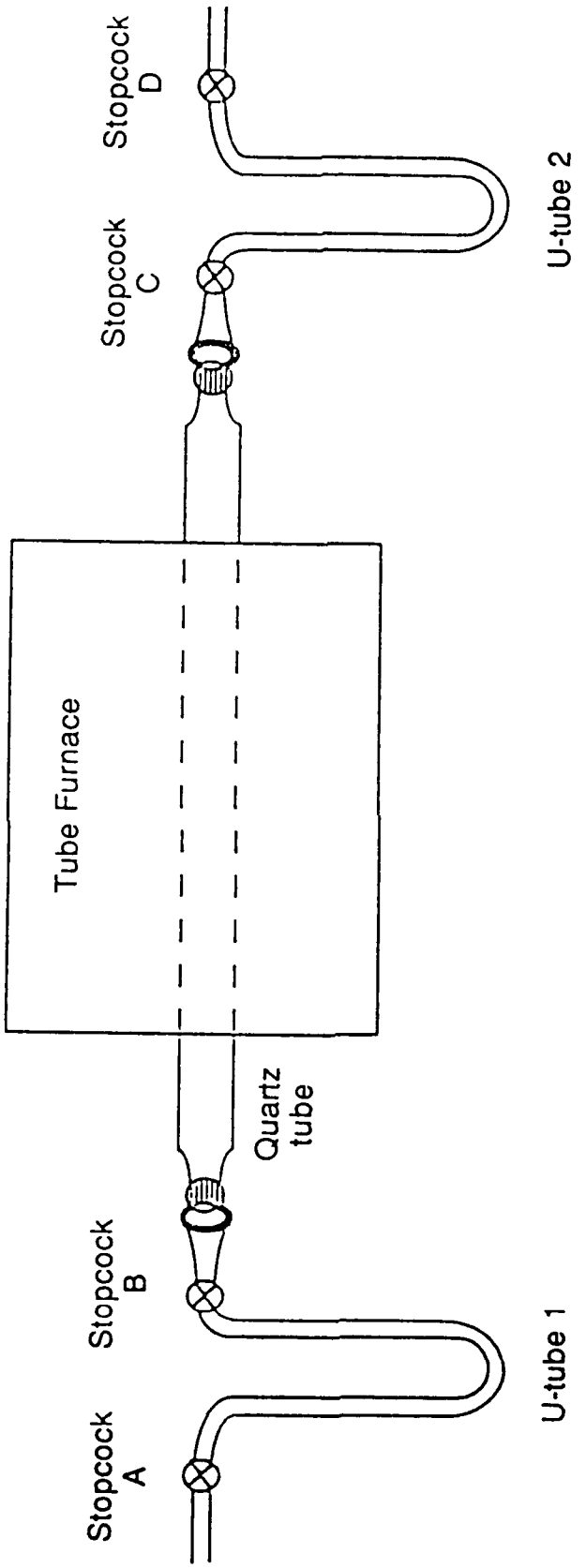

Figure 14. Diagram of Pyrolysis Apparatus.

Liquid nitrogen was also applied to U-Tube 2 to prepare it to serve as a nitrogen trap. Once the halon was frozen, U-Tube 1 was allowed to warm. Stopcock B, leading to the heated quartz tube, was opened, allowing the gaseous halon to pass through the heated quartz tube to U-Tube 2, where the halon and pyrolysis products were trapped. Finally, stopcock A was closed to isolate the vacuum line from U-Tube 1. These last two steps increased the rate of halon transfer between U-Tubes 1 and 2.

Once all the halon and its pyrolysis products had been trapped in U-Tube 2, the sequence was reversed. The vacuum line was reopened to U-Tube 1 and liquid nitrogen was applied to it, and both the liquid nitrogen and vacuum line were removed from U-Tube 2. This caused the halon and pyrolysis products to pass back through the hot quartz tube to U-Tube 1. By this technique, materials could be passed back and forth through the tube furnace. Multiple passes were required in this series of experiments due to the low pressure within the tube system. The low pressure reduced heat transfer to Halon 2402 and resulted in only limited pyrolysis in each pass.

3. Flowing-Gas Pyrolysis Procedure

In the flowing-gas pyrolysis work, a carrier gas was connected to U-Tube 1 through the connection at stopcock A. The gas was allowed to flow through the system for several minutes while the quartz tube was heated in the tube furnace to 800 ^{o}C. This was done to purge the system of all gases other than the carrier gas. Stopcocks A, B, and D were then closed, and the carrier gas line was removed from U-Tube 1. Halon 2402 was injected into U-Tube 1 through stopcock A, and the carrier gas line was reconnected. All stopcocks were opened, and the carrier gas was allowed to flow past the liquid halon through the quartz tube to U-Tube 2 and out of the system. After a few seconds, liquid nitrogen was applied to U-Tube 2 to trap the halon and its pyrolysis products as they moved through the system. Only one pass was performed under these conditions since reversal was difficult and since significant halon pyrolysis was achieved at these higher gas pressures with only one pass.

After the halon had been pyrolyzed by either the vacuum method or the flowing gas method, it was transferred to a vacuum line and stored. Vacuum distillation was used to fractionate the pyrolyzed halon sample. The fractions were analyzed by two methods. First, each fraction was captured in a sealable quartz tube, which was then placed directly into the Raman spectrometer for spectral data acquisition. Second, a Gas Chromatograph-Mass Spectrometer (GC-MS) spectrum was taken of each fraction to determine composition. GC-MS information was used to assign unknown bands in the Raman spectrum.

4. Vacuum Pyrolysis Results

In the initial experiments, Halon 2402 was pyrolyzed in a vacuum since this was expected to produce the least complicated results. The first attempt at the vacuum pyrolysis of the halon involved only a single pass through the pyrolysis tube. The resulting purple-red solution was analyzed by both GC-MS and Raman spectroscopy and was found to contain only Halon 2402 and bromine. Since the presence of bromine could only result from halon decomposition, other products must have been present but undetected. To increase the concentration of pyrolysis products, a multipass procedure was developed.

The multipass vacuum pyrolysis employed four transfers of Halon 1211 and decomposition products through the pyrolysis tube. This procedure produced a purple-red solution, which was darker than that from the single pass experiments. When this material was opened to the atmosphere, it boiled vigorously. The rapid boiling indicated that a portion of the material recovered was gaseous at room temperature. Vacuum distillation techniques were used to isolate the components of the pyrolysis products. In addition to Halon 2402 and free bromine, four products - Halon 1301 (CF_3Br), Halon 1202 (CF_2Br_2), bromine, and tetrafluoroethene (CF_2CF_2) - were isolated from the purple-red solution. Raman spectra of these substances in the gas phase at low pressures (approximately 50 Torr) are illustrated in Figures 15 through 18. A vapor-phase Raman spectrum of Halon 2402 is also

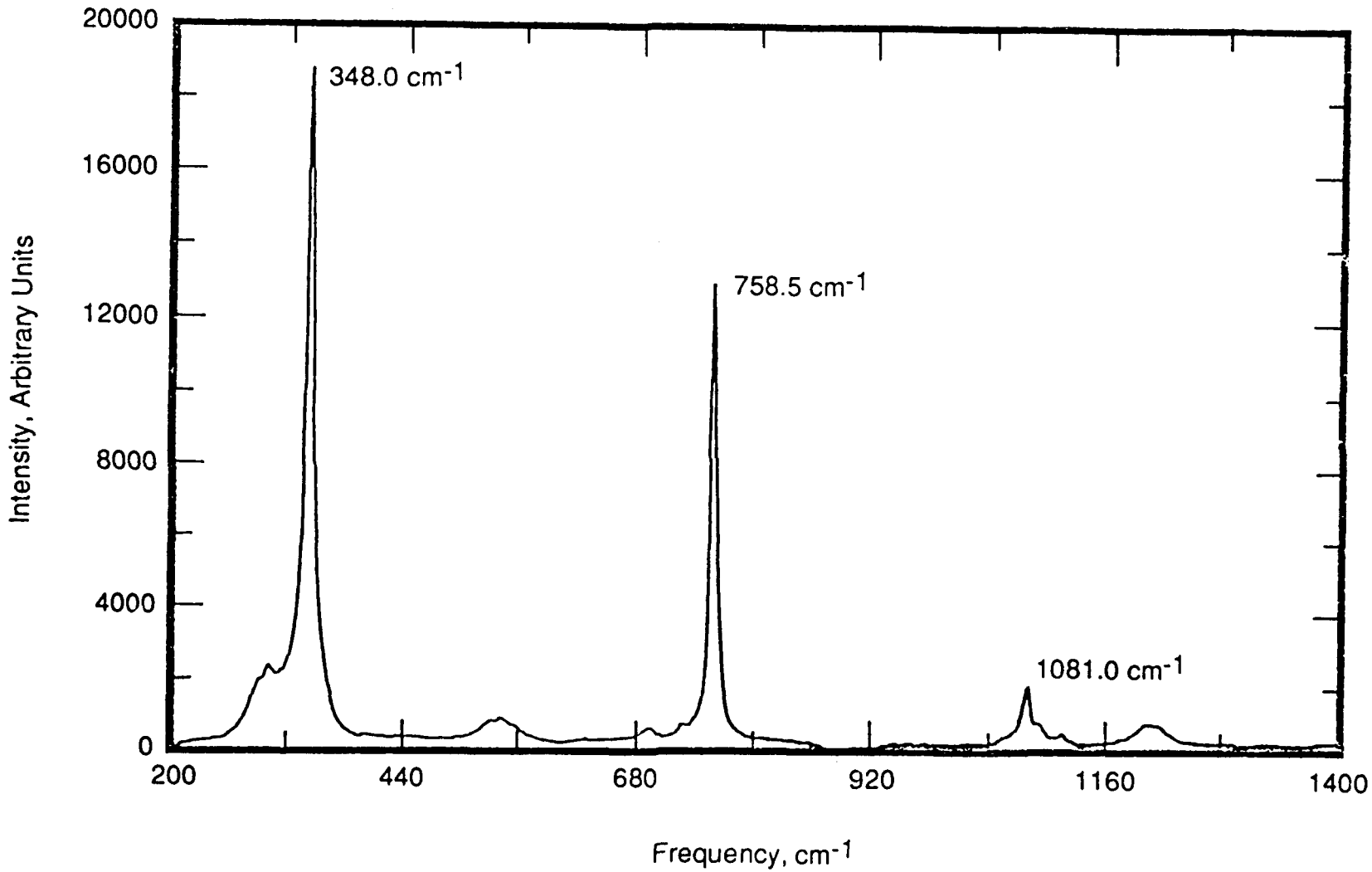

Figure 15. Raman Spectrum of Halon 1301 in the Gas Phase.

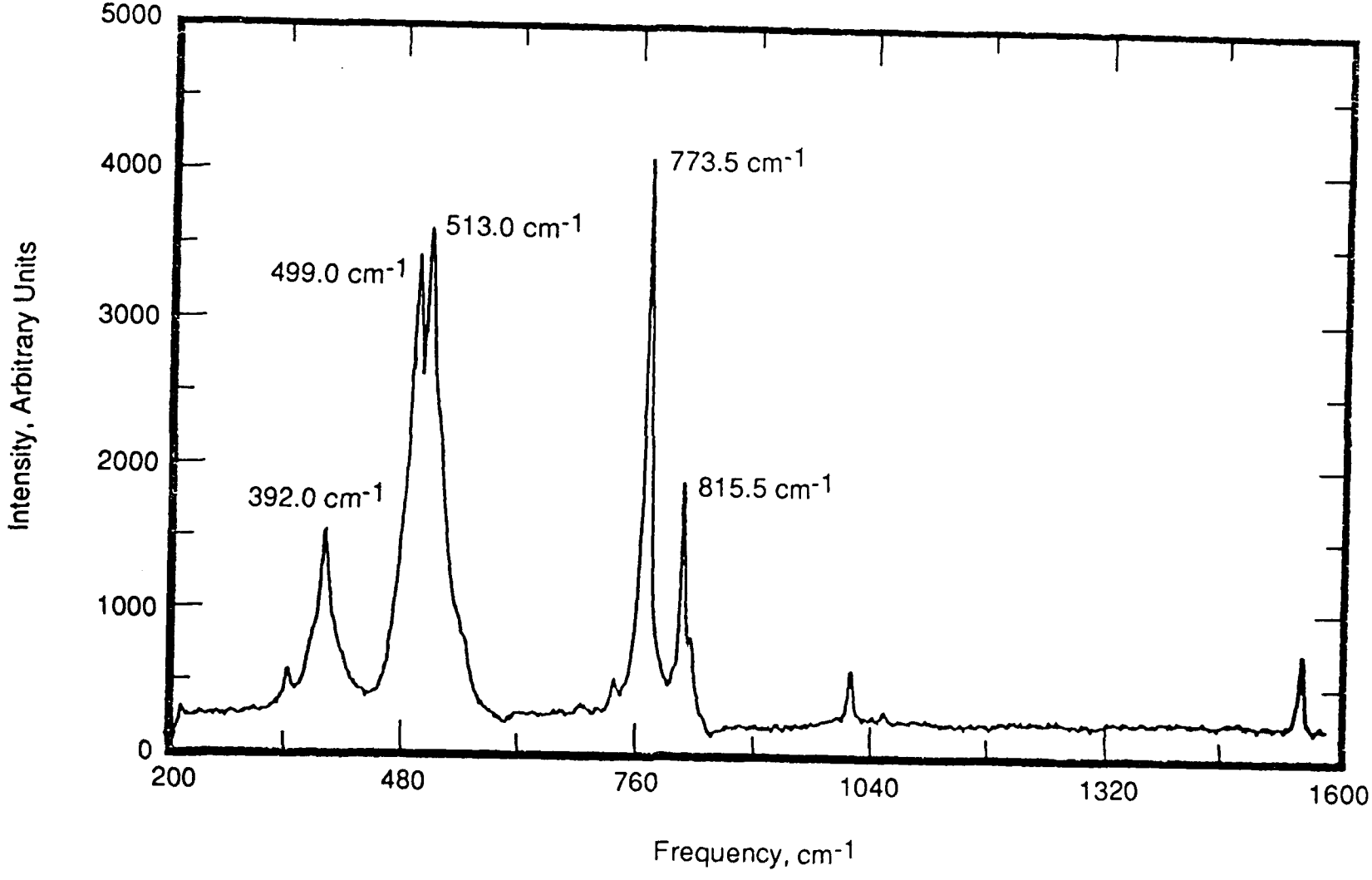

Figure 16. Raman Spectrum of Tetrafluoroethene, C_2F_4, in the Gas Phase.

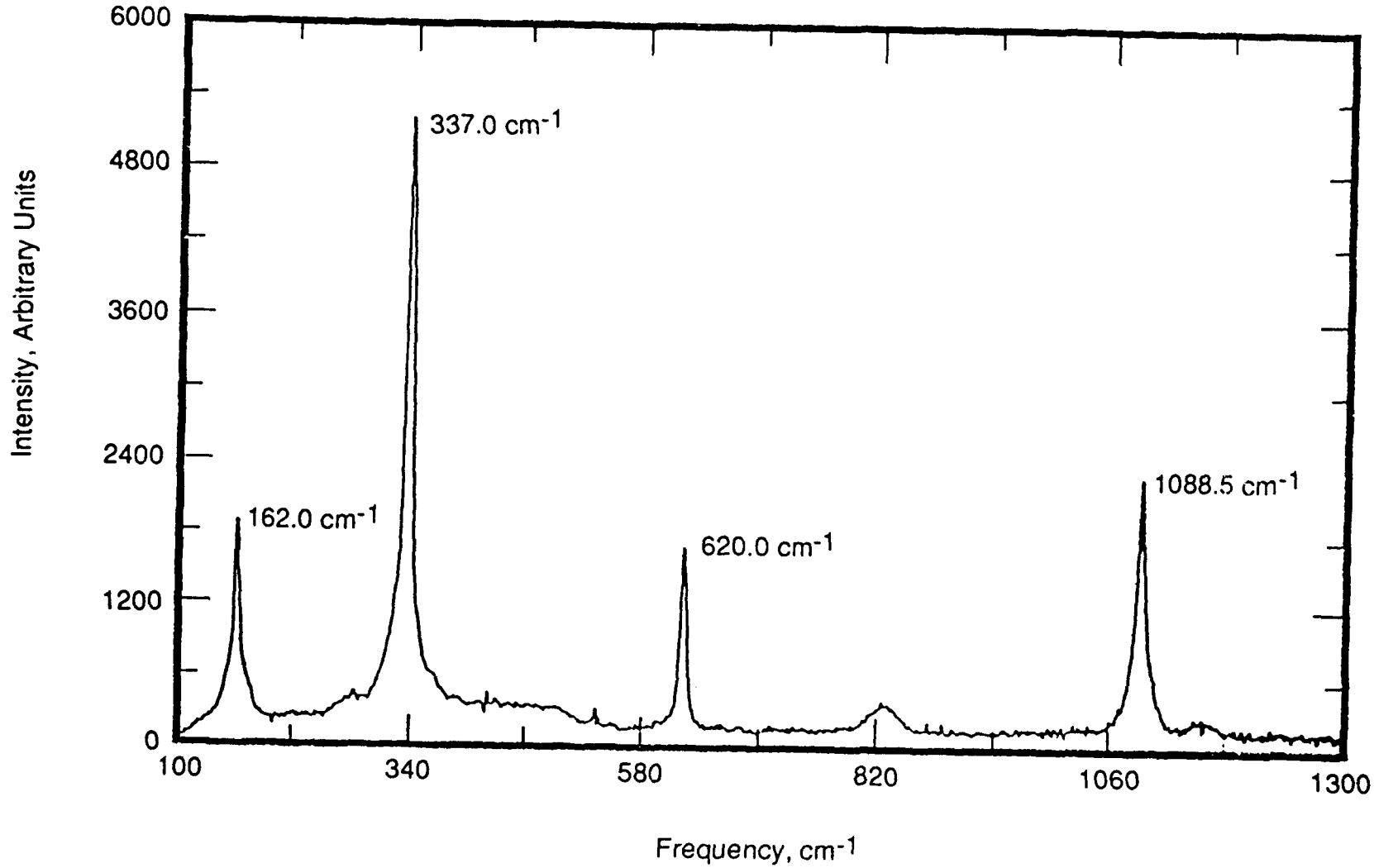

Figure 17. Raman Spectrum of Halon 1202 in the Gas Phase.

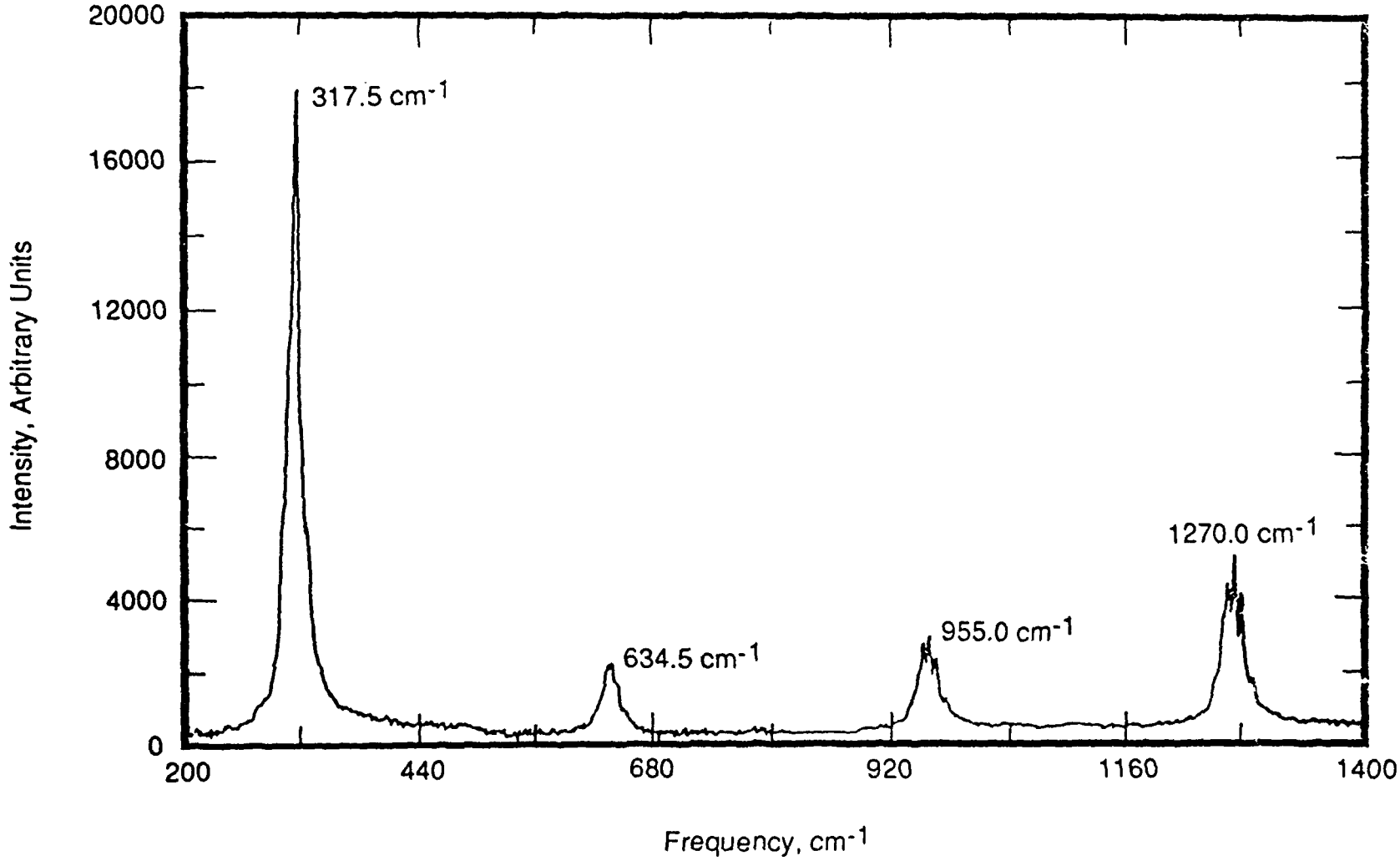

Figure 18. Raman Spectrum of Halon-Produced Bromine, Br_2, in the Gas Phase.

presented in Figure 19. A spectrum of the undistilled vacuum-pyrolyzed product of Halon 2402 is shown in Figure 20. All but one (circled in Figure 20) of the vibrational bands in the Raman spectrum of the undistilled product were assigned to one of the materials whose spectra are shown in Figures 15 through 18. This band was later assigned to a silicon compound.

Many more products than those found are expected for the product mixture. Apparently either the analytical techniques were insufficiently sensitive for detection of these compounds or spectral bands from other materials were masked by those from the primary products.

5. Nitrogen Pyrolysis Results

In the next phase of the pyrolysis experiments, flowing nitrogen was used as the carrier gas for the Halon 2402. Since nitrogen should not react with Halon 2402 at the temperature of 800 ^{o}C used for the experiment, the results from the flowing nitrogen pyrolysis were expected to mirror those of the vacuum pyrolysis.

The product mixture from the flowing nitrogen pyrolysis was a dark purple-red liquid while confined inside the sealed U-Tube. When the tube was open to the atmosphere, much of the material evaporated immediately. Analysis showed the major products of the nitrogen pyrolysis to be the same as those of the vacuum pyrolysis.

Although the percent of total product for each gas was not calculated, it was apparent that Halon 1301 and bromine were the most significant products of the nitrogen pyrolysis. Figure 21 shows the Raman spectrum of the undistilled nitrogen pyrolysis, indicating that Halon 2402 is no longer present, or is present at a much lower concentration than in the products of the vacuum experiment. This more effective destruction is due to the better heat transfer achieved. In this experiment, all but three of the Raman bands of the undistilled product

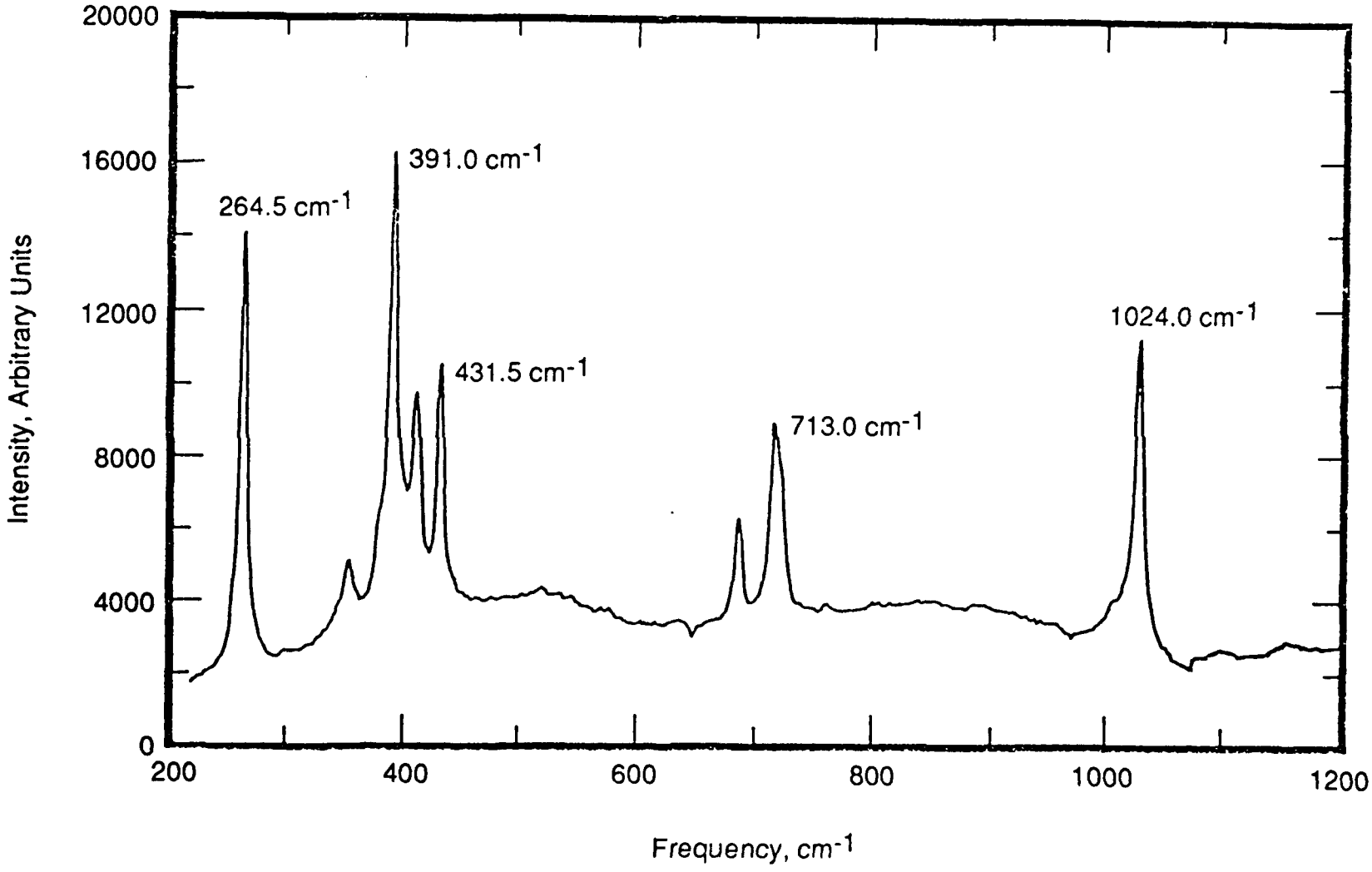

Figure 19. Raman Spectrum of Halon 2402 in the Gas Phase.

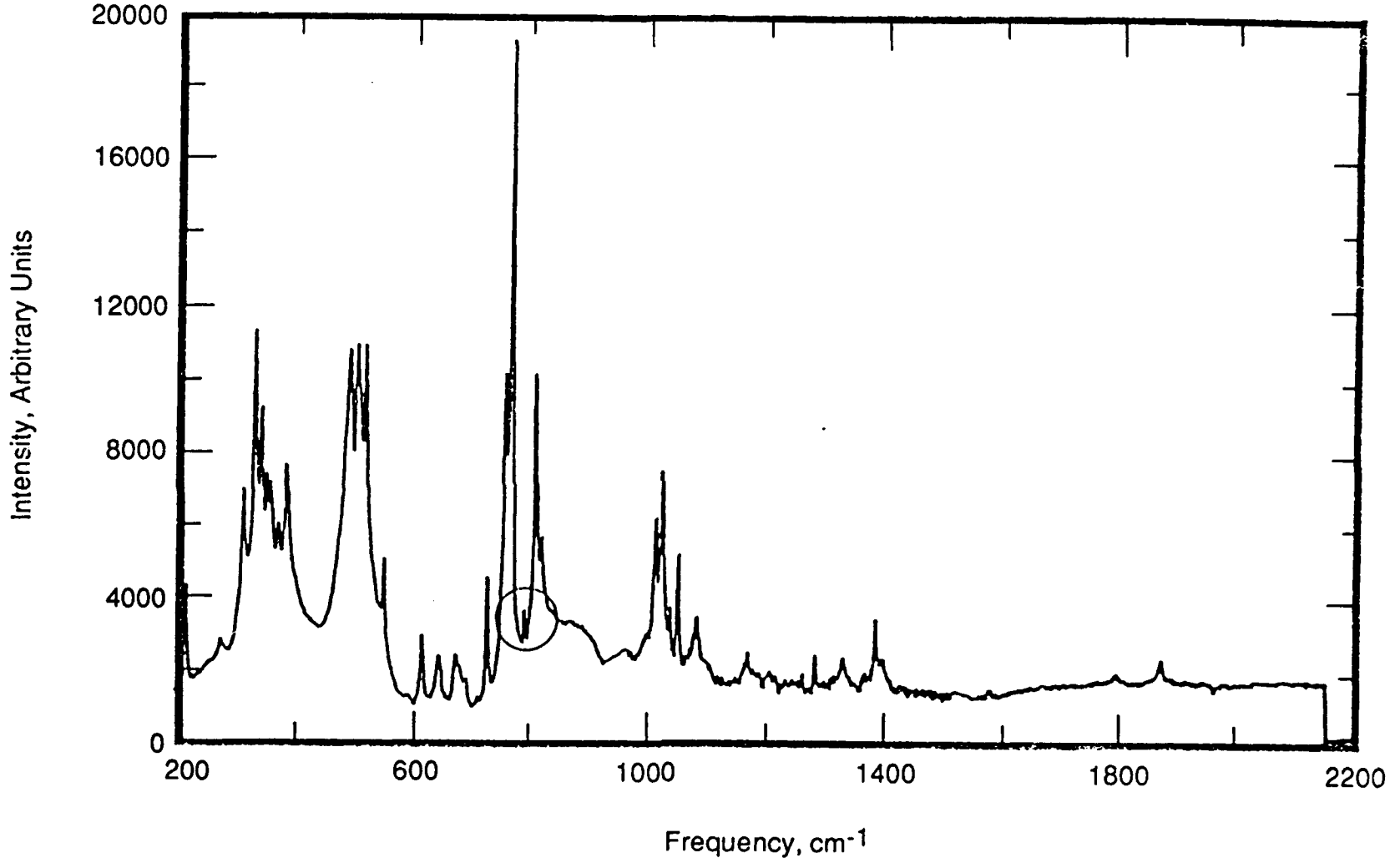

Figure 20. Raman Spectrum of Undistilled Vacuum Pyrolysis Product.

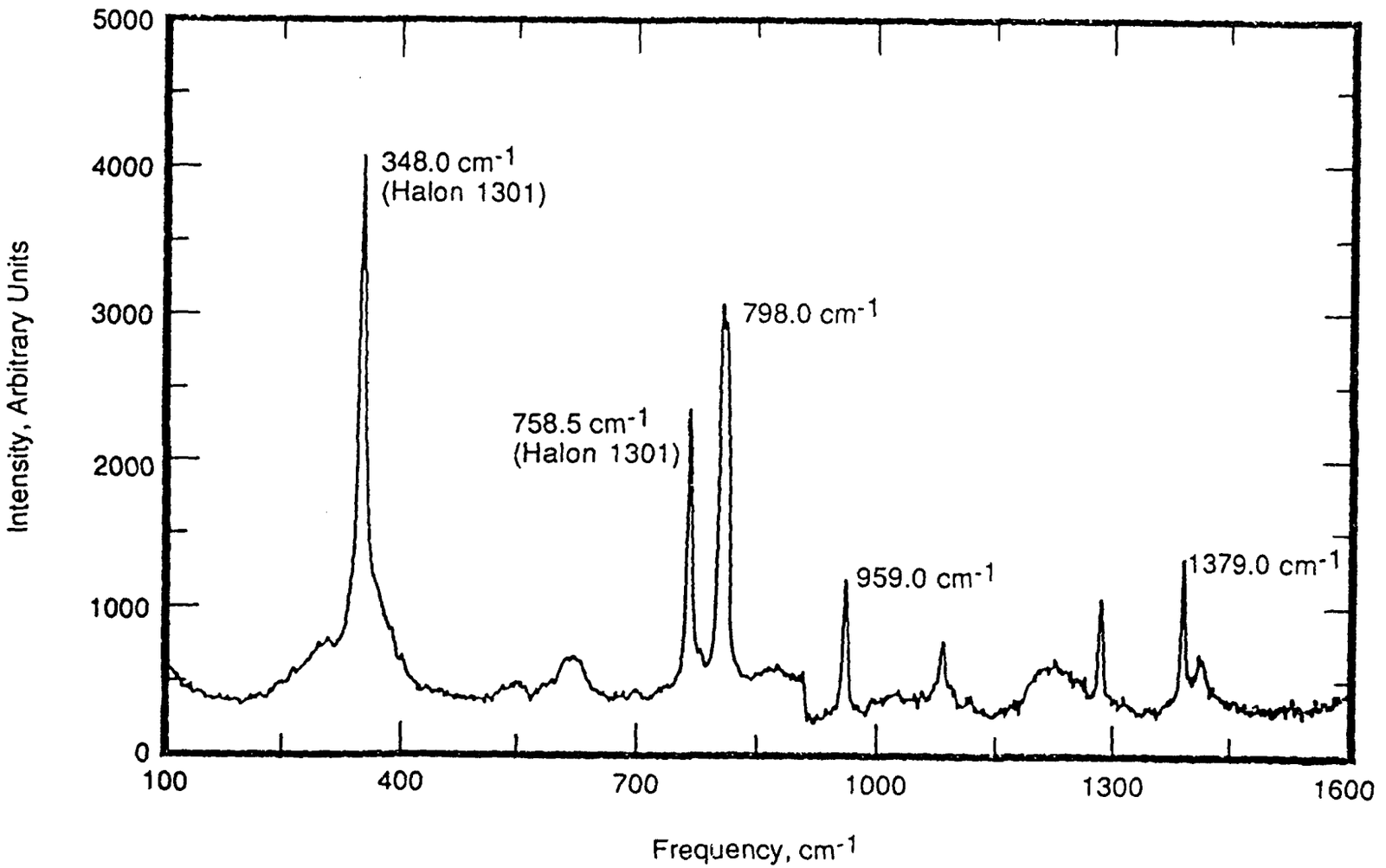

Figure 21. Raman Spectrum of Undistilled Nitrogen Pyrolysis Product.

mixture were assigned to one of the materials shown in Figures 15 through 18. The undistilled spectrum also indicates that the silicon material, represented by the three unassigned bands at 798.0, 959.0, and 1379 cm^{-1}, now make up a higher percentage of the products.

6. Oxygen Pyrolysis Results

In both the vacuum and the flowing nitrogen pyrolysis experiments, Raman bands occurred that could not be assigned to any known product or reactant. Despite the presence of these bands, new phases of the pyrolysis experiments were continued in order to maintain a schedule. It was hoped that later experiments would increase the yield of the unknown material so that GC-MS could be used for identification. Because the unknown bands are so prominent in products obtained in pyrolysis in the presence of flowing oxygen, they must be identified.

7. Silicon Interference

Some material in the Raman spectra of products from the three types of halon pyrolysis experiments remained unidentified. This fact did not become important until pyrolyses of halon in flowing oxygen were performed. This pyrolysis produced such high amounts of unknowns that identification was necessary before continuing further.

The high yield of unknown material is seen in the Raman spectrum of the undistilled oxygen pyrolysis products (Figure 22), where no bands could be identified. Information on the nature of the unknown material was not achieved until the oxygen pyrolysis product had been vacuum-distilled to produce a fraction containing only unknown materials. Figures 23 through 26 show the mass spectrum for this distillation fraction. The important features of this spectrum are the triplets that occur at 28, 29, and 30 amu (Figure 23), 85, 86, and 87 amu (Figure 24), 104, 105, and 106 amu (Figure 25), and 167, 168, and 169 amu (Figure 26). The mass and intensity ratios follow the natural abundance of the silicon isotopes (Reference 37).

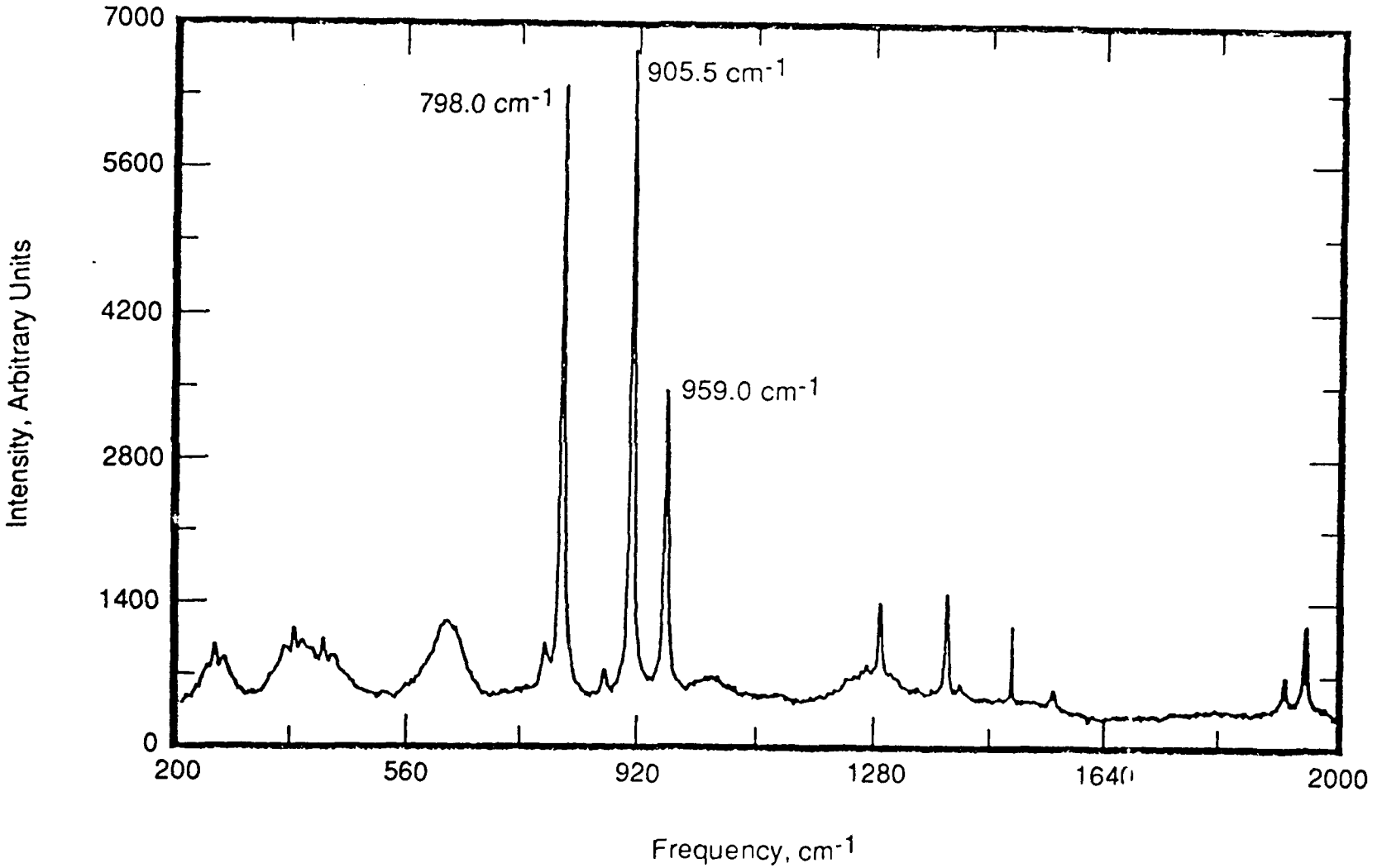

Figure 22. Raman Spectrum of Undistilled Oxygen Pyrolysis Product.

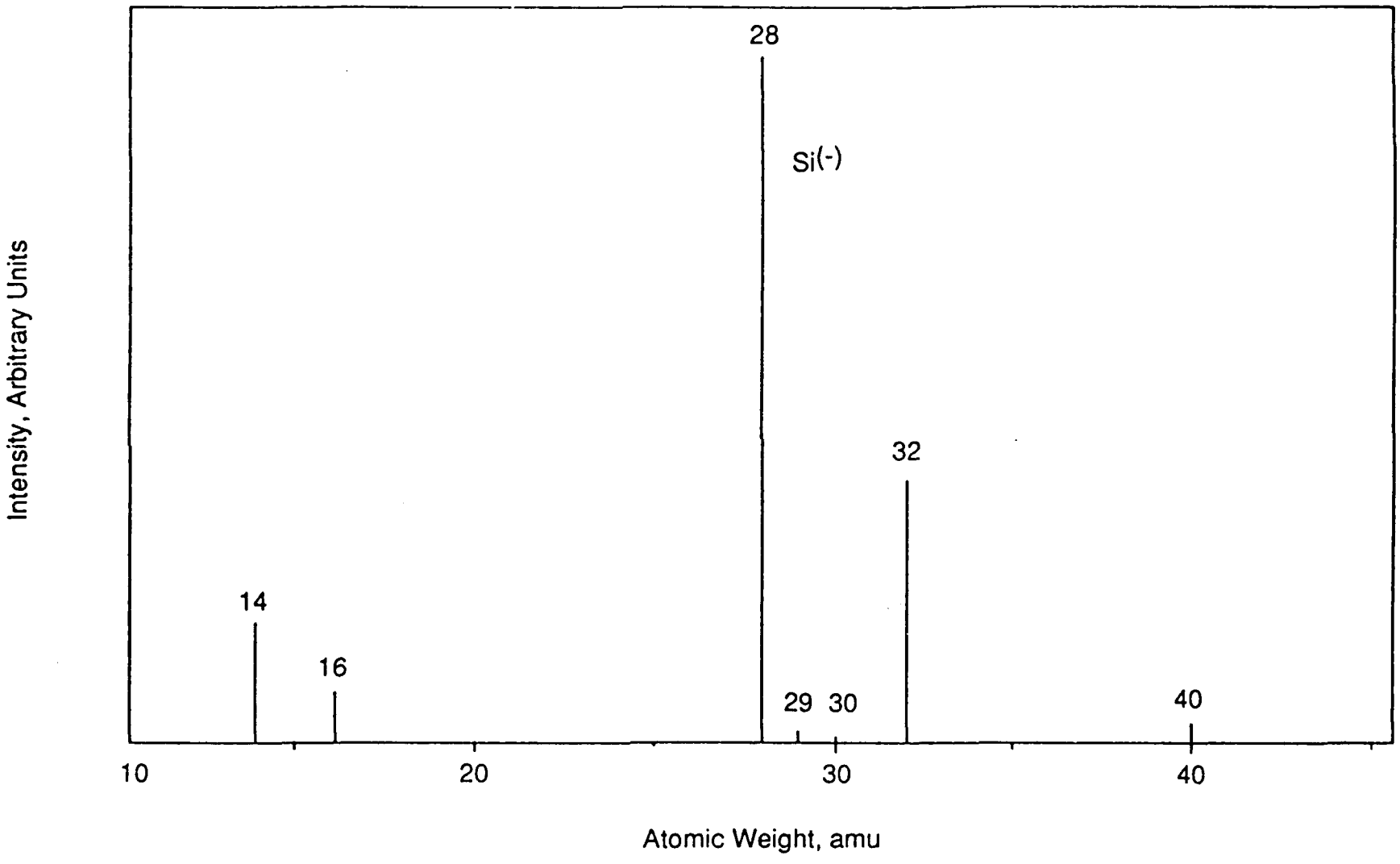

Figure 23. Mass Spectrum of Vacuum Distilled Oxygen Pyrolysis Product from 10 to 45 amu.

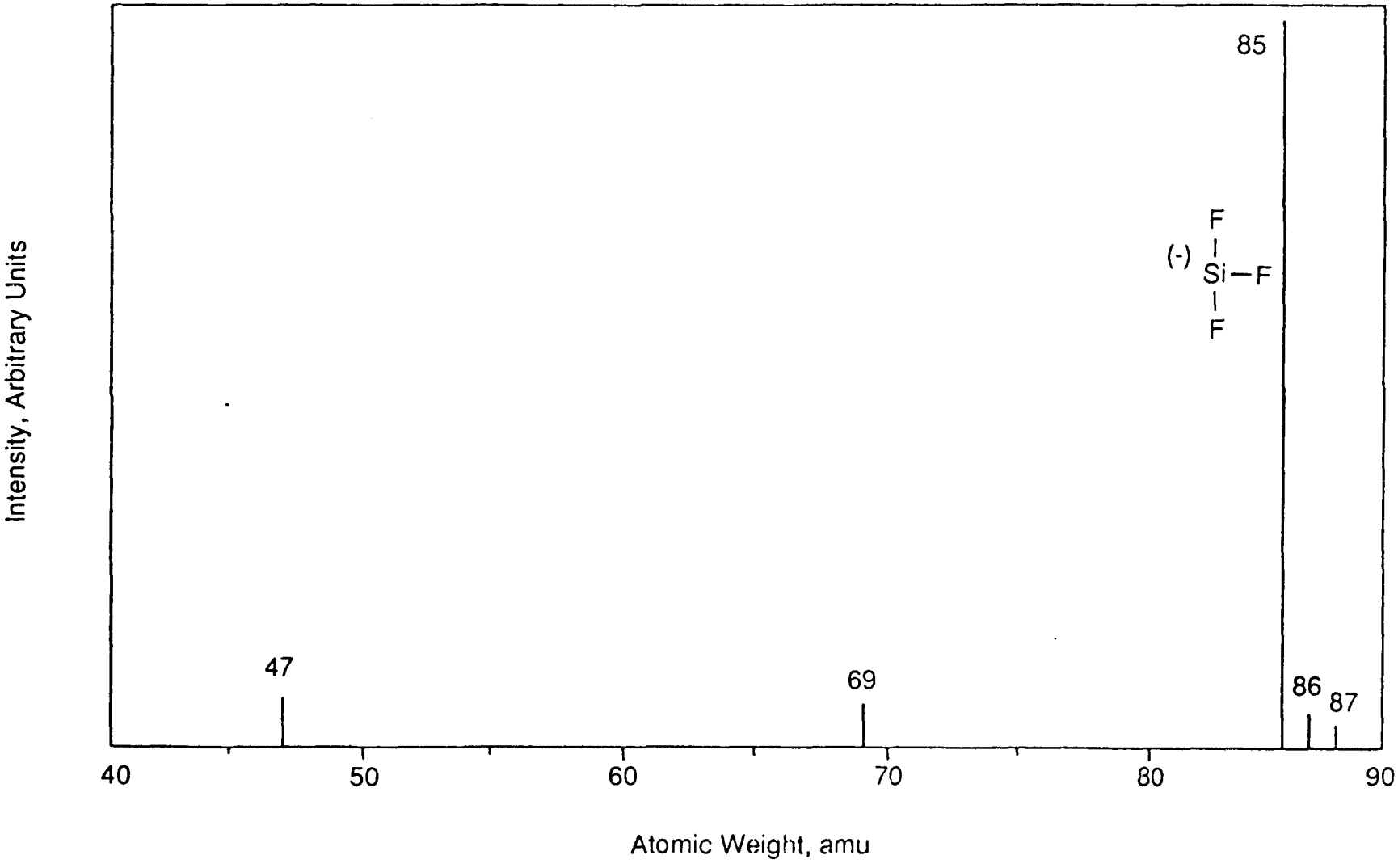

Figure 24. Mass Spectrum of Vacuum Distilled Oxygen Pyrolysis Product from 40 to 90 amu.

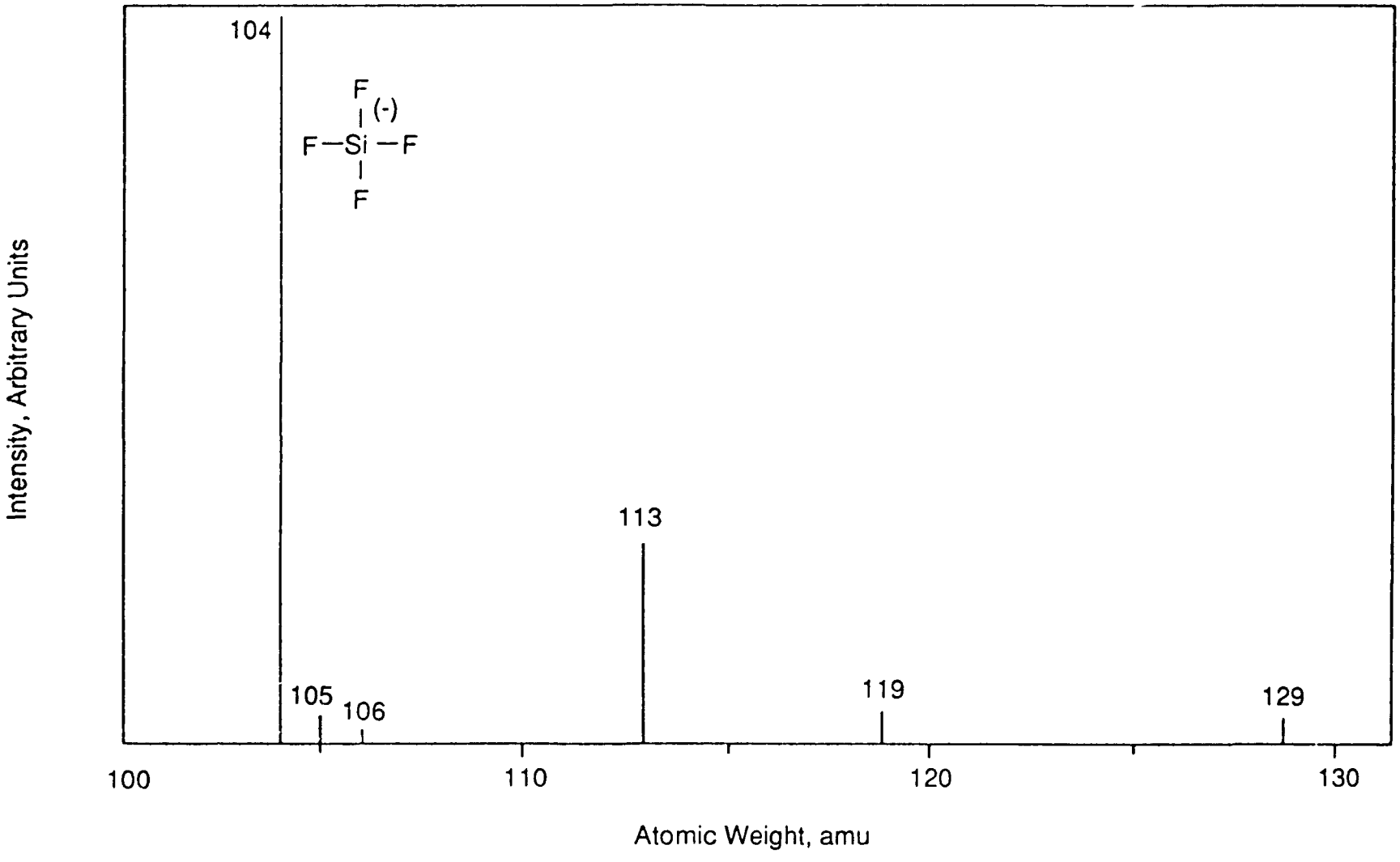

Figure 25. Mass Spectrum of Vacuum Distilled Oxygen Pyrolysis Product from 100 to 130 amu.

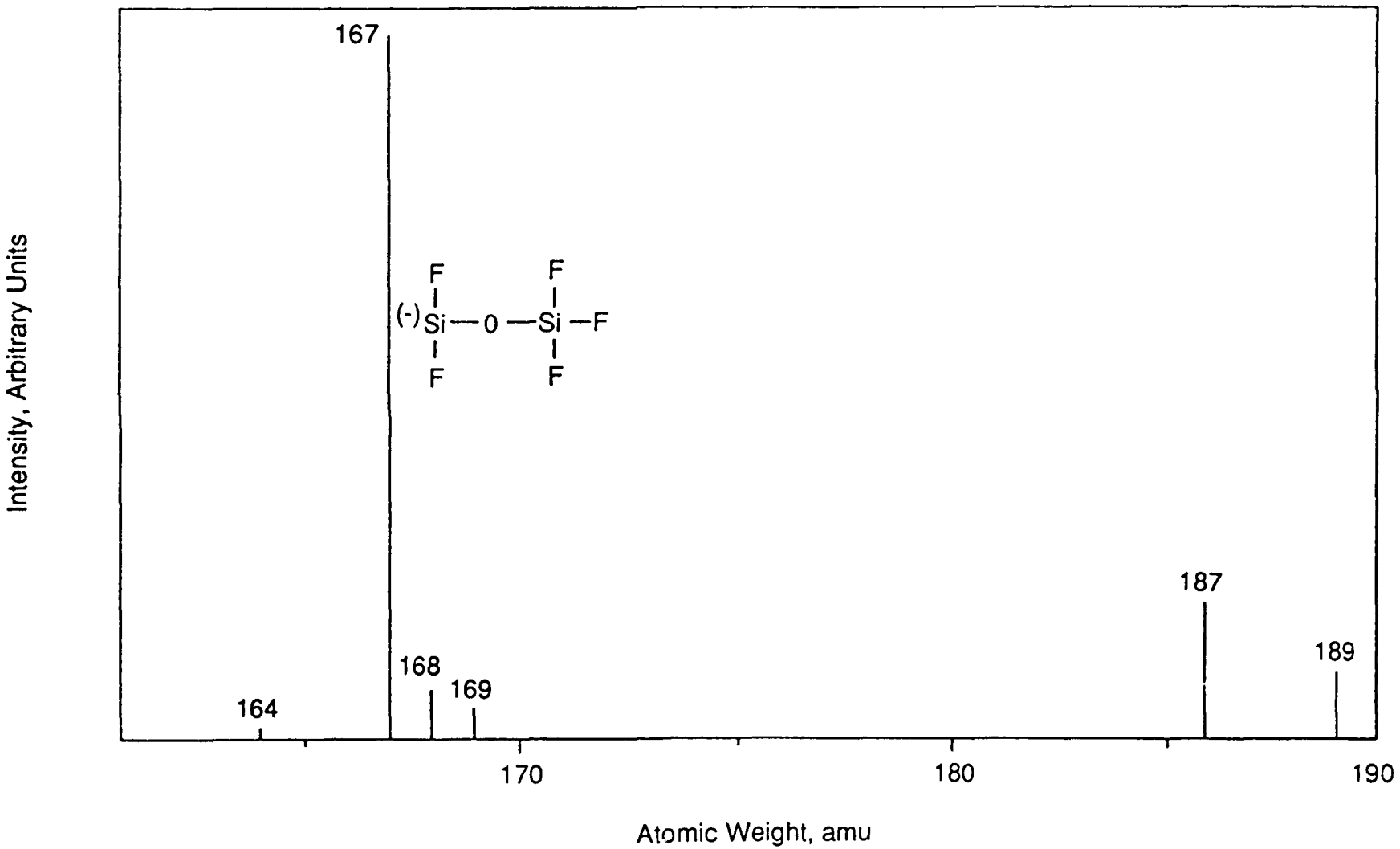

Figure 26. Mass Spectrum of Vacuum Distilled Oxygen Pyrolysis Product from 161 to 190 amu.

For example, the intensity ratio for the triplet starting at mass peak 85 is 93:5:3. The natural abundance is 92:5:3 for silicon isotopes with masses of 28, 29, and 30 amu. The higher mass triplet at 167, 168, and 169 amu has a ratio of 90:6:4. This ratio is similar to that expected for compounds that contain two silicon atoms. The actual ratio should be 85.3:8.6:6.0:0.4:0.1 for the five different sums possible for the three silicon isotopes. Apparently the two lower intensity peaks are not detected. Although the observed ratio does not match the value expected for a compound containing two silicon atoms as well as does that observed for the compound containing a single silicon atom, it is still well within experimental error for these measurements. The final analysis indicated that silicon tetrafluoride (104, 105, and 106 amu) and fluorinated polysilanes were responsible for the unknown bands in the Raman spectra of the pyrolysis products.

Even with the higher production of the silicon compounds in the oxygen pyrolysis experiment, identification of these compounds was difficult. In the first place, silicon compounds were not considered until all other possible compounds containing carbon, fluorine, bromine, and oxygen had failed to identify the peaks seen in the mass spectrum of the unknown compounds. Also, until the pyrolyses in oxygen were performed, the very low signal precluded a natural abundance evaluation. It was finally concluded that silicon compounds originating from etching of the quartz pyrolysis tube by pyrolysis products and intermediates were being observed.

It was concluded further that the interaction of the gases with the quartz perturbed the pyrolysis experiments to the extent that no useful information would be provided by further work on pyrolysis.

SECTION V
CONCLUSIONS AND RECOMMENDATIONS

A. SUMMARY OF PHASE II

In Phase II of this project, a program to find low-ODP chemical alternatives for Halons 1211 and 1301 was initiated. The Phase II effort consisted of (1) laboratory studies of flame suppression and (2) evaluation of laser Raman spectroscopy for analyses of flame extinguishment.

The theory of combustion and extinguishment as developed in Phase I was reviewed and expanded in this Phase II report. Both thermodynamics (energy changes and spontaneity) and kinetics (reaction rates) were used to analyze combustion chemistry. Since kinetic information about reactions must be obtained experimentally, and since experimental probing of combustion is difficult, early kinetic analyses of combustion were limited and unreliable. Newer and better methods for investigating flames now provide reliable data on most elementary combustion reactions, which have allowed scientists to better model flames and to determine the reactions most important in combustion.

Free radicals are generated by initiation and branching reactions. Of these two reaction types, branching reactions dominate because of their lower activation energies. Since branching reactions are usually endothermic (heat absorbing), flames would rapidly self-extinguish if heat were not continuously supplied. The energy required to drive these reactions is provided by the termination reactions, which produce the final combustion products.

To initiate combustion, free radicals must be generated in or supplied to a combustible mixture. This can be done by adding energy to drive the initiation reactions or by adding free radicals to drive the branching reactions. Often (for example, in the case of ignition with a match) heat and free radicals are added simultaneously. Once combustion is started, it

is generally self-supporting because of branching reactions (which generate free radicals) and terminating reactions (which generate heat). With a mechanism known, or at least proposed, the reaction rates of the elementary reactions can be used to draw inferences about which reactions in the mechanism are important. These can be termed "critical" reactions.

Much of this report concerns the hydrogen-oxygen flame. Reactions [9] and [10], given earlier, are considered the most important radical producing reactions in flames of diatomic oxygen and diatomic hydrogen. They are also important in flames of hydrocarbon fuels. Since combustion requires a constant, rapid influx of radical species for maintenance, a perturbation of either of these reactions will have a major effect on the combustion process. Furthermore, it is clear that these two reactions are intimately connected since the products of each act as the reactants for the other. Such intimately connected reactions are said to be "coupled." Anything that affects either of these chain branching reactions will have a major effect on the overall combustion process.

Laboratory-scale cup burner tests were conducted on Halon 1211 and mixtures of Halon-1211 with CFC-12, CFC-22, and CFC-114. These tests were used to scope the potential of compounds containing only chlorine and fluorine as halogen substituents as candidate alternative agents. These tests also examined the applicability of cup burner tests to studies of alternative agents.

Optical techniques for analysis of flame-agent interactions were examined in this study. One of the most important advantages of optical techniques is their ability to investigate the physical properties of matter with little to no perturbation. This lack of disturbance is particularly important when one investigates flame properties, where introduction of even small perturbations may have major effects on the processes occurring. Optical techniques are particularly useful tools for investigations of the mechanisms by which halons inhibit combustion.

From the optical techniques available, spontaneous Raman scattering was chosen as a technique for evaluation of halon inhibition of flames. This technique was selected because of the large amount of molecular information available from the vibrational and rotational spectra. In addition, since Raman signal intensity is directly proportional to species concentration, correlations between intensity and concentration may be made. Lastly, Raman spectroscopy permits measurements of flame temperature from the vibrational and rotational spectra.

An apparatus was constructed for evaluation of laser Raman spectroscopy in studies of flame-agent interactions; however, no studies of actual flame-halon chemistry were performed in this phase. Several techniques were used to design a system to overcome the problems associated with spectroscopic measurements on flames. A stable, laminar flow, premixed hydrogen-oxygen slot burner was constructed to produce a safe, stable flame cell. Special mirrors and multipass techniques were developed to increase the laser power and, therefore, the signal intensity of the Raman scattering. The high stray light rejection and flat, undistorted focal plane of a triple monochromator allowed the maximum use of an OMA for detection of the Raman signal. Together, these elements made up a Raman spectrometer capable of measuring many of the molecular species in an hydrogen-oxygen flame.

Raman spectral analyses were performed on some halons of interest and on pyrolysis products from Halon 2402. These experiments were useful in providing a library of the Raman spectra of many of the products that might be expected in later work. Halon 1301, Halon 1202, diatomic bromine, and tetrafluoroethene were found to be the most abundant products of both vacuum pyrolysis and flowing-nitrogen pyrolysis of Halon 2402. In addition to generating spectral data, the experiments also provided experience in the construction, alignment, and operation of a flame Raman spectrometer. This last point was of particular importance considering the low-intensity signals obtained with flame Raman spectroscopy.

During this Phase II effort, it became increasingly apparent that halons might be banned entirely owing to their impact on stratospheric ozone. An international treaty, the Montreal Protocol, was signed, limiting the production of CFC-11, -12, -113, -114, and -115 and Halons 1211, 1301, and 2402. It also became apparent that firefighter training causes a large percentage of the emissions of halons by the Air Force.

B. CONCLUSIONS

1. In stable flames, the rate of free radical loss must be balanced by the rate of free radical generation. It is not necessary for a chemical agent to remove all free radicals to effect extinguishment. It is only necessary to upset the balance sufficiently for loss (which includes diffusion from flames, chain termination, and recombination on surfaces) to exceed generation. Chain branching reactions, which are often tightly coupled to other elementary reactions, are particularly important in maintaining combustion.

2. Knowledge of the microreactions that occur during reaction allow inferences about the relative importance of various reaction steps in maintaining combustion. This information also permits the development of computerized models of the overall combustion process. A paper by Chang, Karra, and Senkan (Reference 15) demonstrates the use of normalized first-order sensitivity gradients,

$$S_g = d \ln(v)/d \ln(A) \qquad (26)$$

where v is flame velocity and A is the preexponential term in the rate constant, to determine on which reactions flame velocities are most dependent. These "critical" reactions can be targeted in agent development. It is generally agreed that the chain branching reaction given earlier in Reaction [9] is a critical reaction step.

3. Since reaction rates are exponential in temperature, even small changes in temperature can effect large changes in combustion rates. Thus, the heat-absorbing ability of an agent may play an important role in flame extinguishment.

4. Reactions [20] - [24] indicate that, with high pressures, suppression can increase. This indicates that the application of shock waves (or high-intensity sound waves) could increase the effectiveness of halon-like agents.

5. Cup burner test results are highly dependent on air flow rate. Thus it is necessary to either correct for this factor or to hold flow rates constant to compare agent effectiveness using this type of test procedure.

6. For streaming agents, physical properties may be as important as chemical properties. The Phase II work deals only with cup burner tests, which measure extinguishment concentrations and whose results depend only on chemical properties. Work is needed on laboratory-scale tests that take streaming characteristics into account.

7. Laboratory tests indicate that CFCs and HCFCs are potentially useful as clean fire extinguishment agents. Although they are generally not as effective as halons, molecular modifications or the use of suitable blends could produce useful, low-ODP agents.

8. The preliminary testing in this phase shows that inherent flame suppression ability increases in the order CFC-22 ($CHClF_2$, chlorodifluoromethane) < CFC-12 (CCl_2F_2, dichlorodifluoromethane) < CFC-114 ($C_2Cl_2F_4$, dichlorotetrafluoroethane) < Halon 1211 ($CBrClF_2$, bromochlorodifluoromethane). Note that this is precisely the prediction which one would make based on the numbers of halogen atoms of various types, taking into account the fact that effectiveness decreases in the order Br > Cl > F. With a

sufficiently large number of chlorine atoms, it may be possible to use hydrochlorofluorocarbons as alternative agents. Of the agents shown above, only CFC-22 has a low ODP and is not regulated under the Montreal Protocol.

8. Synergistic effects were found in all mixtures tested on a laboratory cup burner apparatus: Halon 1211/CFC-12, Halon 1211/CFC-22, and Halon 1211/CFC-114. The synergism was particularly strong with the mixture containing CFC-22. Thus, the addition of a component having a high extinguishment concentration (such as CFC-22) may cause little decrease in effectiveness of a mixture. This implies that blends of materials may be useful either to improve inherent suppression capability or to improve physical or toxicological characteristics.

9. Laser Raman spectroscopy using a double monochromator and an OMA detector was shown to be a potentially useful tool for the study interactions between flames and halon-like agents. However, studies of flame-agent interactions with this or other spectroscopic tools are sufficiently complex that this work should be established as a separate project.

C. RECOMMENDATIONS

The following recommendations are made:

1. HCFCs, CFCs, and their blends should be targeted for investigation as alternative clean agents for halon replacement.

2. Since the greatest need within the Air Force is a replacement for Halon 1211, which is the clean agent used for aircraft fires and protection of Hardened Aircraft Shelters (HAS), emphasis on Halon 1211 alternatives should be continued.

3. Since the work reported here concerns only extinguishment by chemical processes and does not examine the effects of physical processes on extinguishment, the collection of extinguishment data during discharge of halon-like agents should receive high priority in future work.

4 Laser Raman studies should be split out as a separate project owing to the complexity of these types of experiments.

5. Computerized kinetic analyses should be considered to determine critical reactions for targeting by agents and to predict effectiveness of alternative fire extinguishants.

6. An effort should be initiated to develop an agent to substitute for Halon 1211 in Air Force firefighter training. This effort should encompass known materials for which significant toxicity and environmental impact data are available.

REFERENCES

1. Geyer, G., Equivalency Evaluation of Firefighting Agents and Minimum Requirements at U.S. Air Force Airfields, DOT/FAA/CT-82/109, Technical Center, Federal Aviation Administration, Atlantic City Airport, New Jersey, October 1982.

2. Beeson, H. D., and Zallen, D. M., Three-Dimensional Fire Extinguishant, ESL-TR-85-62, Engineering and Services Laboratory, Air Force Engineering and Services Center, Tyndall AFB, Florida, September 1985.

3. Gann, R. G., editor, Halogenated Fire Suppressants, ACS Symposium Series, Vol. 16, American Chemical Society, Washington, DC, 1975.

4. Tapscott, R. E., and Morehouse, E. T., Jr., Next-Generation Fire Extinguishing Agent, Phase I - Suppression Concepts. ESL-TR-87-03, Engineering and Services Laboratory, Air Force Engineering and Services Center, Tyndall AFB, Florida, July 1987.

5. Purdue University, Fire Extinguishing Agents, Final Report, Contract W 44-009 eng-507, Army Engineers Research and Development Laboratories, Ft. Belvoir, Virginia, July 1950.

6. Glassman, I., Combustion, Academic Press, New York, 1977.

7. Gaydon. A. G., and Wolfhard, H. G., Flames, Their Structure, Radiation, and Temperature, 4th Edition, Chapman and Hall, London, 1979.

8. Gontkovskaya, L. A., and Gontkovskaya, V. T., "Kinetics of Hydrogen Oxidation," Combustion Science and Technology, Vol. 17, p. 143, 1977.

9. Westbrook, C. K., "Inhibition of Hydrocarbon Oxidation in Laminar Flames and Detonations by Halogenated Compounds," 19th Symposium (International) on Combustion, The Combustion Institute, Pittsburgh, pp. 127-141, 1982.

10. Westbrook, C. K., "Numerical Modeling of Flame Inhibition by CF3Br," Combustion Science and Technology, Vol. 34, pp. 201-225, 1983.

11. Ford, C. L., "An Overview of Halon 1301 Systems," in Halogenated Fire Suppressants, ACS Symposium Series, Gann, R. G., editor, Vol. 16, American Chemical Society, Washington, DC, 1975.

12. Hirst, R., and Booth, K., "Measurement of Flame-Extinguishment Concentrations," Fire Technology, Vol. 13, pp. 296-315, 1977.

13. Tapscott, R. E., and Morehouse, E. T., Next-Generation Fire Extinguishing Agent, Phase III - Initiation of Training Agent Development, ESL-TR-89-XX, Air Force Engineering and Services Center, Tyndall AFB, Florida, August 1988.

14. Malcolm, J. E., "Halogenated Extinguishing Agents. Part II. Research at the Corps of Engineers' Laboratories," NFPA Quarterly, pp. 119-131, October 1951.

15. Chang, W. D., Karra, S. B., and Senkan, S. M., "A Computational Study of Chlorine Inhibition of CO flames," Combustion and Flame, Vol. 69, pp. 113-122, 1987.

16. Devore, J. L., Probability and Statistics for Engineering and the Sciences, Brooks/Cole Publishing Co., Monterey, California, p. 455, 1982

17. Gann, Richard G, "Initial Reactions in Flame Inhibition by Halogenated Hydrocarbons," Halogenated Fire Suppressants, ACS Symposium Series 16, American Chemical Society, pp. 318-340, Washington, DC, 1975.

18. Safieh, H. Y., Vandooren, J., and Van Tiggelen, P. J., "Experimental Studies of Inhibition Induced by CF3Br in CO-H2-Ar Flame," 19th Symposium (International) on Combustion, The Combustion Institute, Pittsburgh, pp. 117-125, 1982.

19. Biordi, J. C., Lazzara, C. P., and Papp, J. F., "Flame Structure Studies of CF3Br-Inhibited Methane Flames. II. Kinetics and Mechanisms," 19th Symposium (International) on Combustion, The Combustion Institute, Pittsburgh, pp. 917-932, 1975.

20. Lapp, M., Goldman, L. M., and Penney, C. M., "Raman Scattering from Flames," Science, Vol. 175, p. 1112, 1972.

21. Arden, W. M., Hirschfeld, T. B., Klainer S. M., and Mueller, W. A., "Studies of Gaseous Flame Combustion Products by Raman Spectroscopy," Applied Spectroscopy, Vol. 218, p. 554, 1974.

22. Lapp, M., and Penney, C. M., editors, Laser Raman Gas Diagnostics, Plenum Press, London, 1974.

23. Lapp, M., and Penney, C. M., "Raman Measurements on Flames," Advances in Infrared and Raman Spectroscopy, Vol. 3, Clark, R. J. H., and Hester, R. E., editors, pp. 204-261, Heyden, London, 1977.

24. Stricker, A. W., "Local Temperature Measurements in Flames by Laser Raman Spectroscopy," Combustion and Flame, Vol. 27, pp. 133-136, 1976.

25. Stephenson, D. A., and Aiman, W. R., "A Laser Raman Probe of a Premixed Laminar Flame," Combustion and Flame, Vol. 312, pp. 85-88, 1978.

26. Boiarski, A. A., Barnes, R. H., and Kircher, J. F., "Flame Measurements Utilizing Raman Scattering," Combustion and Flame, Vol. 32, pp. 111-114, 1978.

27. Drake, M. C., and Rosenblatt, G. M., "Rotational Raman Scattering from Premixed and Diffusion Flames," Combustion and Flame, Vol. 33, pp. 179-196, 1978.

28. Penner, S. S., Wang, C. P., and Bahadori, M. Y., "Laser Diagnostics Applied to Combustion Systems," 20th Symposium (International) on Combustion, The Combustion Institute, Pittsburgh, pp. 1149-1176, 1984.

29. Long, D. A., Raman Spectroscopy, McGraw-Hill International Book Company, New York, 1977.

30. Krupa, R. J., Culbreth, T. F., Smith, B. W., and Winefordner, J. D., "A Flashback-Resistant Burner for Combustion Diagnostics and Analytical Spectrometry," Applied Spectroscopy, Vol. 40, p. 729, 1986.

31. Suddendorf, R. F., and Denton, M. B., "Burning Parameters of Premixed Oxygen-Hydrogen and Oxygen-Acetylene Flames," Applied Spectroscopy, Vol. 28, p. 8, 1974.

32. Gutzler, D. E., and Denton, M. B., "Improvements in Flame Emission Spectrometry Through the Use of Ultrasonic Nebulization into a Premixed Oxygen-Hydrogen Flame," Analytical Chemistry, Vol. 47, p. 830, 1975.

33. Mossholder, N. V., Fassel, V. A., and Kniseley, R. N., "Spectrometric Properties and Analytical Applications of Premixed Oxygen-Hydrogen Flames," Analytical Chemistry, Vol. 45, p. 1614, 1973.

34. Fiorino, J. A., Kniseley, R. N., and Fassel, V. A., "A Versatile Long-Path, Slot Burner for Atomic and Molecular Absorption Spectroscopy with Oxyacetylene and Nitrous Oxide-Acetylene Flames," Spectrochimica Acta, Vol. 23B, p. 413, 1968.

35. Gaydon, A. G., Spectroscopy of Flames, John Wiley and Sons, New York, 1957.

36. Zinman, W. G., and Bogdan, S. I., "Influence of Vibration-Rotation Interaction on the Rotational 'Temperature' Determined from an Electronic OH Transition," Journal of Chemical Physics, Vol. 40, p. 588, 1964.

37. Weast, R. C., editor, CRC Handbook of Chemistry and Physics, 64th Edition, CRC Press, Inc., Boca Raton, Florida, p. B236, 1983.

APPENDIX A

AN ARGON-SHEATHED PREMIXED OXYGEN-HYDROGEN BURNER FOR FUNDAMENTAL STUDIES

APPENDIX A

AN ARGON SHEATHED PREMIXED OXYGEN-HYDROGEN BURNER FOR FUNDAMENTAL STUDIES

The following is a copy of a manuscript submitted for publication from this work. The authors are J. H. May and T. M. Niemczyk, Department of Chemistry, University of New Mexico, Albuquerque, NM 87131. To keep from duplicating figures, three of the figure numbers cited (Figures 11, 12, and 13) refer to figures in the main body of the report.

A. ABSTRACT

A laminar-flow, premixed oxygen-hydrogen slot burner has been designed and constructed. The design allows operation over a wide variety of oxygen-hydrogen mixtures without flashback. One of the key design criteria was ease of machining, a feature which has resulted in a considerable flexibility in the dimensions of the slots and the positioning of the sheath slots relative to the flame slot. The flame produced shows high stability and distinct regions which make it ideal for fundamental combustion diagnostics.

B. INTRODUCTION

Most combustion processes are the result of diffusion flames. There are many examples of diffusion flames that include processes as varied as a campfire or a welding torch. There are several advantages to diffusion burners, the most important of these is that flashback cannot occur. Thus, burner designs are simple, and no problems are associated with the use of high-burner-velocity fuel-oxidant mixtures. The major drawback of diffusion flames is that they are both audibly and optically noisy. This problem has been alleviated by burner design in which the reactants are combined in a laminar mixing zone (Reference A-1). This design is certainly an improvement in terms of flame noise and offers no possibility of flashback.

Premixed laminar flow flames have been the most widely used flames in spectroscopic studies over the last decade. In comparison with diffusion flames, they demonstrate lower flame flicker, reduced rise velocities, increased dimensional stability, and improved homogeneity. They have become especially popular for flame atomic absorption studies, where there are a variety of manufacturers that supply premix laminar-flow burners. The great popularity is somewhat due to the properties of the nitrous oxide-acetylene flame, which has proven to be an excellent atom cell. Nitrous oxide-fuel mixtures have relatively low burning velocities and thus can be used in premix burners with a reasonable degree of safety.

When oxygen is used as the oxidant, much higher burning velocities are encountered than when nitrous oxide is used. This is especially the case when hydrogen is used as the fuel. Thus, relatively few reports of flame studies involving a premixed laminar flow oxygen-hydrogen flame have appeared. This is true in spite of the advantages of an oxygen-hydrogen flame: a relatively high temperature, simple flame composition, and relatively low background. These factors can be important in many situations. The low background and simple composition are especially important when performing combustion diagnostics.

Denton and coworkers have studied the burning parameters of oxygen-hydrogen flames (Reference A-2) and have pointed out the usefulness of a premixed oxygen-hydrogen flame in flame emission studies (Reference A-3). The burners used in these studies employed a head that consisted of a pattern of very small diameter holes through which the premixed oxygen-hydrogen mixture flowed. The holes were of small diameter so that laminar flow could be achieved. While this work provided the data needed to design oxygen-hydrogen burners, the design chosen is difficult to machine due to the need for the rather deep, very narrow holes.

Another design approach has been to use a slot burner. Mossholder and coworkers (Reference A-4) evaluated a high flow rate premixed oxygen-hydrogen flame supported on a slot burner originally designed by Fiorino and

others (Reference A-5). The results obtained with their design were not very encouraging, however. This was probably due, in part, to the slot sides not being parallel. Thus, laminar flow was probably not achieved.

We wish to report here the design of a premix laminar flow oxygen-hydrogen burner that is safe to operate and easily constructed. Also, the burner incorporates argon sheathing, a feature which is particularly important if the burner is to be used for combustion diagnostics.

C. EXPERIMENTAL

Flame spectra were measured using a Spex Triplemate Monochromator, Model 1877, and a Princeton Applied Research Optical Multichannel Analyser, Model 1420, equipped with a Model 1218 controller and a Model 1215 console. A Coherent Model I-52-4 argon-ion laser was used as the excitation source for the Raman experiments.

The gas flows to the burner were measured using calibrated rotameters, Matheson Model 604. The halon, CF_3Br, was obtained from Dupont Chemical. The oxygen, hydrogen, and argon were all reagent grade and used without purification.

D. BURNER DESIGN

The theoretical equations required to predict the burner dimensions needed to produce a laminar flame are given below (References A-6 and A-7):

$$R_e = VD/a \qquad \text{(A-1)}$$

and

$$L_m = 0.05 \times R_e \times D \qquad \text{(A-2)}$$

where R_e is the Reynolds number, V is the average gas velocity, a is the viscosity of the gas divided by its density, D is the diameter of the hole through which the gas flows, and L_m is the hole depth. In the case of a slot, D is given by the following equation (Reference A-7):

$$D = 2 \times 1 \times b/(1+b) \qquad (A-3)$$

where 1 is the length of the slot and b is its width. For the case 1>>b, D can be approximated to be equal to 2b. Reynolds numbers less than 23200 then describe laminar flow systems. Since the depth of the slot is proportional to the square of its width, decreasing the slot width reduces the depth required to establish laminar flow. The width chosen was 0.040 centimeter, a value which then required a slot depth of approximately 3 centimeters. The calculated Reynolds number of 900 for a oxygen-hydrogen gas mixture flowing at an average velocity of 4000 centimeters/second, is definitely within the laminar region. These same considerations were also given to the dimensions of the sheathing slots.

As can be seen, some specialized machining is necessary to produce a burner satisfying the above constraints. Previous laminar oxyhydrogen burners have generally used the capillary design where the holes were approximately 0.05 centimeter in diameter (Reference A-2); however, no mention of the actual depth of these holes could be found. By our calculations, these holes must have been approximately 3 centimeters deep, and drilling a 0.05-centimeter diameter hole 3 centimeters into stainless steel is very difficult. An alternative design employing a slot in a conventional burner design, rather than round holes, also presents extreme machining constraints. The design presented here solves the problem of producing deep narrow slots in a manner that allows for simple construction and flexible dimensions and which is shown to produce a stable and well-structured flame.

A diagram of the burner is shown in Figure 11. The burner has three sections: the top section, consisting of four pieces (A, B, C and D), the middle section or baseplate (E), and the bottom section, which serves as the gas mixing chamber (F). Parts A and D are 7.0 x 5.0 x 3.0-centimeter blocks with 0.04-centimeter indents machined into them. Part B is a 7.0 x 0.3 x 3.0-centimeter spacer. Part C is a 7.0 x 0.34 x 3.0-centimeter spacer with a 0.4-centimeter indent. The dimensions of Part E are 7.0 x 5.0 x 1.0 centimeters, and the slot in the center is 3.0 x 0.1 centimeters. Part F is a 5.0-centimeter high piece of 3.0-centimeter OD, 2.0-centimeter ID tubing. All parts of the burner are made of stainless steel.

The key to the design is the four top pieces. The problem of machining deep narrow slots is overcome by grinding an indent into three of the four pieces. The mating surfaces of the pieces are polished flat, and when pulled together, the indents form the slots necessary to achieve laminar flow. The indents in A and D, fed from the side of each piece, form the argon-sheath slots. The argon is introduced of the sheath slots by two 0.125 inch holes drilled through each of parts A and D. The holes are positioned to enter the bottom of the argon-sheath slots. A cavity and connections for water cooling have also been incorporated into these pieces. The water cooling cavities are formed by simply drilling a 0.250-inch hole through the part. The piece labeled B serves as a spacer, and C has the indent that forms the slot for the flame. Two alignment pins, purposely offset to each other, are used to provide an accurate and unique assembly of the pieces (only one pin is shown in Figure 11). The entire group is held together by two bolts that pass horizontally through the pieces. Once the top section is assembled, it is bolted onto the baseplate (E).

The dimensions of the slots as well as their spacing are very flexible. For example, the distance from the argon sheath to the flame is set by the width of pieces B and C. Indeed, by making the vertical bolt holes in pieces A and D slots, different dimensions can be used without remachining the entire burner. Also, as can be seen, there is no difficulty in making extremely narrow slots.

The bottom section (F) serves as the burner mount as well as gas mixing chamber. The top of this piece is welded to the bottom of the baseplate (E). Three connections at the bottom (only two are visible in Figure 11) introduce gases to the mixing chamber.

The pressure relief valve (G) is constructed by welding a short section of 2.0-centimeter OD by 1.5-centimeter ID tubing to a hole in the side of the mixing chamber (F). The cover piece is held closed by springs as shown in Figure 11.

The burner slot used is 0.0404 centimeter wide, 2.0 centimeters long, and 3.0 centimeters deep. The argon sheath slots are 0.040 centimeter wide, 3.0 centimeters long, and 3.0 centimeters deep. These dimensions insure laminar flow under all flow conditions that might be encountered. Consideration was also given to quenching of flame reactions by the burner walls. Very narrow slots can be used for conditions where the flow rate through the slot might be lower than the absolute burning velocity of the fuel oxidant mixture (Reference A-2). This fact can be used to design a burner that will work safely over a wider set of operating conditions than predicted based simply on the burning velocity of the flame.

E. RESULTS AND DISCUSSION

Perhaps the major drawback to the use of a premixed oxygen-hydrogen flame is the possibility of flashback. In order to minimize the possibility of flashback the gas flow through the burner slot must be higher than the burning velocity of the fuel-oxidant mixture, taking into account any wall quenching effects. The gas velocity through the slot must also be in a range that produces a stable, well-structured flame. The slot dimensions used in this design were chosen such that the flow rate of oxygen required for normal operation was 3 liters/minute. With this oxygen flow, the hydrogen flow required for normal operation was 3.5 to 9.5 liters/minute depending on the desired oxidizing or reducing nature of the flame.

Conditions that would produce a flashback were tested for by setting one of the flows (oxygen or hydrogen) and slowly decreasing the flow of the other until flashback occurred or the flow was zero.

The data produced in these studies are compiled in Figure 12. As can be seen, the conditions that produce flashback are a function of both the total flow rate through the burner slot as well as the hydrogen to oxygen ratio. It has also been shown that the conditions necessary to produce flashback are dependent on the temperature of the burner (Reference A-2). As the burner used here is water-cooled, it rapidly reaches an equilibrium, and the flashback conditions remain constant.

Also, as can be seen from the data, the total flow rate (for any oxygen-hydrogen mixture) required to produce flashback is more than a factor of two below the normal operating conditions. Thus, the burner is normally operated without any significant possibility of flashback occurring. Indeed, we have never experienced an unintentional flashback when operating the burner. Further reduction or complete elimination of flashback could be accomplished by using even narrower slots than the ones used here.

Another of the desire goals of the burner design was to produce a stable flame with well-defined reaction zones. Such a flame has temperature zones that characterize the processes occurring at each region in the flame. Measurements of temperature as a function of height above the burner head give the results shown in Figure 13. The temperature was determined by measuring the relative intensities of OH vibrational-rotational bands and calculating the temperature according to the method of Zinman and Bogdan (Reference A-8). When one views the flame operating under the conditions used here, the primary reaction zone begins approximately 1.5 millimeters above the burner head. The bright blue primary reaction zone is approximately 2 millimeters high. Above that is a very light blue mantle that extends 20 to 30 centimeters above the burner head. One would expect that the temperature of the flame gases would increase rapidly with height in the preheat zone, reach a maximum in the primary reaction zone, and taper

off with height above the primary reaction zone. This is exactly the behavior seen in Figure 13. The precision and stability of the system is indicated by the data, obtained from two, entirely separate temperature determinations at each height above the burner.

It is planned to use the burner to study the behavior of halon fire retardants when entering a flame. A possible probe of reaction species in the flame is Raman Spectroscopy. The Raman spectra of the molecules of interest must be separable from the Raman spectra of the flame gases as well as separable from the background emission from the flame itself. In the case of halon 1301 this is a particular problem, as the flame background is extremely strong in the region of the halon spectrum. One method of dealing with the problem is to use background subtraction. In order to do so, however, the flame must be very stable. Figure A-1 shows the original and background-subtracted Raman spectrum of halon 1301 in the 284-784 cm^{-1}. In this figure, the spectrum marked A is the Raman spectrum of the flame with CF_3Br added. That marked "B" is the Raman spectrum of CF_3Br after the flame background is subtracted. The total time required to take these spectra was 12 minutes: 6 minutes for the Raman spectra and 6 minutes for the background emission. Note that the flame emission is very intense and almost completely obscures the two halon peaks. In the background subtracted spectrum, the peaks are clearly seen. This demonstrates not only the power of background subtraction, but the high stability of the premixed flame.

The Authors wish to acknowledge the financial support of the Air Force Engineering and Services Center, Tyndall AFB, Florida and discussion with Mr. Joseph L. Walker, AFESC/RDCF, Tyndall AFB, Florida and Dr. Robert E. Tapscott, New Mexico Engineering Research Institute, University of New Mexico.

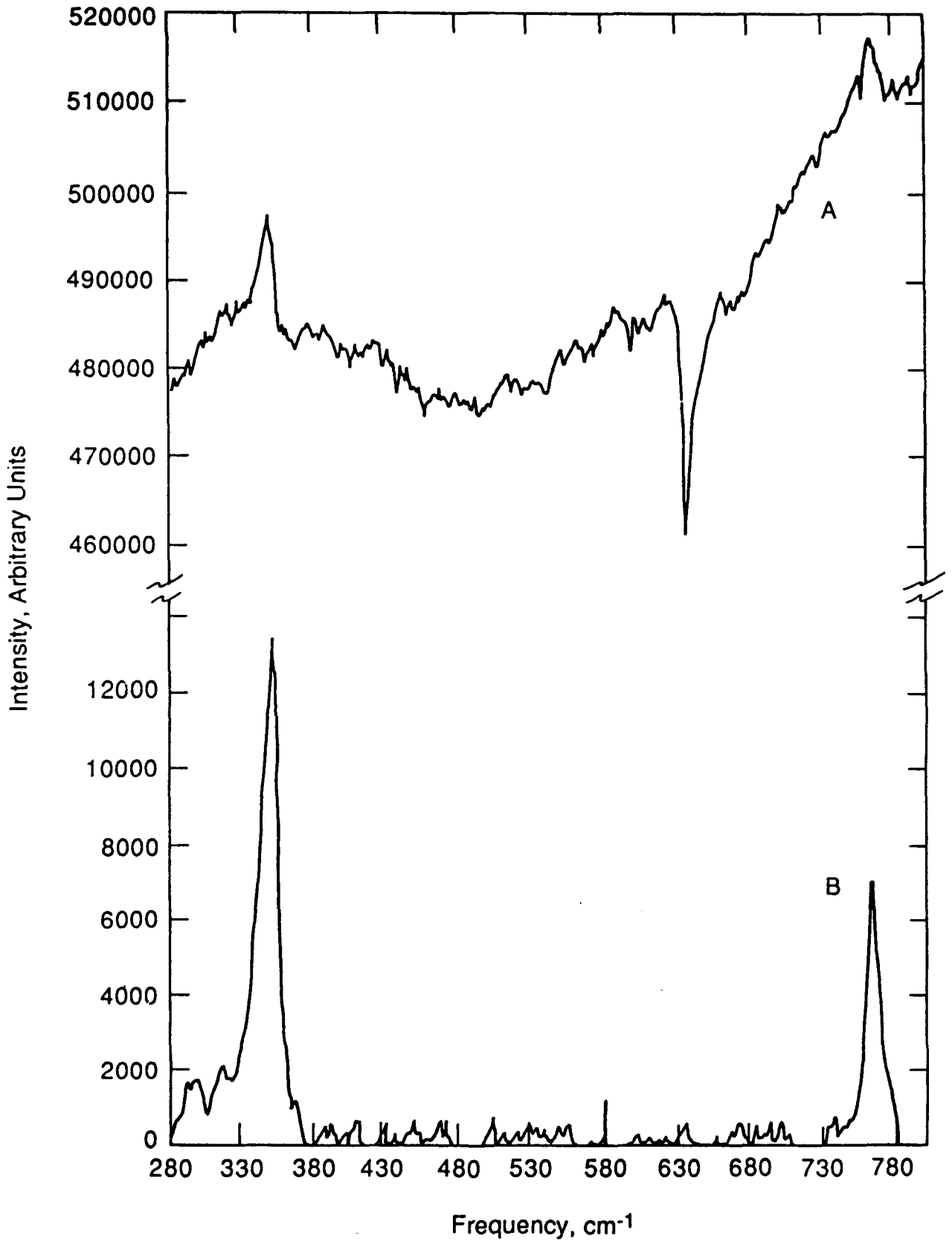

Figure A-1. Spectra of the Flame and CF_3Br.

REFERENCES

A-1. Krupa, R. J., Culbreth, T. F., Smith, B. W., and Winefordner, J. D., Applied Spectroscopy, Vol. 40, p. 729, 1986.

A-2. Suddendorf, R. F., and Denton, M. B., Applied Spectroscopy, Vol. 28, p. 8, 1974.

A-3. Gutzler, D. E., and Denton, M. B., Analytical Chemistry, Vol. 47, p. 830, 1975.

A-4. Mossholder, N. V., Fassel, V. A., and Kniseley, R. N., Analytical Chemistry, Vol. 45, 1614, 1973.

A-5. Fiorino, J. A., Kniseley, R. N., and Fassel, V. A., Spectrochimica Acta, Vol. 23B, p. 413, 1968.

A-6. Gaydon, A. G., and Wolfhard, H. G., Flames, Their Structure, Radiation, and Temperature, 4th Edition, Chapman and Hall, London, 1979.

A-7. Gaydon, A. G., Spectroscopy of Flames, John Wiley and Sons, New York, 1957.

A-8. Zinman, W. G., and Bogdan, S. I, Journal of Chemical Physics, Vol. 40, p. 588, 1964.

APPENDIX B

OUTLINE REPRESENTATIONS OF ENGINEERING DRAWINGS FOR LASER RAMAN SPECTROMETER BURNER

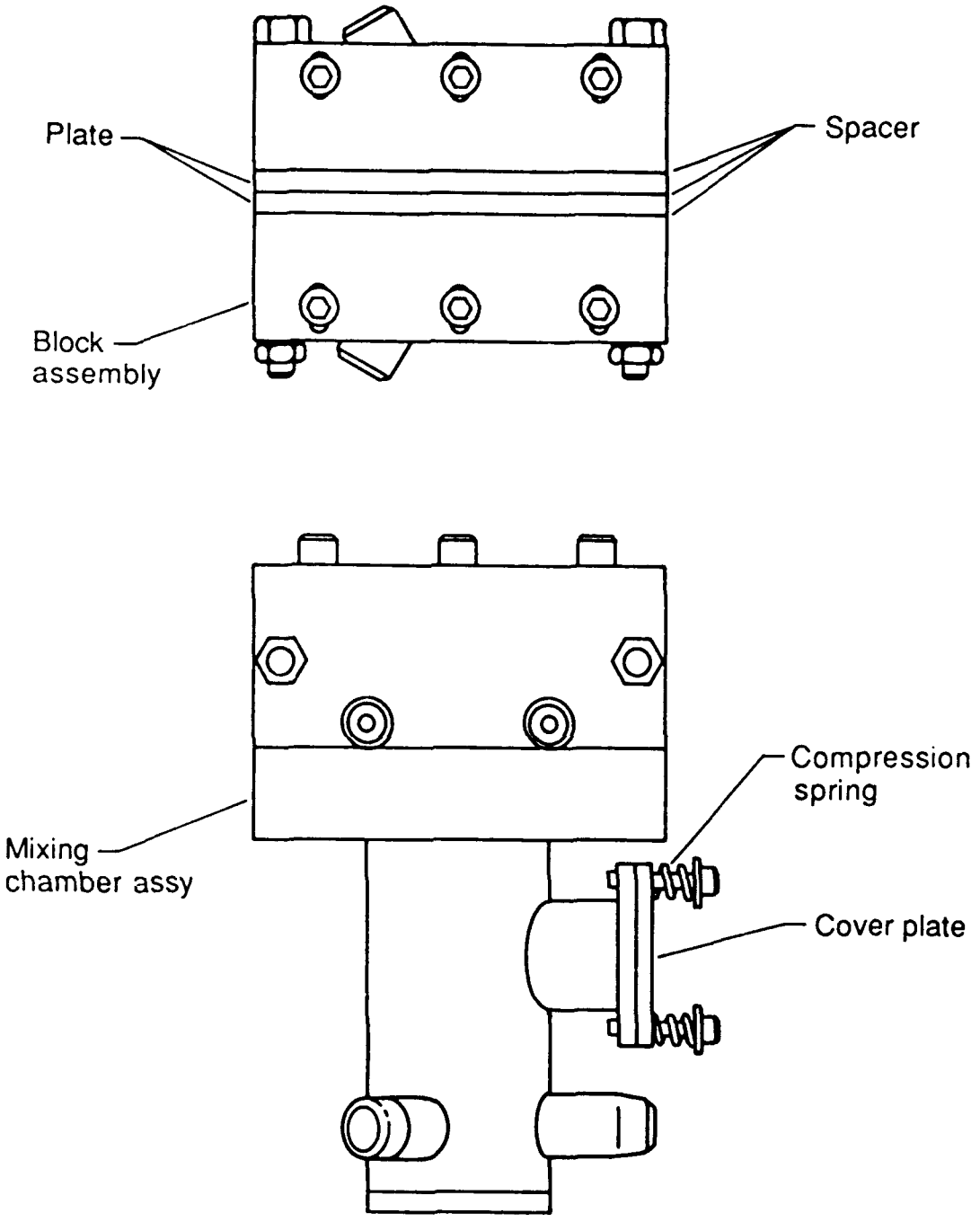

Figure B-1. Assembled Burner with Three Slots and Mixing Chamber with Safety Release.

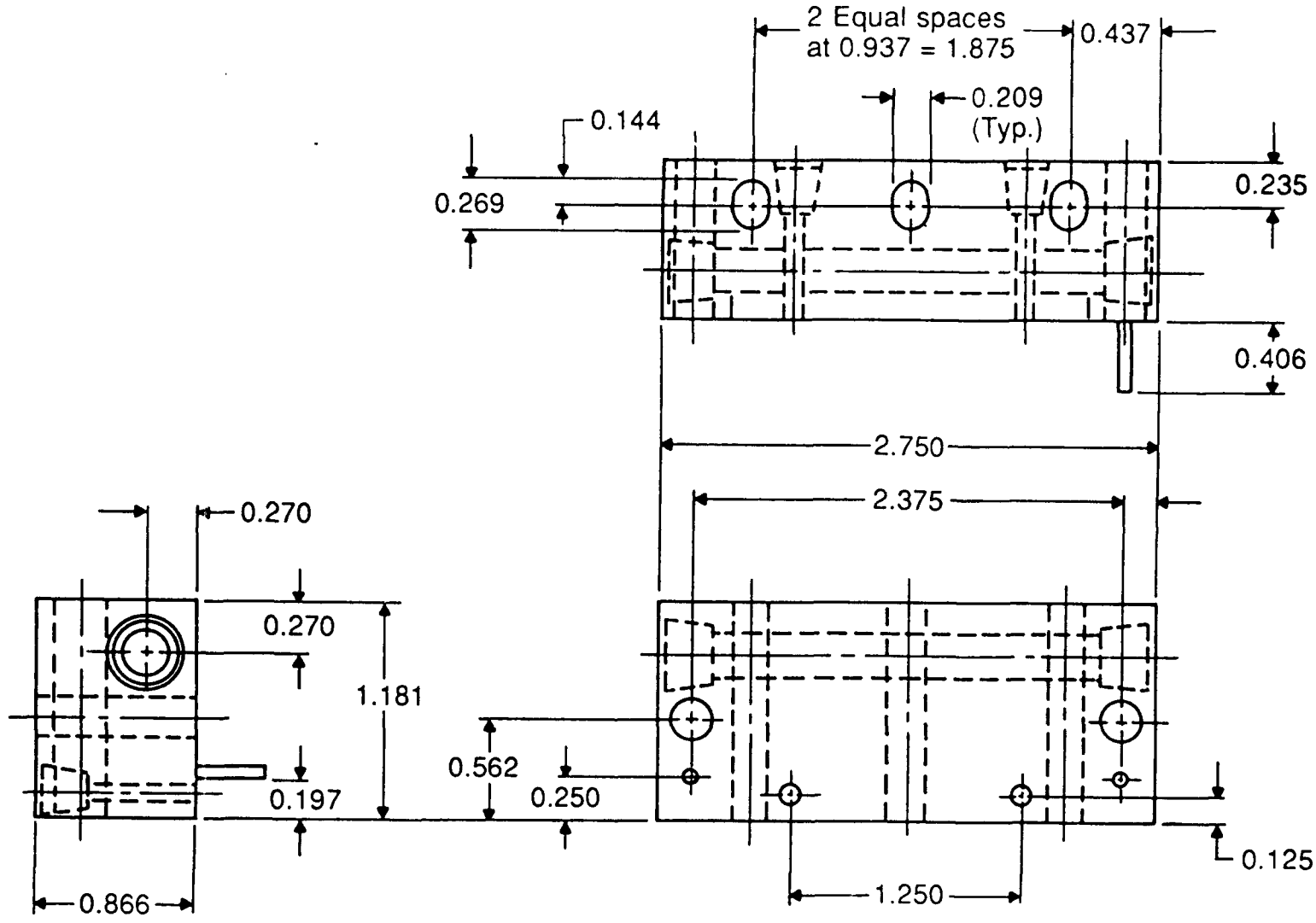

Figure B-2. Outer Blocks of Burner Head with Passages for Argon Gas and Water Cooling.

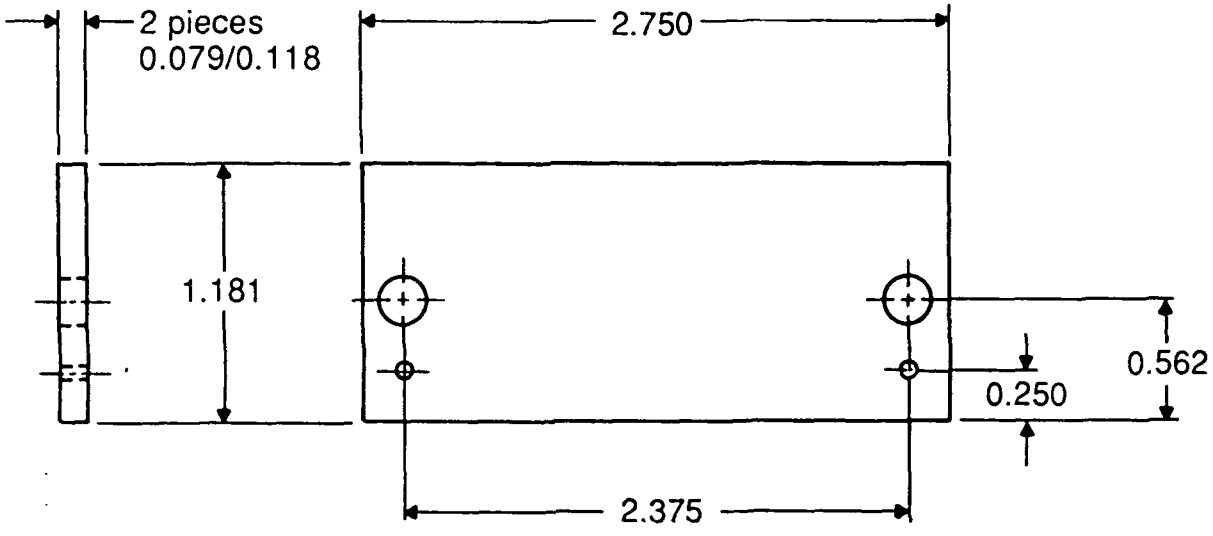

Figure B-3. Spacer, One of Two Separating Three Slots.

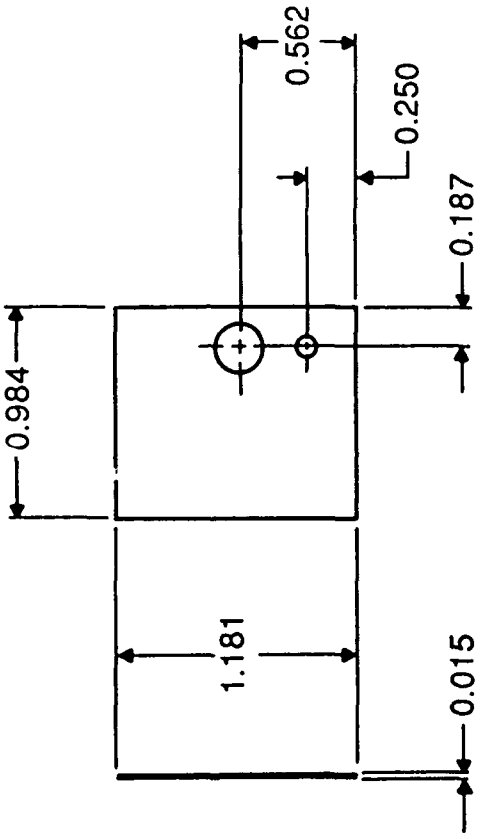

Figure B-4. Short Spacer, One of Six Making Up Outer Slots.

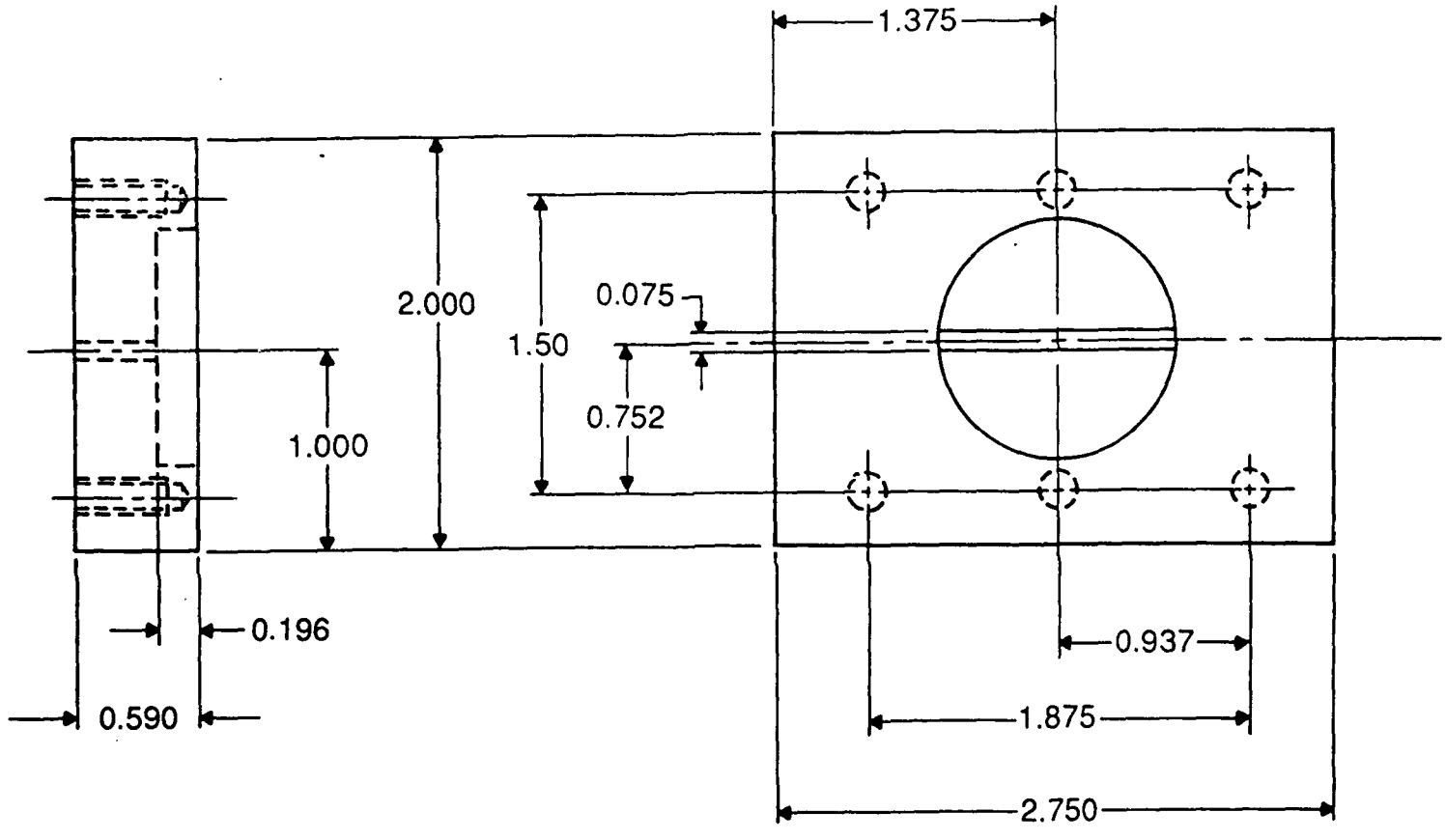

Figure B-5. Bottom Plate to Connect Mixing Chamber and Upper Burner Head.

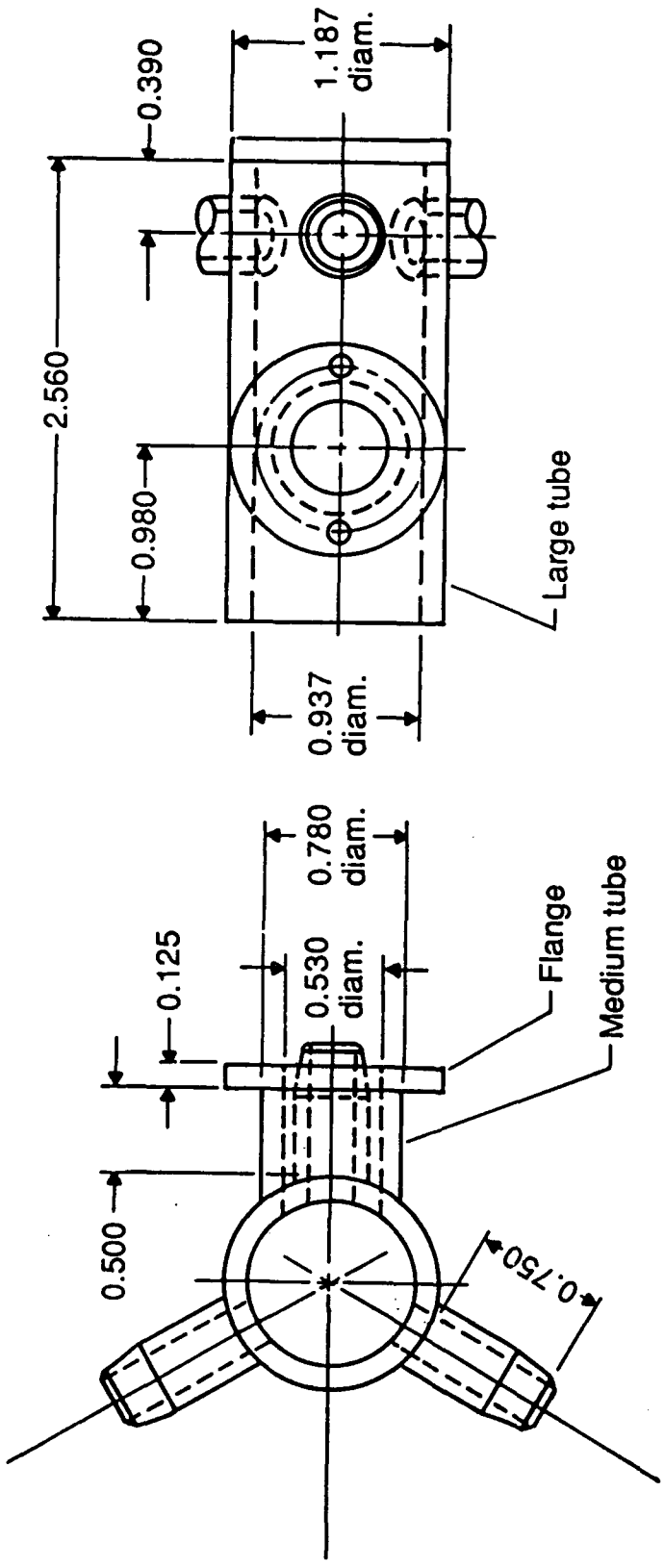

Figure B-6. Mixing Chamber with Safety Release.

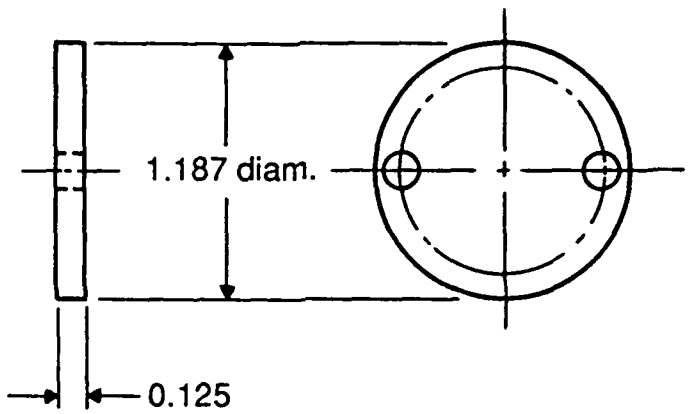

Figure B-7. Plate Cover for Safety Release.

APPENDIX C

RAMAN STUDIES OF HALON FIRE RETARDANTS

APPENDIX C

RAMAN STUDIES OF HALON FIRE RETARDANTS

A. INTRODUCTION

The following is a paper presented in the Division of Fuel Chemistry at the American Chemical Society Meeting, New York, NY, 13-18 April 1986. The authors are J. H. May, F. S. Allen, M. R. Ondrias, Department of Chemistry, and R. E. Tapscott, H. D. Beeson, and D. M. Zallen, New Mexico Engineering Research Institute, University of New Mexico, Albuquerque, NM 87131. The paper has been revised slightly to meet format and other requirements for this report.

B. PAPER

Raman spectroscopy can be used as a passive probe for the study of active systems. Various types of analytical determinations can be made without perturbing the system under study. Of interest is the elucidation of the extinction processes employed by halon extinguishing agents. In the past, Raman has been used to study such molecules as H_2O, N_2, and CO_2 in flames (Reference C-1). Halons and pyrolysed products have vibrations that are more polarization sensitive than the above molecules and should, therefore, be readily analysed in flames. In an initial approach to this problem, the pyrolysis of Halon 2402 (1,2-dibromotetrafluoroethane) is being studied. The pyrolysis products are isolated using vacuum line techniques and are identified using GC-MS and Raman. A library of the Raman spectra from each component is being formed for subsequent use in flame analysis.

The experiment uses a tube furnace with a specially designed tube, which has detachable nitrogen traps capable of holding a vacuum on each end. In a simulation of combustion, the system is brought to high vacuum. The halon is then allowed to vacuum transfer through the pyrolysis tube, which

is at approximately 790 ^{o}C, to the other nitrogen trap. This process is repeated several times. The products are then vacuum distilled, and the fractions are captured in different sealable cuvettes. At present, all fractions are studied in the gas phase at room temperature.

The Raman data are collected on an instrument constructed of the following components:

1. An EG&G Princeton Applied Research Model 1420 intensified Silicon Photodiode Array tube coupled with a Model 1218 solid state detector controller and a Model 1215 computer console.

2. A SPEX Model 1877 Triplemate monochromator.

3. A Coherent Model CR-4 Argon ion laser, capable of producing over 3 watts of continuous-wave (CW) power at the 488.0-nanometer line.

Spectra in the range of 100 to 1000 cm^{-1} can be obtained at a single setting of the monochromator. Since Raman spectra of many of the thermal degradation products are not available, a Finnigan Series 4900 GC-MS is used to identify the products obtained from the pyrolysis experiment. Raman spectra collected on these components will form a spectral library of the pyrolysis products.

Figures C-1 and C-2 show the Raman spectra of the first fraction collected from the vacuum distillation process on the pyrolysed 2402. The complexity of the spectra suggests that more than one component is present. The GC-MS spectra shows that the gas contains only tetrafluoroethene and bromotrifluoromethane (Halon 1301) in significant concentrations. Figures C-3 and C-4 present Raman spectra of pure 1301. It is evident that the spectral bands match many of the bands in the distilled fraction.

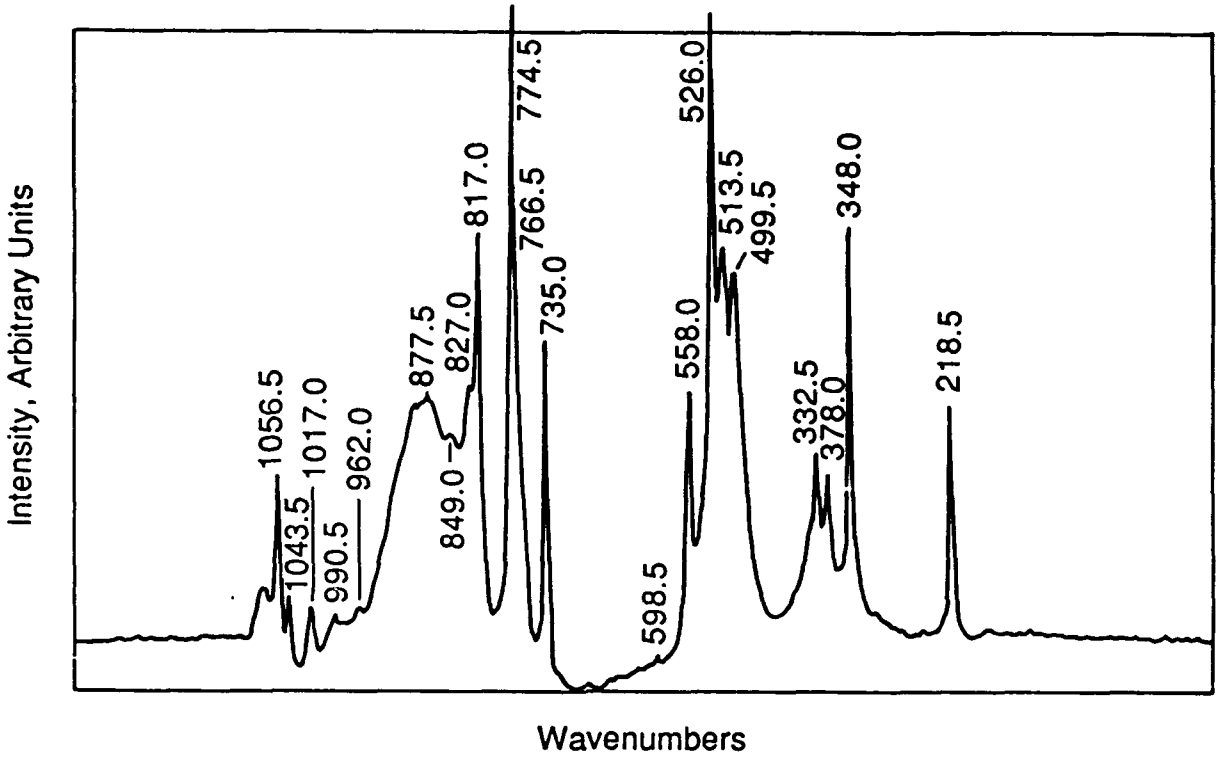

Figure C-1. Raman Spectrum of First Fraction Collected from Vacuum Distillation of Products from Pyrolysed Halon 2402.

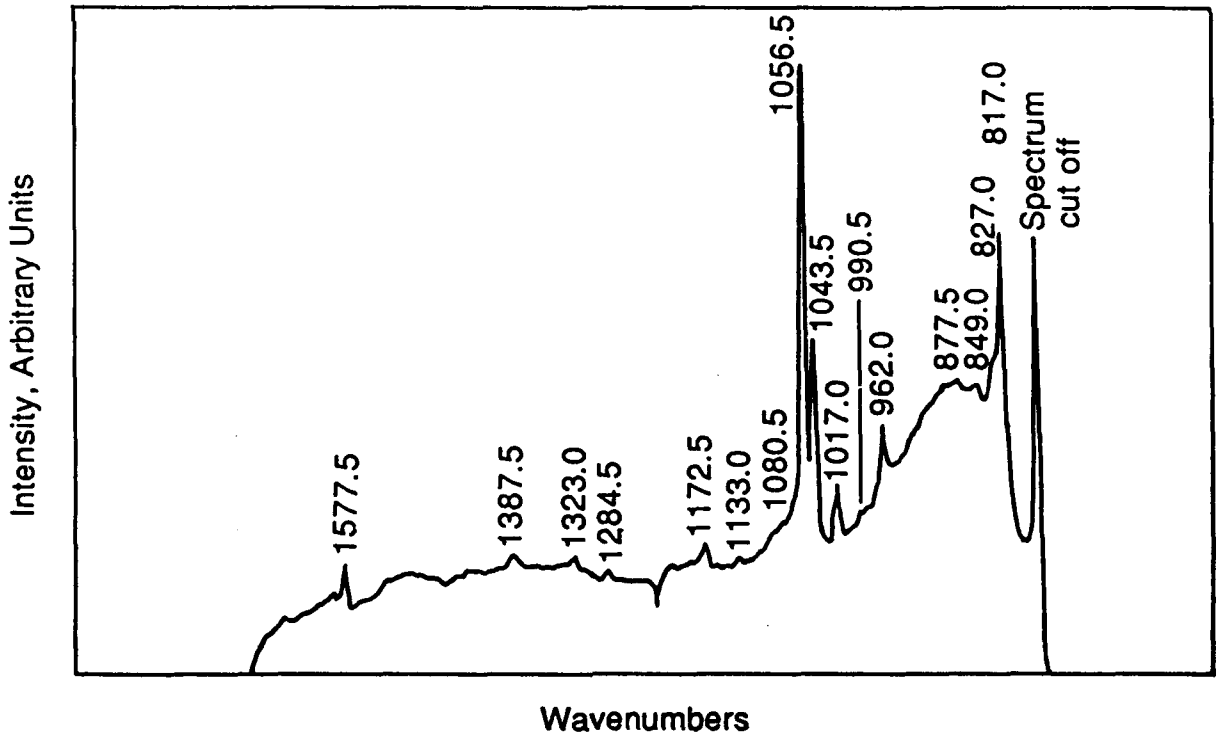

Figure C-2. Expanded Region of Raman Spectrum of Pyrolysis Products.

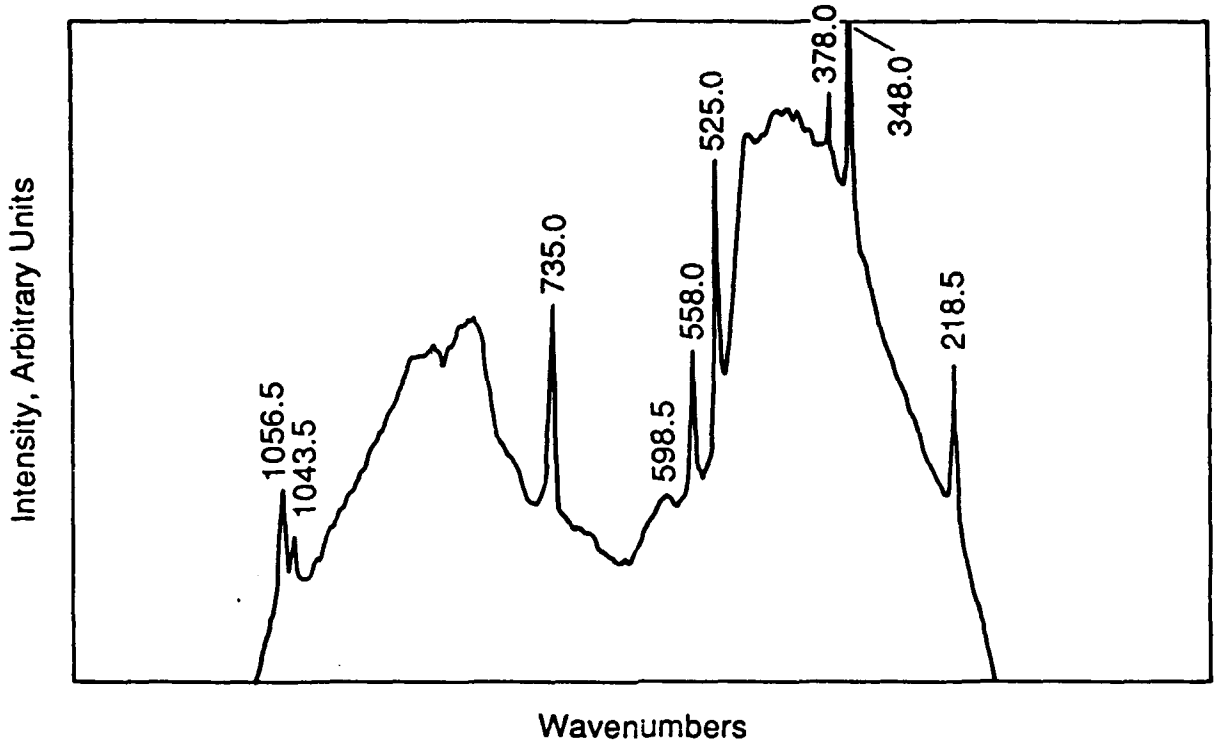

Figure C-3. Raman Spectrum of Pure Halon 1301.

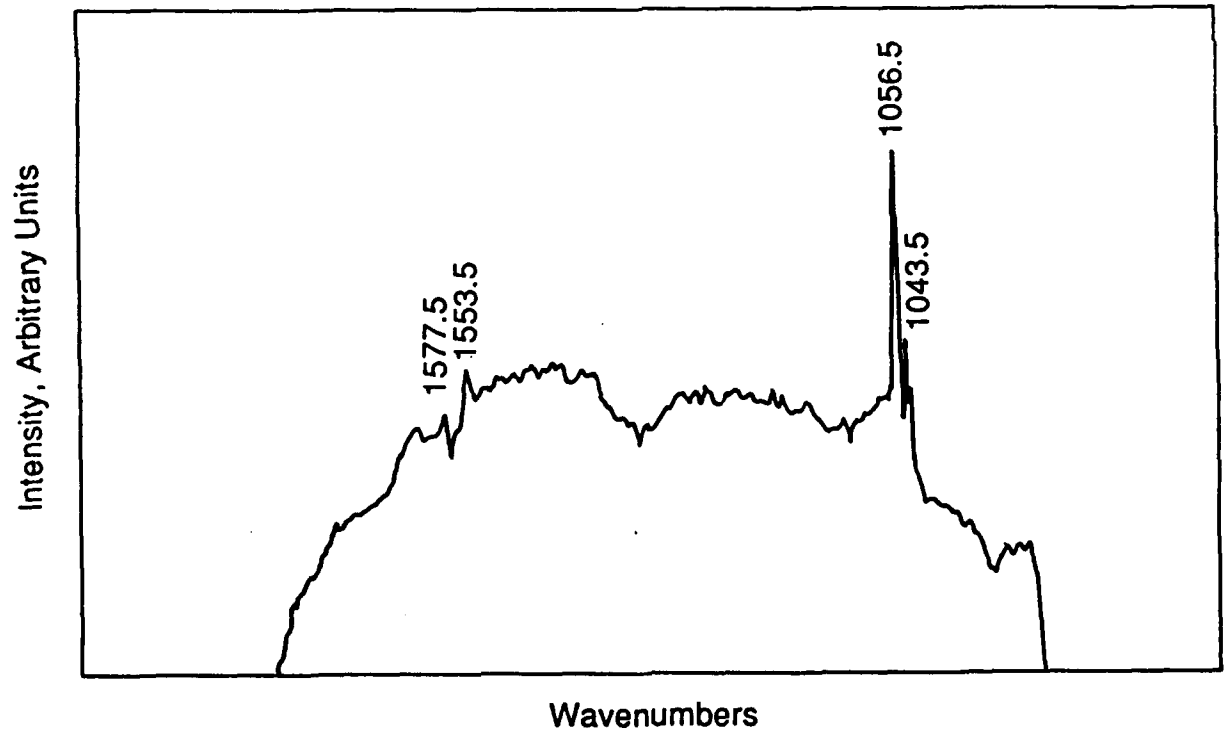

Figure C-4. Expanded Region of Raman Spectrum of Halon 1301.

Pure tetrafluoroethene will be examined to identify its spectral contribution to spectra of the pyrolysis products. The vacuum distillation was performed at 500 millitorr. Planned distillations using higher pressures should provide better separation of the fractions.

Each of these spectra required 30 minutes to collect: 15 minutes for the signal spectra and another 15 minutes for the background. (Raman spectra normally require the subtraction of the background spectra, taken with the excitation source off, from the signal spectra. This is particularly true for photodiode array detectors.) Accurate spectra, to within 2 cm^{-1}, of all but the weaker bands can be taken in a minute or less (this includes background spectra). With pulsed or higher intensity CW lasers, spectra could be taken in less time with even better signal-to-noise ratios.

These studies will permit the development of a library of Raman spectra for the stable products produced by the simulated combustion of Halon 2402 in a vacuum and in oxidizing and reducing environments. This library will be used in subsequent studies to identify the products present in flames near extinction due to the presence of Halon 2402.

ACKNOWLEDGEMENTS

Partial support for this project was provided by the Air Force Engineering and Services Center, Tyndall AFB, Florida. Mr. Joseph L. Walker contributed through many fruitful discussions.

REFERENCE

C-1. Lapp, M., and Penny, C. M., Laser Raman Gas Diagnostics, Plenum Press, New York and London, 1974.

APPENDIX D

RESEARCH PLAN FOR PHASES III AND IV

APPENDIX D

RESEARCH PLAN FOR PHASES III AND IV

A. TRAINING AGENT DEVELOPMENT

The results of testing in this phase indicate that blends of CFCs and/or HCFCs can be used to develop an agent having a decreased ODP to replace Halon 1211 in firefighter training only. Since training accounts for more than 70 percent of Air Force halon emissions, the availability of a training agent would reduce the environmental impact of Air Force operations and would increase the availability of Halon 1211 for essential fire protection requirements. The feasibility of an early development of a training agent is based on the following rationale.

1. A temporary training agent does not need an ODP as low as that required for permanent halon replacements. This is not to say that a training agent must be temporary; however, such a decision could be made depending on the attainable ODP.

2. A training agent needs to mimic the action of Halon 1211 only in one specific scenario--firefighter training with a pool fire containing JP-4 fuel.

3. Since firefighters are professionals and are trained outdoors, toxicity requirements are not as stringent as for a general-purpose agent.

4. Cleanliness and compatibility with advanced airframe materials are not important criteria for an agent intended to be used solely in firefighter training.

5. A decreased agent effectiveness is not a critical drawback since it may serve to give firefighters better training.

6. Since decreased agent effectiveness and a slightly higher toxicity level could be acceptable for a training agent, off-the-shelf materials may be available. Such availability would greatly reduce the work required.

Accordingly, the Air Force tasked work toward the development of a training agent in Phase III and Phase IV of the Next-Generation Agent project. The research plan for these phases is presented below and corresponds to the work as tasked.

B. PHASE III PLAN

The Phase III tasks include the identification and screening of candidates for firefighter training agents in laboratory-scale Class B fire tests. As needed, additional laboratory testing for characterization should be performed. To the extent possible, known materials for which significant toxicity and environmental impact data are available should be used.

From the Phase II results a decision has been made to investigate blends of CFCs and/or HCFCs or the pure materials themselves. Since the performance of an agent to replace Halon 1211 in firefighter training depends in large part on the delivery characteristics, the use of tests that deliver agent by streaming is essential. The following plan was developed.

1. Since discharge characteristics are important, investigations of laboratory methods to determine droplet size for streaming will be made. A photographic technique will be evaluated.

2. Laboratory-scale discharge extinguishment test will be developed to complement the cup-burner test. The availability of two laboratory-scale tests will permit measurements of both extinguishment concentration and

discharge suppression. While extinguishment concentration is a good measure of capability for a total-flood agent, the capability of a streaming agent depends on both extinguishment concentration and streaming performance.

3. A small-scale discharge extinguishment test will also be developed. This test will employ pan fires having an area of 1 ft^2.

4. Sufficient tests will be run on blends and pure materials to evaluate both laboratory-scale and small-scale discharge extinguishment tests for measurements of fire suppression capability for a streaming application.

5. Discharge extinguishment tests will also be run on blends and pure materials to scope the potential of CFCs and HCFCs as firefighter training agents.

C. PHASE IV PLAN

The Phase IV requirements task selected field studies of a firefighter training agent. Class B pool fire field tests are to be performed on the most promising candidate agents. Both medium-scale and large-scale tests are to be conducted. An important requirement is the survey and compilation of toxicity and environmental data.

1. A brief survey of generally available CFCs and HCFCs will be made with particular emphasis on toxicity and environmental characteristics.

2. Medium-scale tests involving pool fires having areas from 4 to 28 square feet will made on selected CFCs, HCFCs, and/or blends.

3. Large-scale pool fire tests from 100 to 300 square feet will be performed on selected CFCs, HCFCs, and/or blends. These tests will employ handheld extinguishers and 150-pound wheeled units.

(The reverse of this page is blank.)